Modeling and Dynamic Optimization of Microalgae Cultivation in Outdoor Open Ponds

A DISSERTATION
SUBMITTED TO THE FACULTY OF
UNIVERSITY OF MINNESOTA
BY

Abdulla Abdul Rahman Malek

IN PARTIAL FULFILLMENT OF THE REQUIREMENTS
FOR THE DEGREE OF
DOCTOR OF PHILOSOPHY

Advised by Prodromos Daoutidis

December 2016

(قُلْ سِيرُوا فِي الْأَرْضِ فَانْظُرُوا كَيْفَ بَدَأَ الْخَلْقَ ۚ ثُمَّ اللَّهُ يُنْشِئُ النَّشْأَةَ الْآخِرَةَ ۚ إِنَّ اللَّهَ عَلَىٰ كُلِّ شَيْءٍ قَدِيرٌ)

Say: "Travel through the earth and see how Allah did originate creation; so will Allah produce a later creation: for Allah has power over all things.

Acknowledgements

I would like to sincerely thank my advisor Professor Prodromos Daoutidis for the guidance, encouragement, and support throughout my wonderful PhD journey.

I would like to express my gratitude to all my office-mates who enriched my research life: Dr. Fernando V. Lima, Dr. Milana Trifkovic, Dr. Ana I. Torres, Dr. Dimitrios Georgis, Dr. Srinivas Rangarajan, Dr. Seongmin Heo, Dr. Adam Kelloway, Dr. William Alex Marvin, Dr. Nahla Al Amoodi, Michael Zachar, Udit Gupta, Mustafa Caglayan, Dr. Davood Babaei Pourkargar, Conor O'Brien, Manjiri Moharir, Nitish Mittal, Matthew Palys, Wentao Tang, and William Allman. To Dimitrios and Nitish, I appreciate your help in gPROMS. To Michael and Alex, I appreciate the enriching discussions in modeling and optimization. To Udit and Srinivas, I appreciate the mind opening discussions during the long working nights. Also, thank you Dr. Yasser Al Wahedi for your helpful advice.

I am grateful to my family, especially my mother (Nadia Salem), my father (Abdulrahman Ghaleb) and my wife (Aala Alhuwait) for always being extremely supportive and encouraging throughout my life.

Table of Contents

Acknowledgements i

List of Tables v

List of Figures vi

1 Introduction 1

1.1 Motivation 1

1.2 Objectives and Approach 4

1.3 Computational Tools and Packages 7

2 Growth of Microalgae in an Outdoor Open Pond 9

2.1 Background 9

2.1.1 Autotrophic and Heterotrophic Microalgae 9

2.1.2 Reactor Configurations 11

2.1.3 Harvesting of Algal Biomass 12

2.2 Process Description and Modeling 13

2.2.1 Water Material and Energy Balances 14

2.2.2 Microalgae Mass Balance and Growth Kinetics 18

2.2.3 CO_2 Sump Stations 22

2.3 Process Economics 24

2.4 Model Validation 25

2.4.1 Experimental Setup and Model Assumptions 25

2.4.2 Simulation Results 29

2.5 Dynamic Optimization 30

2.5.1 Problem Definition 30

2.5.2 Major Operating Parameters 32

2.5.3 Base Case 36

2.5.4 Optimization Problem 37

2.5.5 Optimization Results 38

2.6 Conclusions 43

3 Cultivation Coupled with Recovery of Flue Gas CO_2 44

3.1 Background 44
3.2 Process Description and Modeling 45
3.2.1 Microalgae Cultivation System 45
3.2.2 Microalgae Cultivation and Flue Gas CO_2 Utilization 46
3.2.3 Direct Contact Condensing Heat Exchanger Model 47

3.3 Process Economics 49
3.4 Dynamic Optimization 51
3.4.1 Base Case 52
3.4.2 Optimization Problem 52
3.4.3 Optimization Results 53

3.5 Conclusions 58

4 Cultivation Coupled with Recovery of Waste Heat 59

4.1 Background 59
4.2 Process Description and Modeling 60
4.2.1 Microalgae Cultivation System 60
4.2.2 Microalgae Cultivation and Flue Gas Heat Recovery 61
4.2.3 Indirect Contact Condensing Heat Exchanger Model 62

4.3 Process Economics 63
4.4 Optimization 64
4.4.1 Base Case 65
4.4.2 Optimization Problem 68
4.4.3 Optimization Results 69

4.5 Conclusions 75

5 Cultivation Coupled with Recovery of Waste Nutrients 76

5.1 Background 76
5.2 Process Model 79
5.2.1 Microalgae Cultivation System 79
5.2.2 Treated Wastewater Utilization 79
5.2.3 Kinetics of Nutrient Limitation on Growth 84

5.3 Process Economics 86
5.4 Supply Chain Optimization 88
5.4.1 Microalgae Cultivation at Wastewater Treatment Plants 90
5.4.2 Microalgae Cultivation at Power Plants 91
5.4.3 Optimization Results 92

5.5 Conclusions 96

6 Conclusions and Future Work 97

6.1 Conclusions 97
6.2 Future Work 100
6.2.1 Integration of Waste Heat and CO_2 Recovery 100
6.2.2 Siting of Algae Facilities Worldwide 101
6.2.3 Alternative Harvesting Schemes 102

Nomenclature 103
Bibliography 107
Appendix 120

List of Tables

Table 2.1: Parameter definitions and values for the mass and energy balances. 17

Table 2.2: Parameter definitions and values for the microalgae growth kinetics model. 28

Table 2.3: Values assigned to the parameters of the CO_2 mass balance and transfer model. 31

Table 2.4: Parameter definitions and values for the process economics model. 32

Table 3.1: Parameter values for the heat transfer coefficient correlation. 49

Table 3.2: Parameter definitions and values for the process economics model. 51

Table 4.1: Parameter definitions and values for the process economics model. 64

Table 5.1: Effluent characteristics of wastewater treatment plants in Imperial County. 81

Table 5.2: CO_2 emissions data for natural gas fired power plants in Imperial County. 81

Table 5.3: Parameter definitions and values for the nitrogen deficiency model including initial values. 86

Table 5.4: Parameter definitions and values for the wastewater transportation cost. 88

Table A.1: Daily weather conditions from typical metrological year data in imperial county California USA. 120

Table A.2: Travel distances in miles between the considered wastewater treatment plants and power plants in Imperial County, California, United States of America. 128

List of Figures

Figure 2.1: Open Ponds (left image) and photobioreactors (right image). 13

Figure 2.2: Approximation of the open pond model as a cascade of compartments. 14

Figure 2.3: Modeling the open pond as a cascade of continuous stirred-tank reactors (CSTRs) with an internal and an external recycle stream. 17

Figure 2.4: Daily global solar radiation and average air temperature at Málaga from September 23, 1997 to July 31, 1998 [87], [88]. 27

Figure 2.5: Simulation results for Spirulina cultivation in Málaga, Spain from September 1997 to July 1998: Algal biomass areal concentration and temperature of the pond water. 29

Figure 2.6: Comparison between monthly-averaged values of the predicted productivity and the productivity determined experimentally in reference [85]. 30

Figure 2.7: Demonstration of the heuristic approach for finding the optimal dilution rate. The dilution rate is increased in steps of 0.05 day^{-1} each time the microalgae reach a stationary phase. 34

Figure 2.8: Effect of the nutrient and light limitations on the growth rate during the search for the optimal dilution rate and biomass algal concentration in the pond using the heuristic approach. The base case CO_2 gas and makeup water flowrates were used in this simulation. 35

Chart 2.1: Breakdown of the unit production cost for the base and optimized cases. 37

Figure 2.9: Algal biomass areal concentration in the open pond for the base case and the optimized case. .40

Figure 2.10: Optimal monthly operating profile for the dilution rate compared to the base case profile. 40

Figure 2.11: Optimal monthly operating profile for the CO_2 gas flowrate compared to the base case daily profile. 41

Figure 2.12: Optimal monthly operating profile for the makeup water flowrate compared to the base case daily profile. 41

Figure 2.13: Effect of the nutrient and light limitations on the growth rate for the optimized case. 42
Figure 2.14: Effect of the temperature limitation on the growth rate for the optimized case. 42
Figure 3.1: Schematic of the open pond and packed tower proposed configuration for the crude flue gas cooling and injection scenario. 47
Figure 3.2: Optimal monthly schedules for the CO_2 gas flowrate in the flue gas and pure gas (base case) scenarios. These are the flowrates at each of the two sump stations.....55
Figure 3.3: Optimal monthly schedules for the dilution rate in the flue gas and pure gas (base case) scenarios. 55
Figure 3.4: Optimal monthly schedule for the cooling water in the optimized flue gas injection scenario...56
Figure 3.5: Profile of the resulting flooding factor in the packed column during operation under the optimized flue gas injection scenario.....56
Figure 3.6: Difference between the CO_2 limitation on the growth rate in the flue gas and pure gas (base case) scenarios. 57
Chart 3.1: Breakdown of the unit production cost for the flue gas and pure gas (base case) scenarios. 57
Figure 4.1: Schematic of the open pond and shell and tube heat exchanger proposed configuration for the waste heat recovery coupling.....62
Figure 4.2: Effect of the temperature limitation on the growth rate for the base case (no-heating). 66
Figure 4.3: Heat gains and losses from the open pond surface for the base case (no-heating).....67
Figure 4.4: Comparing water and air temperatures in the base case (no-heating).....67
Figure 4.5: Difference between the temperature of the open pond water in the heating case and the base case (no-heating).....70
Figure 4.6: Difference between the temperature limitation on the growth rate between the heating case and the base case (no-heating).....70
Figure 4.7: Comparison between the growth rate of microalgae in the open pond for the heating case and the base case (no-heating).....71

Figure 4.8: Comparison between the heat losses through water thermal radiation for the heating case and the base case (no-heating). 71
Chart 4.1: Unit production cost breakdown for the heating case and the base case (no-heating). 72
Figure 4.9: Dilution rate profile for the heating case and the base case (no-heating). 73
Figure 4.10: Optimal monthly schedule for the hot flue gas flowrate. 73
Figure 4.11: Optimal monthly schedule for the splitting ratio (*S*). This fraction determines the amount of harvest water redirected to the heat exchanger for heating. 74
Figure 4.12: Algal biomass concentration in the open pond for the optimized case where culture heating is employed. 74
Figure 5.1: Map of Imperial County displaying the considered power plants locations (white font and black marker) and land availability: developed land (red), developed open-space (pink), agricultural (brown), and pasture land (yellow) [135], [136]. 82
Figure 5.2: Map of Imperial County displaying the geographic distribution of the considered wastewater treatment plants and CO_2 power plants [134], [135], [138]. 83
Figure 5.3: Daily evaporation losses from open surfaces in Imperial County. 89
Figure 5.4: Nitrogen requirement for sustaining the growth rate of microalgae for the optimized case presented in Chapter 2. 89
Figure 5.5: Necessary concentration of nitrogen in the makeup water calculated based on the profiles shown in Figures 5.3 and 5.4. 90
Figure 5.6: Map of Imperial County displaying the optimal solution for the supply chain optimization scenario. The optimal microalgae cultivation site is the Niland Gas Turbine Plant with treated wastewater received from Niland wastewater treatment plant. 94
Chart 5.1: Comparing breakdown of the unit production costs for cultivating microalgae at a power plant and at a wastewater treatment plant. 95
Figure 5.7: Limitation on the growth rate due to nitrogen deficiency in the optimal supply chain scenario. 95

CHAPTER 1

Introduction

1.1 Motivation

Climate change can have a strong impact on physical and biological systems [1]. Stricter environmental policies are continuously being imposed by the global community in efforts toward limiting global warming and avoiding its potential risks [2]. Human influence on climate change is mainly caused by the emissions of long-lived greenhouse gases (GHGs), which have increased by 70% between 1970 and 2004 [3]. The most important anthropogenic GHG is carbon dioxide (CO_2), which represented more than 75% of total anthropogenic GHG emissions in 2004 [4]. In 2013, global CO_2 emissions reached 35.3 billion tonnes [5]. Cutting greenhouse gas emissions towards achieving the targets pledged under the United Nations Framework Convention on Climate Change (UNFCCC) is a universal challenge [6]. The consumption of fossil fuels is the main source of global increase in CO_2 emissions [7]. In 2009 around 41% of the energy consumed globally was

based on petroleum [8]. This is stimulating a global interest in finding eco-friendly renewable alternatives to fossil fuels, thus ensuring environmental and energy sustainability.

A potential replacement for petroleum is biofuel, which can be integrated with the current fuel infrastructure. The most commonly produced biofuel is ethanol, which is made from a carbohydrate source such as cornstarch or sugarcane. Biodiesel is another widely used biofuel that can be produced from lipid-based oils such as rapeseed and soybean. Replacing 50% of all transportation fuels in the United States (US) with biofuels produced using corn or soybean as feedstock would require devoting 846% or 326% of the US existing cropping land, respectively [9]. Thus, relying on energy crops as feedstock for biofuels production could disrupt the food supply chain leading to a food crisis. To avoid the food vs. energy competition, using agricultural waste as an alternative feedstock for biofuels production is currently under consideration. Agricultural waste contains polysaccharides (cellulose and hemicellulose) surrounded by a matrix of lignin and hemicellulose [10]. The crosslinked structure of the lignocellulosic material traps the polysaccharides from enzymatic hydrolysis and microbial fermentation [11]. The costly biomass pretreatment necessary to make the polysaccharides accessible for the enzymes is one of the reasons why cellulosic ethanol production is not widely used.

The need for biofuels production at a commercial level has prompted reconsidering the production of biofuels using algal biomass, which was a hot research topic during the 1980's [12]. The great potential of algae lies in its high photosynthetic efficiency, achieving

biomass productivities that are orders of magnitude higher than productivities of other crops [13], [14]. Using algal oil for replacing 50% of all transportation fuels in the US will require devotion of only 2.5% of the US cropping land. Furthermore, the food supply chain would be entirely intact, because algae can flourish in non-arable land [15].

Moreover, carbon constitutes up to 50% of dry weight algal biomass (DW), hence, microalgae cultivation would assist in mitigating CO_2 as approximately 1.83 kg of CO_2 is required to produce each kg of DW [16]. A well-to-pump net CO_2 emissions of -20.9 kg per GJ of energy generated has been reported in a life cycle analysis study for an algal biodiesel process [17].

In addition to mitigating CO_2 and addressing the energy issue, improving algal technology economics would help addressing food sustainability issues as well. This is due to the fact that algal biomass is protein rich, of high nutritional value, and can be used as domestic animal feed [18], [19] or aquaculture feed [20]. This could substantially help in managing the predicted protein gap that might threat food supply for the growing world population [21]. Furthermore, algae do not require freshwater to proliferate; they can be cultivated using brackish or wastewaters that have few competing uses, and for some strains, even using saline water [22], [23]. Thus, an additional advantage of algae cultivation is wastewater treatment, because algae feed on nutrients contaminating water, e.g. nitrogen (N) and phosphorous (P), thus cleaning wastewater in an ecologically safe way [24], [25].

Microalgae are widely cultivated for a variety of products including food additives, pigments, antibiotics, and nutraceuticals [26]. However, the production cost remains too high for high-volume, low-value markets; for example, a conservative estimate for the cost of producing algae-based green diesel is around \$10 gal^{-1} [27]. However, the analysis also projects a potential cost range of \$3-5 gal^{-1} of green diesel considering the room for significant improvement in algal biotechnology [27]. Serious efforts have been invested in genetically engineering some algae strains to increase their rates of growth [28]. Additionally, several reactor configurations with improved mass transfer and enhanced utilization of sunlight were recently developed [29]. In parallel with advances in algal biotechnology, process systems engineering can play an important role in optimizing the economics of algae-based commodity products such as biofuels. Several optimization studies have appeared in the literature focusing on the design and synthesis of downstream processes for biofuels production and CO_2 mitigation using microalgae [30], [31]. Studies on bioreactor design and optimization based on computational fluid dynamics (CFD) modeling have been carried out as well [32].

1.2 Objectives and Approach

The economics of algae cultivation are highly sensitive to the productivity of microalgae and maintaining steady operation in outdoor cultivation at commercial scale is challenging, because varying weather conditions greatly affect the growth rate [27]. The identification of optimal operating conditions mitigating the impact of such environmental

factors can maximize the productivity of microalgae over a production cycle. Most of the studies on optimization of microalgae cultivation are based on trial-and-error and/or design heuristics [33]–[36]. Some model-based optimization studies have appeared focusing on laboratory algae growth systems without accounting for weather variations [37], [38].

The premise of this thesis is to develop a dynamic optimization framework for determining optimal operating conditions for improving outdoor algae production over a production period. Specifically in Chapter 2, a first principles model is developed for algae cultivation in outdoor open ponds considering the effect of daily varying local climatic conditions on algae growth. The model accounts for the effect of medium temperature, irradiance level, and nutrient availability on the growth of microalgae as well as the transfer of CO_2 from a CO_2 rich gas to the growth culture. Model validation against experimental results from the literature is then conducted. A dynamic optimization problem is formulated to determine the optimal dilution rate, makeup water flowrate and CO_2 gas flowrate monthly profiles that minimize the cost of producing microalgae in a representative location (Imperial County in California, USA) over the course of a year.

An important component of the economics of microalgae cultivation is the cost of CO_2 supply for providing the carbon necessary to grow the microalgae [16]. Many studies suggest the integration of microalgae cultivation with power production where the cost of CO_2 can be reduced through the sequestration of flue gases CO_2 [39]–[41]. Another vital operational challenge in outdoor microalgae cultivation is maintaining the temperature within the range favoring the growth of microalgae. Several studies in the literature suggest

utilizing waste heat from power plants in algal biomass production and preparation, namely culture heating, biomass dewatering and biomass drying [27], [42]–[44]. Another objective of this thesis is to assess the economic advantage of integrating outdoor cultivation of microalgae with nearby natural gas-fired power production for the supply of waste heat and CO_2.

In Chapter 3, heat exchanger models are developed to estimate the performance and operational costs of heat exchangers used for cooling the CO_2 gas and transferring the heat to the pond water. The derived dynamic process model for the outdoor production of algal biomass is used to predict the growth of microalgae under the aforementioned algae and power production coupling scenarios in Chapters 3 and 4. Furthermore, the dynamic optimization formulation developed in Chapter 2 is used to optimize the operations of the open pond and heat exchangers as well.

Cultivating microalgae using nutrients from waste sources could potentially reduce the algal biomass production cost by eliminating the need for fertilizers typically added to the culture to support the growth of microalgae. Growth inhibition due to the presence of metals was not detected when a strain of the algal species *Nannochloropsis Salina* was cultivated in treated municipal wastewater and diluted digester centrate [45]. Moreover, outdoor cultivation of microalgae in diluted anaerobic digestion effluent can be comparable to the use of commercial nutrients [46]. Therefore, another objective addressed in this thesis is the evaluation of the economic impact of utilizing municipal wastewater secondary effluent in microalgae cultivation. In Chapter 5, first the savings on nutrients and makeup

water costs are evaluated for an algae cultivation case using locally available treated wastewater. Since microalgae consume carbon more than any other nutrient, the cost of transporting wastewater from a nonlocal municipal wastewater treatment plant to a CO_2 rich source can be a serious drawback for the utilization of wastewater nutrients. Hence, a supply chain model is proposed and optimized to determine the optimal daily amounts of wastewater transported and the location of an algae facility coupled with municipal wastewater treatment. The model accounts for the transportation distances between the candidate locations and wastewater treatment plants in Imperial County as well as the nutrient content of the wastewater treatment plants effluents. Only sites with adequate land and CO_2 availability are considered as candidate locations.

1.3 Computational Tools and Packages

The mathematical models developed in this thesis are coded in gPROMS ModelBuilder v4.0 modeling platform installed on a 64-bit Windows 7 CPU equipped with an i7 processor at 3.4 GHz and 16 GB of RAM [47]. Physical properties are determined with Multiflash v4.3.25 using the Peng-Robinson equation of state [48].

Time integration of ordinary differential equations is performed using the DASOLV solver which is based on variable time step Backward Differentiation Formulae (BDF) [47]. This solver embeds the MA48 sub-solver which uses a direct LU-factorization algorithm to solve sets of linear algebraic equations. To increase numerical stability the default value of the “PivotStabilityFactor” was changed to 0.9, which is one of the setting

parameters of the MA48 sub-solver. To solve sets of nonlinear algebraic equations during initialization the DASOLV solver uses the BDNLSOL (Block Decomposition NonLinear SOLver) solver. Dynamic optimization runs are performed using the CVP_SS solver which implements a control vector parametrization algorithm based on the single-shooting method [47]. CVP_SS employs the DASOLV solver to perform integration of sets of differential-algebraic equations. For nonlinear programs, the CVP_SS solver uses the NLPSQP solver which is based on sequential quadratic programing (SQP) algorithm. For nonlinear programs involving discrete decision variables, the CVP_SS solver uses the OAERAP solver which employs an outer approximation method. The OAERAP solver relies on the NLPSQP solver as well.

CHAPTER 2

Growth of Microalgae in an Outdoor Open Pond*

2.1 Background

2.1.1 Autotrophic and Heterotrophic Microalgae

Microalgae, i.e. microscopic algae, are fresh/marine microorganisms that convert nutrients, using an energy source, to biomass consisting of carbohydrates, lipids, and proteins [26]. Microalgae that use sunlight as their energy source are called autotrophic microalgae. The class of microalgae that depends on other energy sources, such as glucose, is called heterotrophic microalgae [49]. Because of their reliance on sunlight, autotrophic microalgae can be cultivated during daytime only. On the other hand, heterotrophic

* Reprinted in part with permission from A. Malek, L. C. Zullo, and P. Daoutidis, "Modeling and Dynamic Optimization of Microalgae Cultivation in Outdoor Open Ponds," *Ind. Eng. Chem. Res.*, vol. 55, no. 12, pp. 3327–3337, 2016 [145]. Copyright © 2015 American Chemical Society.

microalgae can be cultivated continuously as long as essential nutrients and an energy source are supplied. Despite this advantage, supplying heterotrophic microalgae with an energy source incurs an additional cost impacting negatively the cultivation economics. As a result, research conducted on employing microalgae for commodity markets is more focused on autotrophic microalgae.

Carbohydrates and proteins created within microalgae are necessary for cell division, while lipids contribute to proliferation as an energy source during night [49]. Algal lipids are triglycerides composed of mainly (~80%) saturated and monounsaturated fatty acids that can be converted to biodiesel and green diesel [50]. The lipid content of microalgae varies from 1-85% of dry weight depending profoundly on strain and growth conditions. It has been found that growing algae under nutrient deficiency increases the lipid content [51]. Nitrogen deficiency demonstrates maximum effect on increasing the lipid content compared to silicon or phosphorus deficiency [50]. Although, increasing the lipid content is advantageous, growing algae under nutrient deficiency reduces biomass productivity. Therefore, the practice in batch (semi-continuous) mode cultivation is to accumulate lipids using nutrient deficiency after creating enough biomass under nutrient replete conditions [12]. In continuous-mode cultivation, the supply of nutrients is controlled based on targeting a balance between productivity and lipid accumulation.

2.1.2 Reactor Configurations

Autotrophic microalgae are conventionally cultivated in open ponds and photobioreactors, shown in Figure 2.1. Although, these cultivation systems are principally similar, their economics are entirely different. An open pond can be a raceway open to the atmosphere and made of concrete and lined with plastic or compacted clay. The algal culture in an open pond is continuously mixed using air bubbling or a paddle wheel to achieve better nutrient distribution and uniform cell exposure to sunlight. Usually, makeup water and nutrients are added in front of the paddle wheel to maximize mixing, while biomass is harvested prior to the paddle wheel. Dissolved CO_2 is supplied to open ponds by bubbling CO_2 gas throughout the culture using, for instance, countercurrent sumps located at the pond center. Since open ponds are open to the atmosphere, controlling the culture temperature and contamination from the surrounding environment are on-going challenges. Another disadvantage of using open ponds is the high rate of water evaporation from cultures to the atmosphere, requiring enormous amounts of water makeup, especially for large-scale production.

Photobioreactors have higher surface-to-volume ratio, achieving better exposure to sunlight and leading to increased (up to 13 times higher) biomass productivity compared to using open ponds [9]. However, this improvement in productivity is obtained at the expense of using costly transparent reactor materials, such as tubing. Moreover, dense algal cultures in photobioreactors generate dissolved oxygen in excessive concentrations, which inhibits photosynthesis and can cause photooxidative destruction of algae [52]. As a result,

using degassing vessels to prevent O_2 accumulation becomes necessary [53]. These huge capital costs in addition to cooling requirements make open ponds a more suitable candidate for developing algae based processes for commodity markets [27].

2.1.3 Harvesting of Algal Biomass

Microalgae form stable suspensions in water, because of their small size, low specific gravity, and negative surface charges [54]. Efficient harvesting technologies are lacking which adds another hurdle to the production process. Generally, the high moisture content of algal biomass (>99 wt%) is reduced in a primary harvesting step using for example sedimentation, or dissolved air flotation (DAF) [55]. Further thickening is done using sunlight drying or through a secondary harvesting step, concentrating algal biomass from 1.5% to 3% using for instance a belt filter press or a centrifuge [9], [56]. Separation and purification techniques employed would depend on the final product targeted. For example, recovering algal oil requires chemical/mechanical cell disruption and lysis, e.g. using high pressure homogenizers, before extracting the oil with butanol using liquid-liquid extraction [57]. Alternatively, algal oil can be extracted in a single step using hydrothermal liquefaction (HTL), which directly converts wet algal biomass into oil (bio-crude) through heating under pressure [58].

Figure 2.1: Open Ponds (left image) and photobioreactors (right image) [59], [60].

2.2 Process Description and Modeling

The economics of mass cultivation of microalgae are more favorable for the open pond system than the photobioreactor configurations; hence the entire analysis in this thesis is based on microalgae cultivation in an open pond [27], [61]. Several open pond modeling studies in the literature have adopted the concept proposed and validated in references [62], [63] where the hydrodynamics of an open pond are modeled by a cascade of continuous stirred-tank reactors (CSTRs) [64][65]. In this approach, an individual open pond is approximated as a series of *n* compartments where the content leaving the last compartment is recirculated to the first compartment as demonstrated in Figure 2.2. Assuming each compartment to be well-mixed, it can be modeled as a CSTR and the corresponding mass and energy balances can be constructed for the species considered in this model: microalgae, water and CO_2. Models for the growth of microalgae in open ponds can be found in references [63], [66], [67], whereas references [62], [63], [65]–[68] also

incorporate modeling of the CO_2 transfer. The microalgae growth kinetics formulation presented herein is based on the work in reference [67] and the CO_2 transfer modeling is adopted from reference [68].

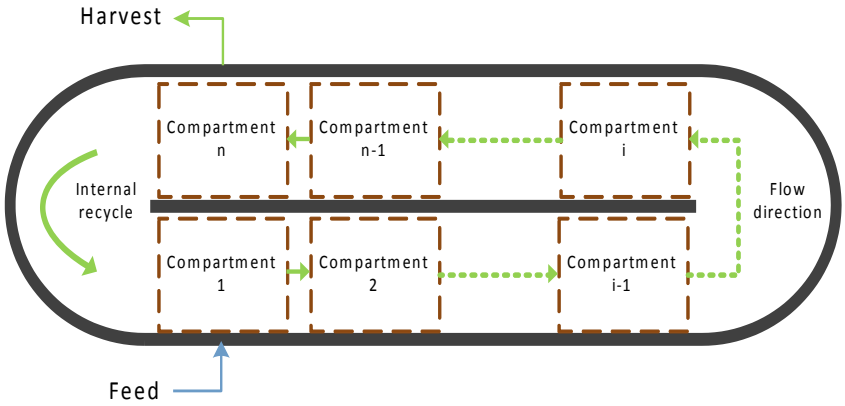

Figure 2.2: Approximation of the open pond model as a cascade of compartments.

2.2.1 Water Material and Energy Balances

In an insulated open pond, water enters through the pond feed (F_{feed}), or from precipitation, and leaves via evaporation (F_{evap}), harvest ($F_{harvest}$), or consumption by microalgae in photosynthesis. Typically algae are grown in geographic areas lacking rains, hence the amount of water added by precipitation is hereby neglected. Water consumed during photosynthesis is also negligible. For any CSTR in the pond, water flows in (F_{in}) from the preceding CSTR and flows out (F_{out}) to the succeeding CSTR in the direction of flow. Therefore, the depth of water (H) in an arbitrary CSTR in a segmented open pond can be found from

$$LW\frac{\mathrm{d}H_i}{\mathrm{d}t} = F_{\mathrm{in},i} - F_{\mathrm{out},i} - F_{\mathrm{evap},i} \tag{2.1}$$

where L is the length and W is the width of each CSTR, which are assumed constant and identical for all of the CSTRs. The following relations govern the flow within the pond between the i-th CSTR and the preceding CSTR

$$F_{\mathrm{in},i} = F_{\mathrm{out},i\text{-}1} = W H_{i\text{-}1} v \tag{2.2}$$

where v is the water velocity, and $i \in [1,n]$. The pond feed and harvest are taken into account by adding F_{feed} and subtracting F_{harvest} from eq 2.1 for the 1st and nth CSTRs, respectively. The dilution rate (D) dictates the rate of algal biomass harvest

$$F_{\mathrm{harvest}} = D L W \sum_{i=1}^{n} H_i \tag{2.3}$$

To compensate for evaporation losses, after harvesting the algal biomass the water is combined with makeup water (F_{makeup}) and recycled back to the pond as F_{feed} as shown in Figure 2.3. Regardless of the microalgae type, i.e. freshwater vs. marine, only freshwater is considered for F_{makeup}, because even for a seawater pond to maintain the salinity at the desired level freshwater has to be added. Water blowdown for preserving culture quality is neglected. The amount of water evaporating from each CSTR is calculated accordingly

$$F_{\mathrm{evap},i} = \frac{L W E_{\mathrm{v},i}}{\rho L_{\mathrm{e},i}} \tag{2.4}$$

where ρ is the water density. The latent heat flux (E_{v}), according to Dalton's Law, and the latent heat of evaporation (L_{e}) are given by

$$E_{\mathrm{v},i} = \left(19.0 + 0.95\ U^2\right)\left(P_{\mathrm{sat},i} - P_{\mathrm{air}}\right) \tag{2.5}$$

$$L_{\mathrm{e},i} = 597.3\ -\ 0.57\ T_{\mathrm{w},i} \tag{2.6}$$

where U is the wind speed above the pond water and Tw is the water temperature [69]. The saturation vapor pressure at the water temperature (P_{sat}), and the vapor pressure in the overlaying air (P_{air}) are computed using Antoine's equation.

The temperature of the water greatly affects the growth rate of algae. Hence, an energy balance for water is derived to track the water temperature in each compartment

$$LW\,\rho\,c_{\mathrm{p}}\,\frac{\mathrm{d}}{\mathrm{d}t}\left(H_i T_{\mathrm{w},i}\right) = \rho\,c_{\mathrm{p}}\left(F_{\mathrm{in},i}T_{\mathrm{w},i-1} - F_{\mathrm{out},i}T_{\mathrm{w},i}\right) + LW\,E_i \tag{2.7}$$

where c_{p} is the specific heat capacity of water. The term E represents the heat exchanged through the water surface of each compartment. It accounts for the heat addition from the absorbed solar irradiance (E_{s}) and atmospheric long-wave (E_{a}), and the heat loss due to evaporation (E_{v}), water long-wave (E_{w}), and conduction to atmosphere (E_{c}). These terms are calculated based on the model developed in reference [69]

$$E_{\mathrm{a}} = \sigma\left(T_{\mathrm{air}} + 273\right)^4\left(\alpha_1 + 0.031\sqrt{P_{\mathrm{air}}}\right)\left(1 - \alpha_5\right) \tag{2.8}$$

$$E_{\mathrm{w},i} = \varepsilon\,\sigma\left(T_{\mathrm{w},i} + 273\right)^4 \tag{2.9}$$

$$E_{\mathrm{c},i} = \alpha_2\left(19 + 0.95U^2\right)\left(T_{\mathrm{w},i} - T_{\mathrm{air}}\right) \tag{2.10}$$

$$E_{\mathrm{s}} = \alpha_3\,I_{\mathrm{a}} \tag{2.11}$$

where I_{a} is the daily average solar irradiance at the pond surface and T_{air} is the air

temperature. The other parameters are defined in Table 2.1 including their assigned values as well as values for the mass balance parameters.

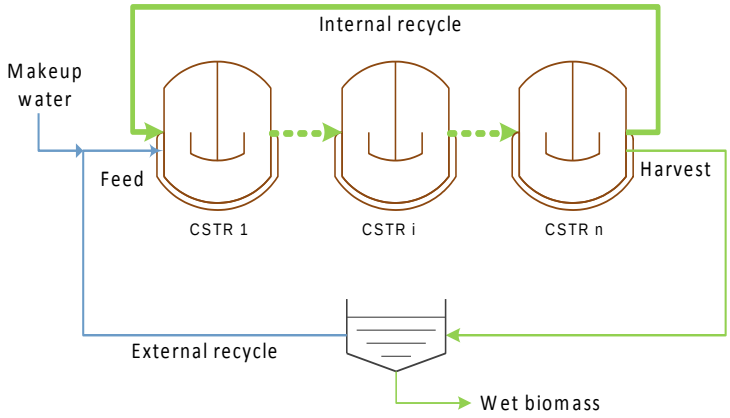

Figure 2.3: Modeling the open pond as a cascade of continuous stirred-tank reactors (CSTRs) with an internal and an external recycle stream.

Table 2.1: Parameter definitions and values for the mass and energy balances [69]–[71].

Parameter	Description	Value
v	water velocity in the open pond (cm s^{-1})	25
ρ	density of water (g cm^{-3})	1.0
c_p	specific heat of water (cal K^{-1} g^{-1})	1.0
σ	Stefan-Boltzmann constant (cal cm^{-2} d^{-1} K^{-4})	11.7×10^{-8}
ε	water emissivity	0.97
α_1	atmospheric attenuation coefficient	0.6
α_2	Bowen's coefficient (mmHg $^oC^{-1}$)	0.47
α_3	radiation absorption factor	0.9
α_5	reflection coefficient	0.03

2.2.2 Microalgae Mass Balance and Growth Kinetics

In the absence of algae grazers, the concentration of algae in the pond (C_{algae}) would depend on the growth rate (μ), the harvest rate and the rate of algal biomass deterioration due to respiration and other basal metabolism processes (B)

$$LW\frac{\mathrm{d}}{\mathrm{d}t}\left(H_i\,C_{\text{algae},i}\right)=F_{\text{in},i}\,C_{\text{algae},i\text{-}1}-F_{\text{out},i}\,C_{\text{algae},i}+\left(\mu_i-B_i\right)LW\,H_i\,C_{\text{algae},i} \tag{2.12}$$

After harvesting the algal biomass, the water is recycled back to the pond and the concentration of algae in the feed is given by

$$C_{\text{algae}_{\text{feed}}}=\left(1-H_{\text{eff}}\right)C_{\text{algae},n}\,\frac{F_{\text{harvest}}}{F_{\text{feed}}} \tag{2.13}$$

where H_{eff} is the harvest efficiency which is around 95% for harvest of algal biomass [72]. The areal productivity of the system (Pr) is often used as an evaluation criterion and could be defined as

$$Pr=H_{\text{eff}}\,\frac{D}{n}\sum_{i=1}^{n}H_i\,C_{\text{algae},i} \tag{2.14}$$

The basal metabolism rate increases exponentially with the water temperature

$$B_i=B_{\text{m}}\,e^{k_{\text{B}}\left(T_{\text{w},i}-T_{\text{B}}\right)} \tag{2.15}$$

where B_{m} is the metabolic rate at a reference temperature (T_{B}), and k_{B} is a fitting constant [67]. Factors affecting the growth rate of algae considered in the model are the temperature of the culture, the irradiance level, and the nutrient concentrations. The maximum algae

growth rate (μ_{max}) is achieved when those factors are at their optimal levels, otherwise the actual growth rate depends on the deviations from these levels as

$$\mu_i = \mu_{\max} \, f_{\text{Nutrient},i} \, f_{\text{T},i} \left\langle f_{\text{I},i} \right\rangle_{\text{average}} \tag{2.16}$$

where f_{Nutrient}, f_{T}, and f_{I}, are the attenuation factors for nutrient, temperature and light limitations, respectively [67]. Most of these factors are species-specific, and so their detailed forms depend on the particular algae strain in study.

The marine alga *Nannochloropsis Salina (N. Salina)* chosen for this study is a promising species for algal biofuels production because of its high lipid content and robustness in outdoor cultivation [73]. Since there are limited studies on outdoor cultivation of *N. Salina* in open ponds, the mass and energy balances in the model are validated using data from the literature for the protein rich freshwater *Spirulina* which is widely cultivated outdoors at commercial scale for food-grade products [74]. Microalgae proliferate within a certain range around an optimal temperature and growth stops completely away from such range of temperature. The term f_{T} can be estimated using the following exponential relation

$$f_{\text{T},i} = \begin{cases} e^{-k_{\text{T},1}\left(T_{\text{w},i} - T_{\text{opt}}\right)^2}, & T_{\text{w},i} > T_{\text{opt}} \\ e^{-k_{\text{T},2}\left(T_{\text{opt}} - T_{\text{w},i}\right)^2}, & T_{\text{w},i} \le T_{\text{opt}} \end{cases} \tag{2.17}$$

where T_{opt} is the optimal temperature for algae growth and $k_{\text{T},1}$, and $k_{\text{T},2}$ are fitting constants [67]. The optimal temperature for *Spirulina* is within the range of 24-42 ^{o}C depending on the particular strain of *Spirulina*, and for *N. Salina* it is around 28 ^{o}C [72]–[75].[28,31]

Autotrophic microalgae drive photosynthesis by the energy from light photons and due to the shading effect the microalgae closer to the pond surface are exposed to higher light intensities, hence, the mean value of f_{I} is considered

$$\left\langle f_{\mathrm{I},i} \right\rangle_{\text{average}} = \frac{1}{H_i} \int_0^{H_i} \left(\frac{1}{t_{\mathrm{p}}} \int_0^{\beta\, t_{\mathrm{p}}} f_{\mathrm{I},i}\, dt \right) dz \tag{2.18}$$

where β is the fractional length of a day having daylight (photoperiod), t_{p} is the length of a day and z is the vertical distance from the water surface. Since autotrophic microalgae do not grow at night, this time integral is formulated to generate an average over the daylight hours; using a daily average instead would lead to overestimation of the growth rate. Various formulas have been developed in the literature [76] for modeling f_{I} and the model proposed in reference [77] fits the experimental data presented in reference [78] for *N. Salina*

$$f_{\mathrm{I},i} = 1 - e^{-\frac{I_i}{I_{\max}}} \tag{2.19}$$

where I is the photosynthetically active radiation (PAR) experienced by the microalgae and $I_{\max}$ is the maximum radiance above which algae growth does not increase any further. However, for some microalgae strains, including *Spirulina*, exceeding $I_{\max}$ actually damages the photosynthetic reaction, known as the photoinhibition effect. This phenomenon is captured in the relation proposed by Steele [79]

$$f_{\mathrm{I},i} = \frac{I_i}{I_{\max}} e^{1-\frac{I_i}{I_{\max}}} \tag{2.20}$$

The Beer-Lambert law is commonly used to model I as corrected for the attenuating effect of the growth culture

$$I_i = \alpha_3 \alpha_4 \frac{I_a}{\beta} e^{-k_{e,i} z} \tag{2.21}$$

where α_4 is a factor for converting from total radiation to PAR. The extinction coefficient (k_e) is related to the water/background turbidity (k_w) and the concentration of algae in the pond

$$k_{e,i} = k_w + .0088 C_{\mathrm{algae},i} R_{\mathrm{Chl}} + .054 \left(C_{\mathrm{algae},i} R_{\mathrm{Chl}} \right)^{2/3} \tag{2.22}$$

where R_{Chl} is the chlorophyll content of the algal biomass [80].

There are at least 30 chemical elements required for growing microalgae of which the most important ones, i.e. usually the growth limiting ones, are nitrogen (N), phosphorus (P), and carbon [81]. However, for the purpose of determining f_{Nutrient} in this chapter, only carbon is considered, as N and P losses from the culture are minimal compared to carbon losses through CO_2 degassing; N and P can be maintained at adequate levels by fertilizers' addition [82]. Assuming that all nutrients are abundant except for carbon, a Monod type equation modified for the inhibitory effect of oversupply of CO_2 can be used to estimate f_{Nutrient}

$$f_{\text{Nutrient},i} = \frac{C_{\text{CO}_2,i}}{K_{\text{C}} + C_{\text{CO}_2,i} + \dfrac{C_{\text{CO}_2,i}^2}{K_{\text{s}}}} \tag{2.23}$$

where K_C and K_s are the half saturation and inhibition constants for CO_2, respectively [68]. Autotrophic microalgae acquire carbon by consuming dissolved CO_2 supplied artificially and/or from diffusion of atmospheric CO_2, hence the balance for the CO_2 in the pond water (C_{CO_2}) is

$$\begin{aligned}\frac{\mathrm{d}}{\mathrm{d}t}\left(H_i C_{\text{CO}_2,i}\right) = {} & \frac{\left(F_{\text{in}} C_{\text{CO}_2,i\text{-}1} - F_{\text{out}} C_{\text{CO}_2,i} + G_i\right)}{LW} \\ & -\left(\mu_i - B_i\right) H_i R_{\text{CO}_2} C_{\text{algae},i} - K_{\text{atm}}\left(C_{\text{CO}_2,i} - C_{\text{CO}_2,\text{atm}}\right)\end{aligned} \tag{2.24}$$

where R_{CO_2} is the CO_2 requirement and G is the rate of CO_2 supplementation by bubbling CO_2 rich gas into the pond water. The mass transfer coefficient K_{atm} regulates the diffusion of CO_2 to/from the atmosphere as driven by the difference between C_{CO_2} and the equilibrium concentration of atmospheric CO_2 in water ($C_{CO_2,atm}$).

2.2.3 CO_2 Sump Stations

Sump stations located at the pond middle are used for bubbling CO_2 gas into the growth culture in a concurrent or countercurrent arrangement. Modeling the CO_2 transfer from the gas bubbles to the pond water in a sump station allows analyzing the effect of bubbling rate on algae growth which is useful for the optimization problem. For a given CO_2 mole fraction in the inlet gas (y_{in}), the term G can be calculated from determining the CO_2 mole fraction in the outgassing bubbles (y_{out})

$$G_i = \frac{P_g Q_{g,i}}{R_g T_g}\left(y_{in} - y_{out,i}\right) \tag{2.25}$$

where R_g is the universal gas constant, and the gas flowrate (Q_g), temperature (T_g), and pressure (P_g) are assumed constant throughout the entire water column. Assuming plug flow for the gas phase, y_{out} is estimated based on the model derived in reference [68]

$$y_{out,i} = \frac{R_g T_g}{P_g} H_e \left(C_{CO_2,i} + \left[\frac{y_{in} P_g}{H_e R_g T_g} - C_{CO_2,i} \right] e^{\frac{-K_L a_i \left(1-\varepsilon_{g,i}\right) W H_i W_s}{Q_{g,i} H_e}} \right) \tag{2.26}$$

where H_e is the dimensionless Henry's constant, K_L is the mass transfer coefficient for the CO_2 transfer from the gas phase to the liquid phase, W_s is the width of the sump station and ε_g is the gas hold up. For countercurrent flow, the gas bubbles' total interfacial area (a) can be approximated from

$$a_i = \pi d_b^2 \frac{N_{o,i}}{W_s W (v_b - v)} \tag{2.27}$$

where d_b is the bubble diameter, and v_b is the gas bubble terminal velocity [68]. According to reference [83], the number of bubbles of gas formed at the sump bottom (N_o) is

$$N_{o,i} = \frac{Q_{g,i}}{\pi \frac{d_b^3}{6} (1 - \varepsilon_{g,i})} \tag{2.28}$$

The gas hold up is determined from the volume ratio of gas in the sump

$$\varepsilon_{g,i} = \frac{\alpha_6 Q_{g,i}}{\alpha_6 Q_{g,i} + v W_s W} \tag{2.29}$$

where α_6 is a correction factor for the compression of gas under water [84].

2.3 Process Economics

The algal biomass unit production cost (*UPC*), a criterion to evaluate different scenarios in this thesis, is defined in this chapter as

$$UPC = \frac{CC_{\text{Pond}} + \sum_{t=1}^{T_c} (cost_{\text{Nutrients},t} + cost_{\text{CO2},t} + cost_{\text{water},t} + cost_{\text{energy},t})}{\sum_{t=1}^{T_c} harvest_t} \tag{2.30}$$

where t is an integer denoting the number of the day starting from the beginning of the production cycle, T_c is the length of the time horizon and CC_{Pond} is the amortized capital cost of the open pond system. The daily amount of algal biomass harvested, cost of nutrients, cost of CO_2, cost of water, and cost of energy are calculated by

$$harvest_t = H_{\text{eff}}\, C_{\text{algae},n,t}\, F_{\text{harvest},t} \tag{2.31}$$

$$cost_{\text{Nutrients},t} = harvest_t (x_{\text{NH}_3} R_{\text{N}} R_{\text{NH}_3} + x_{\text{DAP}} R_{\text{P}} R_{\text{DAP}}) \tag{2.32}$$

$$cost_{\text{CO2},t} = x_{\text{CO}_2}\, \rho_{\text{CO}_2} \sum_{i=1}^{n} Q_{\text{g},i,t} \tag{2.33}$$

$$cost_{\text{water},t} = x_{\text{w}}\, F_{\text{makeup},t} \tag{2.34}$$

$$cost_{\text{energy},t} = x_{\text{e}}\, E_{\text{mixing},t} \tag{2.35}$$

where x_{NH_3}, x_{DAP}, x_{CO_2}, x_{w}, and x_{e} are the prices of ammonia, diammonium phosphate, CO_2, freshwater and electricity, respectively. The terms R_{N} and R_{P} are the nitrogen and phosphorus contents of the algal biomass and the terms R_{NH_3} and R_{DAP} are the nitrogen content of ammonia and the phosphorus content of diammonium phosphate, respectively.

The CO_2 gas density (ρ_{CO_2}) is calculated using the ideal gas law. The daily energy requirement for mixing the open pond water using a paddle wheel (E_{mixing}) is given by

$$E_{\text{mixing}} = \frac{\alpha_8 \alpha_9 \rho \left(h_{\text{friction}} + \sum h_{\text{bend}} \right) v W \sum_{i=1}^{n} H_i}{n M_{\text{eff}}} \tag{2.36}$$

where M_{eff} is the efficiency of the mixing system, α_8 is a unit conversion factor, and α_9 is the number of hours the paddle wheel is running daily [70]. From the Gauckler-Manning formula for open channel flow one can calculate the head losses from friction of the pond bottom (h_{friction}) and flow around each bend (h_{bend})

$$h_{\text{friction}} = v^2 n_o^2 \frac{n L}{r^{4/3}} \tag{2.37}$$

$$h_{\text{bend}} = \frac{3 \alpha_7 v^2}{g} \tag{2.38}$$

where n_o is a roughness factor also known as the Gauckler-Manning coefficient, r is the channel hydraulic radius, α_7 is the kinetic loss coefficient and g is the acceleration of gravity [85].

2.4 Model Validation

2.4.1 Experimental Setup and Model Assumptions

Spirulina was cultivated in a 450 m^2 outdoor open pond for 10 months in Málaga, Spain [86], [87]. The experiment resembles a scenario for commercial scale algal biomass production, especially given the prolonged cultivation period and varying environmental

conditions. Therefore, the water temperature, biomass areal concentration, and productivity profiles reported in references [86], [87] were used to validate the ones predicted by the developed model.

In the experiment, the depth of water was maintained at 30 cm and the growth culture was prepared with modified Zarrouk's Medium providing adequate nutrient levels [86]. Moreover, the pond was inoculated with a concentration of 15 g DW m^{-2} and harvest was started after 13 days and only interrupted during February due to heavy rains [87]. The corresponding model assumptions and parameters are: (1) the open pond was discretized into n = 18 compartments each having a length and width of $L = W$ = 5 m; (2) the makeup water flowrate was set to match the evaporation losses to fix the depth at H = 0.3 m; (3) the nutrient concentrations were at their optimal values, therefore eq 2.23 was set to $f_{\text{Nutrient},i}$ = 1 and eqs 2.24-2.29 were excluded; (4) after the inoculation period (13 days), the dilution rate was set to an estimate D = 0.10 day^{-1} based on reference [88] except for 17 days during February where there was no harvest.

The initial conditions and values assigned to the kinetic parameters for *Spirulina* growth are shown in Table 2.2. Figure 2.4 shows the solar radiation and air temperature data for the period of the experiment at Málaga, which were obtained from the European Database of Daylight and Solar Radiation [89] and the Tutiempo Network [90], respectively. These data, including the data for the humidity, wind speed, and photoperiod, were used in the simulation of the model consisting of eqs 2.1-2.18 and 2.20-2.23.

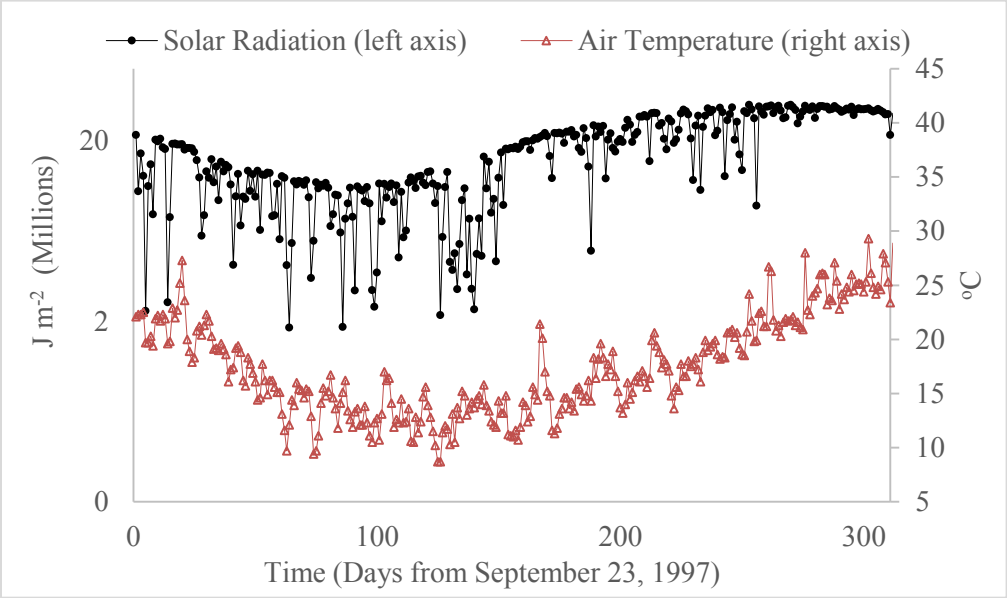

Figure 2.4: Daily global solar radiation and average air temperature at Málaga from September 23, 1997 to July 31, 1998 [89], [90].

Table 2.2: Parameter definitions and values for the microalgae growth kinetics model.

Parameter	**Description**	**Value**	
B_m	metabolic rate at reference temperature (day^{-1})	0.04 [67]	
T_B	reference temperature for metabolic rate (^oC)	20 [67]	
k_B	metabolic rate exponential fitting constant ($^oC^{-1}$)	0.069 [67]	
B	fractional length of a day having daylight	0.5	
t_p	length of a day (h)	24	
k_w	water (background) turbidity (m^{-1})	0.3 [69]	
α_4	coefficient for photosynthetically active radiation	2.05 [91]	
	Species-specific parameters	*Spirulina*	*N. Salina*
μ_{max}	maximum algae growth rate (day^{-1})	1.4 [92]	1.3 [78]
T_{opt}	optimal temperature for algae growth (^oC)	27.5 [67]	27 [93]
$k_{T,1}$	temperature limitation fitting constant ($^oC^{-2}$)	0.005 [67]	0.01 [93]
$k_{T,2}$	temperature limitation fitting constant ($^oC^{-2}$)	0.004 [67]	0.03 [93]
I_{max}	maximum irradiance for algal growth ($\mu E\ m^{-2}\ s^{-1}$)	200 [94]	58 [78]
R_{Chl}	chlorophyll content of microalgae (g Chl g^{-1} DW)	.007 [86]	.017 [95]
	Initial conditions	*Spirulina*	*N. Salina*
H	depth of water in a CSTR in the open pond (m)	0.3	0.3
T_w	temperature of the water in the CSTR (^oC)	22.1 *	12.4 *
C_{algae}	microalgae concentration in culture (g DW m^{-3})	15	45
C_{CO_2}	molar concentration of CO_2 in the pond (mol m^{-3})	-	0.02 *

* assumed in equilibrium with the ambient environment.

2.4.2 Simulation Results

The predicted water temperature profile shown in Figure 2.5 is slightly lower than the one determined experimentally which is due to the fact that the air temperature data used herein are marginally lower than the measurements at the experiment [86], [87]. As a result, the growth was inhibited in the winter, but advanced in the summer and consequently the areal concentration profile was slightly altered. However, as shown in Figure 2.6 the predicted productivity is in good agreement with the experimentally determined productivity with a mean percent error of 16.3%, which demonstrates the adequacy of the proposed model.

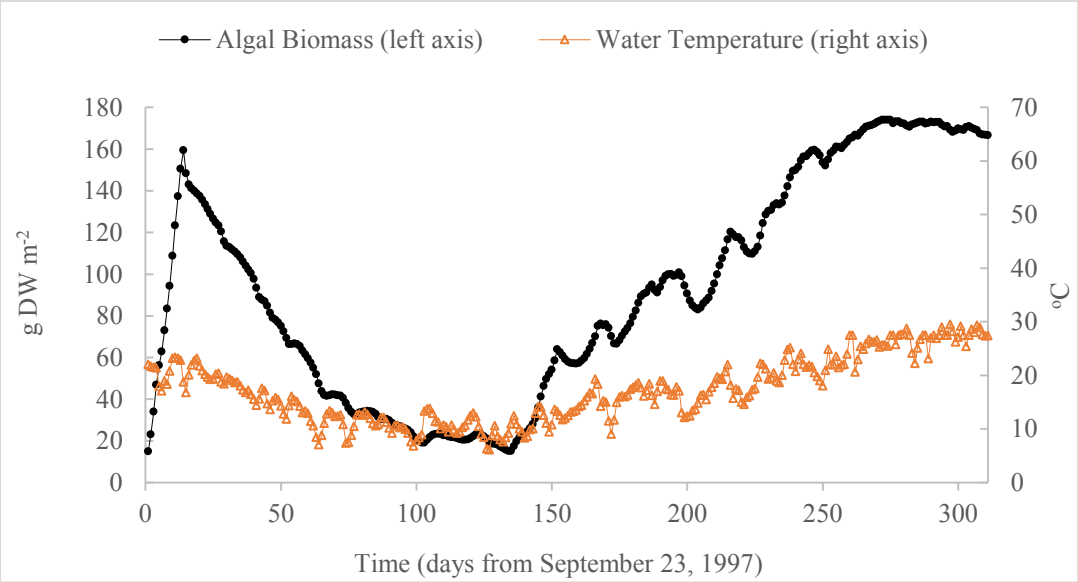

Figure 2.5: Simulation results for Spirulina cultivation in Málaga, Spain from September 1997 to July 1998: Algal biomass areal concentration and temperature of the pond water.

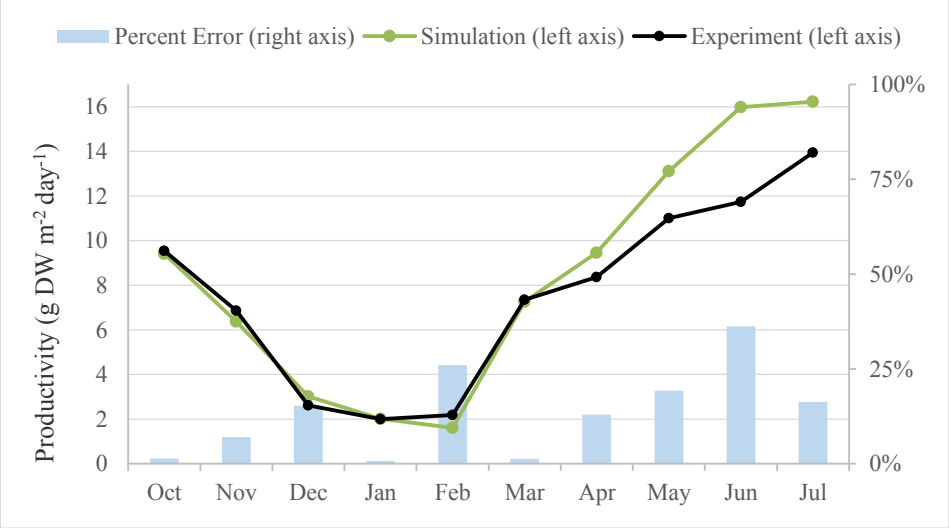

Figure 2.6: Comparison between monthly-averaged values of the predicted productivity and the productivity determined experimentally in reference [87].

2.5 Dynamic Optimization

2.5.1 Problem Definition

Imperial County in California is one of the suitable places for cultivating *N. Salina* in USA owing to the warmer weather and availability of resources including land, water and CO_2 [70]. This site was selected for the optimization case study and the daily weather conditions in a typical meteorological year for this site shown in the Appendix were obtained from the National Solar Radiation Data Base [96]. The 4 ha open pond proposed in reference [70] for the production of algal biofuels at commercial scale was adopted herein. Therefore, the pond was discretized into 44 compartments with $L = W = 30$ m and the CO_2 gas was set to be introduced at the bottom of the 12th and 34th compartments. Drying of the wet algal biomass is to be accomplished by spreading a shallow layer of the

harvested algal suspension over a bed lined with low-density polyethylene [70]. The cost of the cultivation system, including the land, open pond, sump stations, water transfer system, and drying beds, amortized for 20 years is estimated at CC_{Pond} = \$17,888 [70]. The parameter values selected for the growth kinetics of *N. Salina* are shown in Table 2.2. The values assigned to the parameters of modeling the CO_2 transfer and process economics are shown in Tables 2.3 and 2.4, respectively. For a production cycle of one year the program, comprising eqs 2.1-2.19 and 2.21-2.38, contains 1044 variables, and 1883 parameters.

Table 2.3: Values assigned to the parameters of the CO_2 mass balance and transfer model.

Parameter	Description	Value
K_C	half saturation constant for CO_2 (mol CO_2 m^{-3})	9×10^{-4} [68]
K_s	inhibition constant for CO_2 (mol CO_2 m^{-3})	180 [68]
$C_{CO_2,atm}$	equilibrium concentration of atmospheric CO_2 in water (mol m^{-3})	0.02
R_{CO_2}	CO_2 requirement per unit of algae (mol CO_2 g^{-1} DW)	0.042 [97]
v_b	CO_2 gas bubble terminal velocity (cm s^{-1})	30 assumed
T_g	temperature of CO_2 gas (°C)	316 [70]
P_g	pressure of CO_2 gas (atm)	1.2 [70]
y_{in}	mole fraction of CO_2 in the bubbling gas at inlet	1.0
R_g	universal gas constant (atm m^3 mol^{-1} K^{-1})	8.2×10^{-5}
H_e	dimensionless Henry's constant	0.8317
W_s	width of the CO_2 gas sump station (m)	0.3 [70]
d_b	diameter of CO_2 gas bubble (mm)	2 [102]
α_6	Coefficient for gas compression under water depth of 30 cm	0.96 [84]
K_{atm}	mass transfer coefficient for diffusion of CO_2 to/from atmosphere (m day^{-1})	2.4 [16]
K_L	mass transfer coefficient for CO_2 transfer from gas bubbles to water (m day^{-1})	9.59 [100]

Table 2.4: Parameter definitions and values for the process economics model.

Parameter	Description	Value
x_w	price of agricultural water (\$ m^{-3})	0.016 [101]
x_e	price of electricity (\$ kWh^{-1})	0.04 [102]
x_{NH_3}	price of ammonia (\$ $tonne^{-1}$)	934 [103]
R_N	nitrogen content of algal biomass (g N g^{-1} DW)	0.05 [104]
x_{DAP}	price of diammonium phosphate (\$ $tonne^{-1}$)	706 [103]
R_P	phosphorus content of algal biomass (g P g^{-1} DW)	0.0071 [104]
x_{CO_2}	price of pure CO_2 gas (\$ $tonne^{-1}$)	40 [105]
M_{eff}	efficiency of the paddle wheel mixing system	40% assumed
n_o	Gauckler-Manning coefficient	2.08×10^{-7} [70]
r	channel hydraulic radius	0.29 [70]
α_7	kinetic loss coefficient	2 [70]

2.5.2 Major Operating Parameters

This section addresses the current practice for the major operating parameters as suggested in the literature for commercial scale cultivation in continuous-mode. The considered parameters are the dilution rate (D), the CO_2 gas flowrate and the makeup water flowrate.

2.5.2.1 Dilution rate

The dilution rate is one of the main operating parameters affecting the productivity of an algal system. A low D creates a dense culture where light availability becomes limited due to the shading effect. This reduces the growth rate of microalgae and consequently leads to a lower productivity. On the other hand, a high D would reduce the concentration

of microalgae in the pond also resulting in a lower productivity. Moreover, in an extremely sunny day this could be damaging to the growth rate for a microalga that experiences photoinhibition which would lead to an even lower productivity. Therefore, local climatic conditions have to be considered when searching for the optimal *D*.

The dilution rate for the base case scenario is determined by employing the empirical harvest scheme proposed in reference [88]. It starts by holding off harvest and allowing the algae to grow until the stationary phase of growth is reached, followed by ramping up *D* in steps of 0.05 day^{-1} as demonstrated in Figure 2.7. Each time the concentration of algae in the pond is stabilized for several days the dilution rate is increased and the optimum is the one yielding the maximum algae productivity. The next step is to determine the algal biomass areal concentration, which when reached after inoculation, harvest at the identified *D* should commence. The productivity profile shown in Figure 2.7 is consistent with the experimental results reported in reference [88]; note that the highest productivity was achieved when *D* is 0.10 day^{-1}, which is the same conclusion reached in reference [88]. From Figure 2.8, it was observed that the growth rate is mostly inhibited by the limited availability of sunlight and this limitation is higher for sunnier days. Considering that *N. Salina* does not experience photoinhibition, this could only mean that the shading effect of the high algal biomass concentration is the main factor responsible for limiting the productivity of the system. Comparing Figures 2.7 and 2.8, it was noticed that the light limitation improves when the areal concentration is less than 35 g DW m^{-2}; hence this could be the optimal areal concentration. An alternative to finding a single

dilution rate is to aim for the optimal areal concentration and adjust the dilution rate accordingly [88]. However, in outdoor cultivation the optimal areal concentration is a function of the uncontrolled environmental conditions, therefore, the dilution rate profile needs to be determined using dynamic optimization.

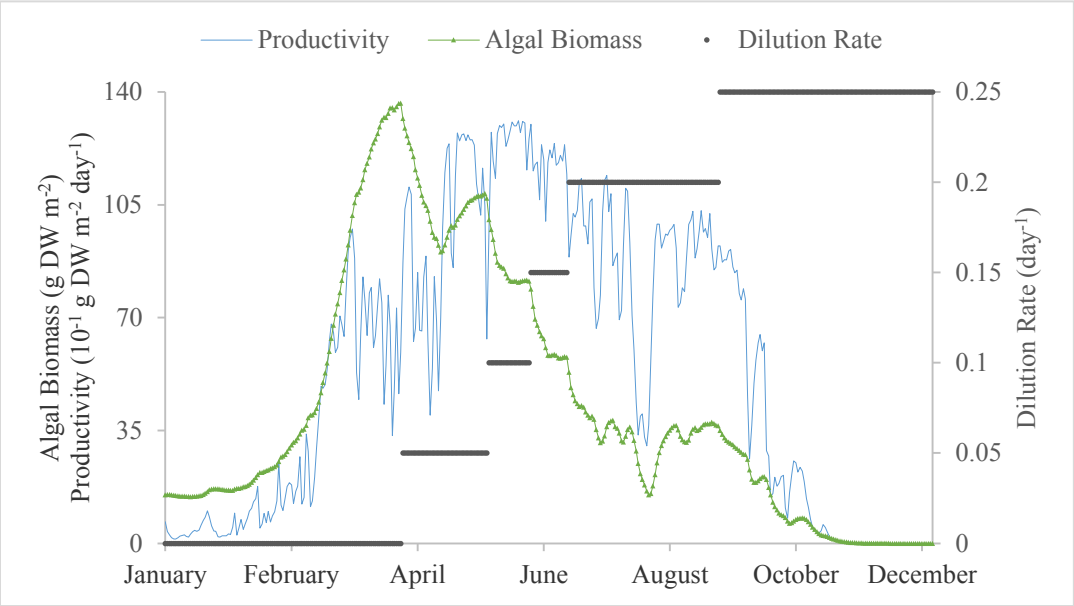

Figure 2.7: Demonstration of the heuristic approach for finding the optimal dilution rate. The dilution rate is increased in steps of 0.05 day^{-1} each time the microalgae reach a stationary phase.

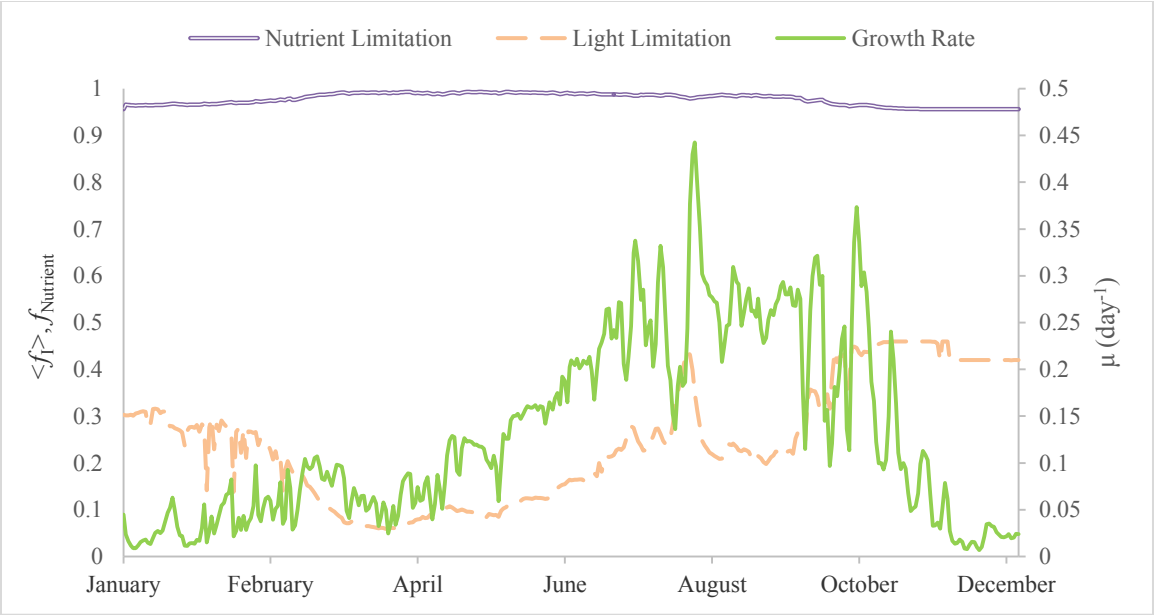

Figure 2.8: Effect of the nutrient and light limitations on the growth rate during the search for the optimal dilution rate and biomass algal concentration in the pond using the heuristic approach. The base case CO_2 gas and makeup water flowrates were used in this simulation.

2.5.2.2 CO_2 gas flowrate

Another important operating parameter is the rate of bubbling of the CO_2 gas (Q_g) into the pond culture. Increasing Q_g provides more dissolved CO_2 to the growth culture, but it increases the loss of CO_2 through degassing as well, and CO_2 is a costly feedstock. Typically, the CO_2 gas is added to the growth medium on-demand serving as a pH regulator targeting a value within the range of 7-8 to maximize the CO_2 utilization [88], [104]. According to [106], the optimal pH for growing *N. Salina* is between 8 and 9, and hence, using buffers to separate the CO_2 supply from the pH regulation is recommended for

achieving better growth rates and eliminating algae competitors including other microalgae species, grazers, and bacteria. Furthermore, this would also allow optimizing the CO_2 supply focusing on providing enough CO_2 to prevent any nutrient limitation by carbon deficiency while minimizing atmospheric losses. Alternatively, the pH of the growth medium could be adjusted by fertilizing with monopotassium phosphate as a substitute to diammonium phosphate, as the potassium content greatly affects the algal culture pH [37].

2.5.2.3 Makeup water flowrate

The operating depth of water in the pond, controlled by F_{makeup}, influences the system productivity and economics through affecting the light penetration, CO_2 absorption and mixing energy requirement. The depth of culture is usually maintained at a certain level within 20-40 cm [16], [70].

2.5.3 Base Case

The base case was simulated starting with no harvest followed by $D = 0.10$ day^{-1} once the concentration exceeded 50 g DW m^{-2}. The CO_2 gas flowrate was set based on the rate of CO_2 uptake from the growth medium. The makeup water flowrate was set to the level that compensates for evaporation losses. The simulation took 39 seconds to generate the results shown as the blue line in Figures 2.9-2.12. Using the unoptimized operating parameters it would cost \$758 tonne^{-1} to produce 40 tonne of DW year^{-1}. Chart 2.1 shows that the cost of the CO_2 gas constitutes 16% of the base case *UPC*, which is around 40% of the operating cost which means there is potential in optimizing the CO_2 supply. Also,

although the cost of makeup water compared to the other cost components is insignificant as Chart 2.1 shows, optimizing the makeup water flowrate would affect the CO_2 absorption.

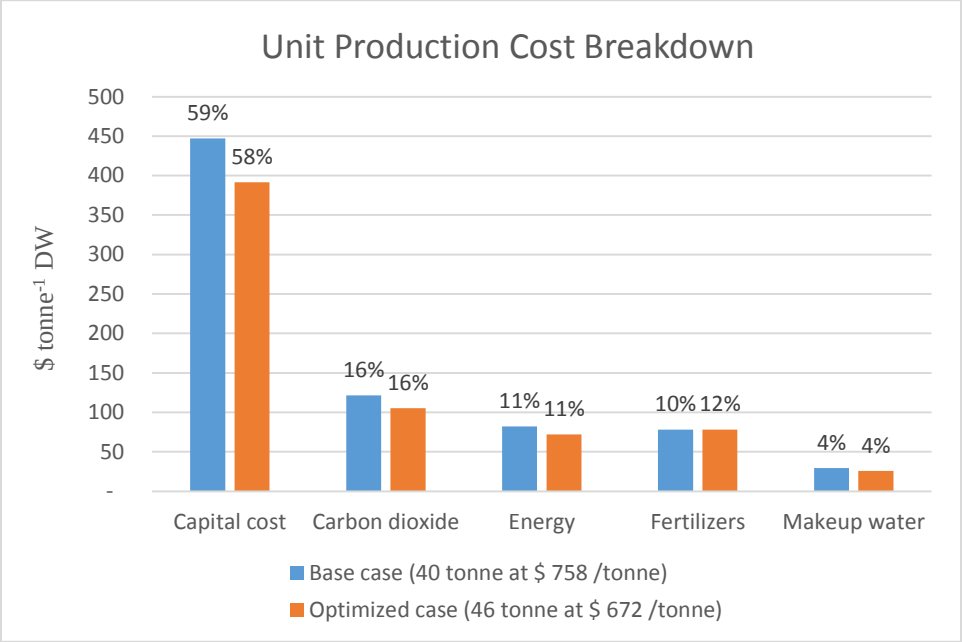

Chart 2.1: Breakdown of the unit production cost for the base and optimized cases.

2.5.4 Optimization Problem

The optimization problem considered determines the profiles of the dilution rate, CO_2 gas flowrate, and makeup water flowrate that

$$\underset{D,Q_g,F_{makeup}}{\text{minimize}} \qquad UPC \text{ (eq 2.30)}$$

subject to the following constraints:

(1) mass and energy balances (eqs 2.1-2.14)

(2) growth kinetics (eqs 2.15-2.19 and 2.21-2.23)

(3) CO_2 transfer (eqs 2.24-2.29)

(4) process economics (eqs 2.31-2.38)

Note that this formulation contains nonlinear growth kinetics and transient balances making it a nonlinear dynamic optimization problem. Assuming that the optimal areal concentration varies only on a monthly basis, the time horizon was divided into 12 control intervals creating 36 optimization decision variables which are subject to the following bounds:

$$Q_g \geq 0,\ F_{makeup} \geq 0,\ 0 \leq D \leq 0.5,\ 0.2 \leq H \leq 0.4$$

assuming that the CO_2 gas and makeup water availability are unlimited. The bounds on the dilution rate and depth were set based on typical operation in commercial algae facilities [16]. The base case assigned values for the decision variables were used as an initial guess.

2.5.5 Optimization Results

It took the optimizer 11,715 seconds to find the optimal operating profiles shown in Figures 2.10-2.12 corresponding to a production of 46 tonne DW $year^{-1}$ which is around 11% cheaper than the base case at a *UPC* of \$672 $tonne^{-1}$ and a cost break down as shown in Chart 2.1. Interestingly, Figure 2.9 shows that the algal biomass areal concentration in the optimized case is kept around 30 g DW m^{-2} which reduces the light limitation as shown in Figure 2.13 when compared with the light limitation in Figure 2.8. Also, this supports the prediction made earlier regarding the optimal areal concentration being close to 35 g DW m^{-2}. As demonstrated in Figures 2.9 and 2.10 the optimal dilution rate profile follows

the algal biomass areal concentration during the year, but toward the end of the production cycle *D* goes up so that the remaining algae in the pond is completely harvested.

The optimal makeup water flowrate profile maintains the depth around 30 cm throughout the year, but towards the end of the production cycle it stops making up for the evaporation losses as shown in Figure 2.12. This explains the higher algal concentration at the end of the production horizon for the optimized case when compared to the base case as Figure 2.9 shows. The main reason for optimizing the makeup water flowrate is to minimize the cost of water while maintaining suitable CO_2 absorption. Since there is no flow of CO_2 gas in November and December, the optimizer decides to lower the makeup water flowrate substantially to reduce the cost of makeup water. Notice from Figure 2.11 that the optimal CO_2 flowrate on average is less than in the base case. Although this causes growth limitation due to CO_2 deficiency as shown in Figure 2.13, the cost of CO_2 requirement reduces to \$107 tonne^{-1} DW from a base cost of \$121 tonne^{-1} DW.

Chapter 3 of this thesis evaluates the utilization of waste CO_2, namely industrial flue gas CO_2, because as shown in Chart 2.1 the most expensive operating component is the CO_2 supply. Moreover, the combined cost of makeup water and fertilizers constitutes 16% of the *UPC*, hence wastewater utilization supplying both elements at a potentially reduced cost is evaluated in Chapter 5. As shown in Figure 2.14, the growth rate is mostly inhibited by the temperature limitation making cultivation during winter, first part of the spring and last part of the fall nearly impossible. Utilizing waste heat to warm up the pond water to assist the growth during those cold periods is evaluated in Chapter 4 of the thesis.

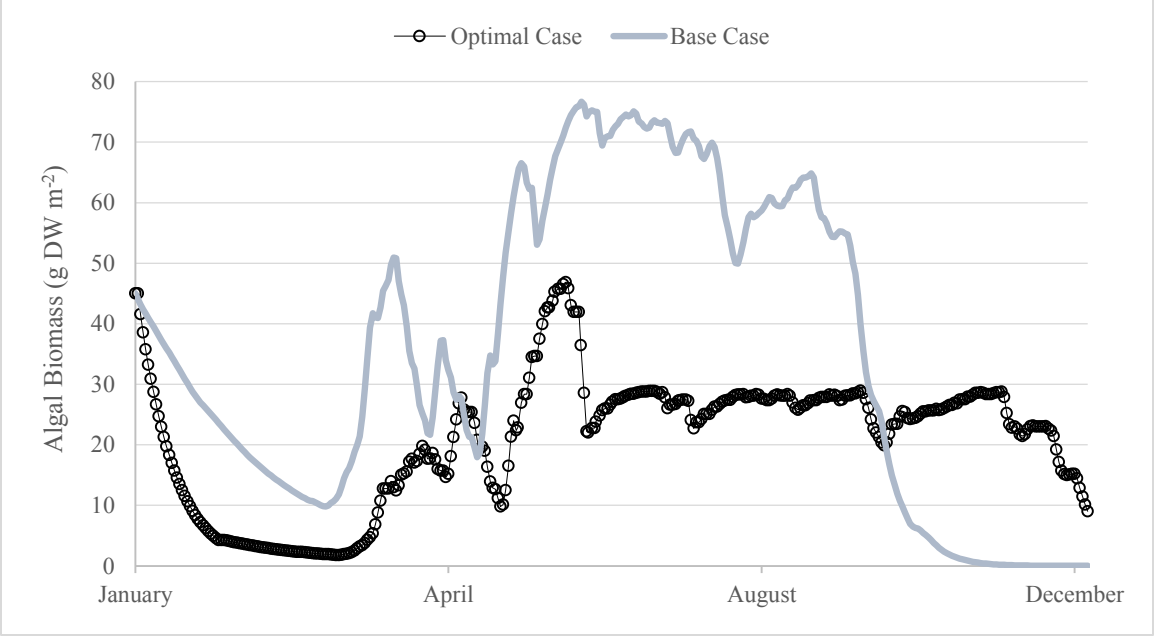

Figure 2.9: Algal biomass areal concentration in the open pond for the base case and the optimized case.

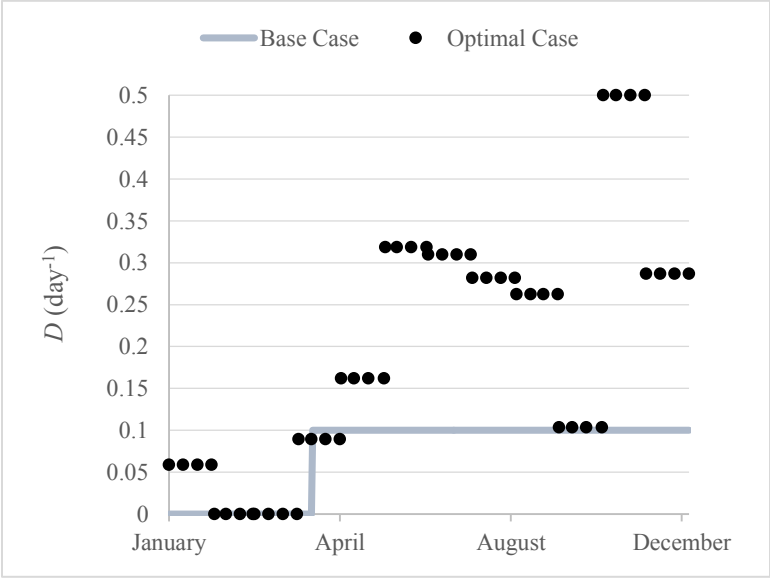

Figure 2.10: Optimal monthly operating profile for the dilution rate compared to the base case profile.

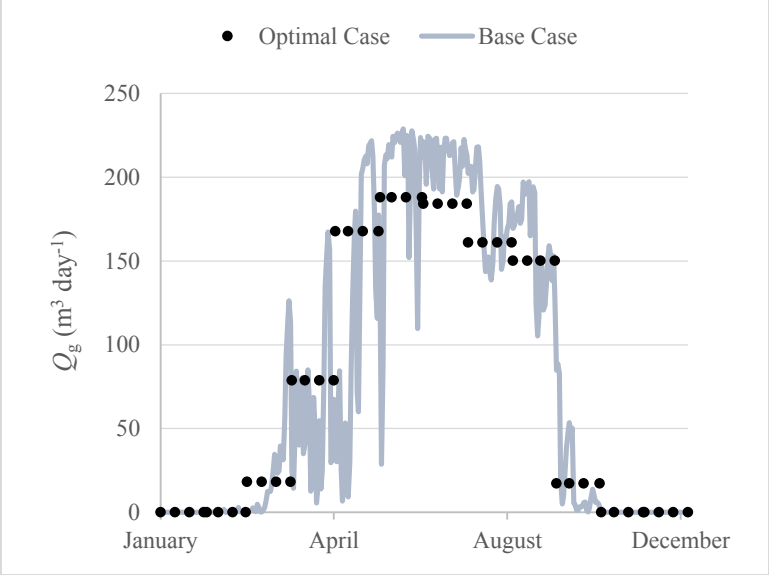

Figure 2.11: Optimal monthly operating profile for the CO_2 gas flowrate compared to the base case daily profile.

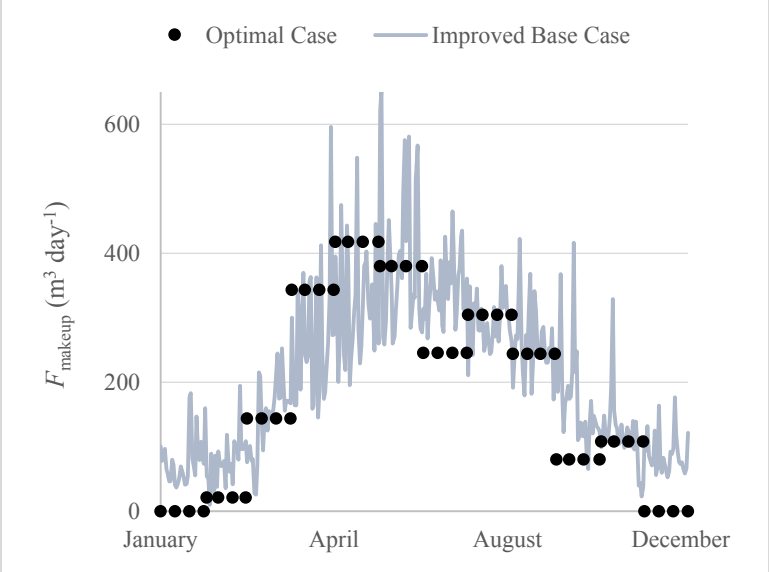

Figure 2.12: Optimal monthly operating profile for the makeup water flowrate compared to the base case daily profile.

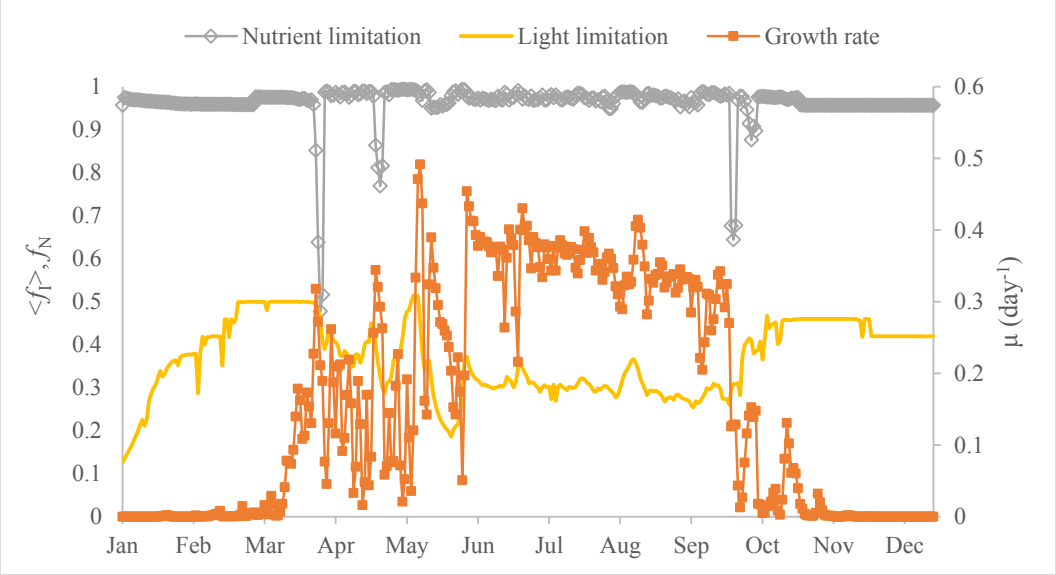

Figure 2.13: Effect of the nutrient and light limitations on the growth rate for the optimized case.

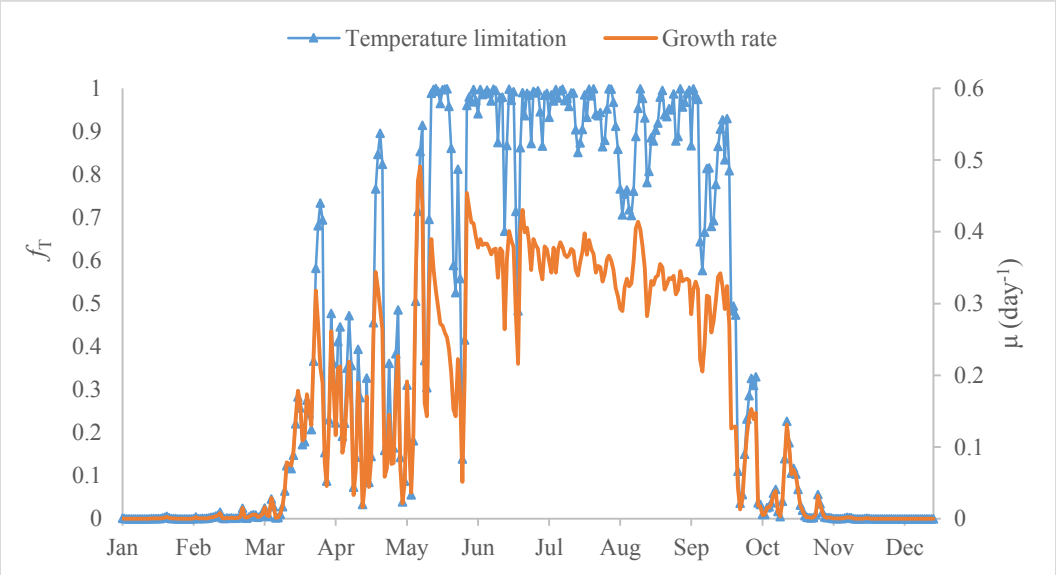

Figure 2.14: Effect of the temperature limitation on the growth rate for the optimized case.

2.6 Conclusions

A mathematical model for estimating the growth of microalgae in an outdoor open pond based on local climatic conditions was developed in this chapter. The model was validated against literature data for the production of *Spirulina* in an outdoor open pond in Málaga, Spain. The simulated algal biomass productivity agreed with experimental data, with a mean percent error of approximately 16%. A dynamic optimization problem was formulated for determining the location-specific optimal monthly operating profiles for the dilution rate, CO_2 gas flowrate, and makeup water flowrate. A case study was conducted for the cultivation of *N. Salina* in California, USA. The operating profiles generated by the optimization lowered the cultivation cost by at least 11% when compared with the base case scenario where common practice operation was employed.

CHAPTER 3

Cultivation Coupled with Recovery of Flue Gas CO_2

3.1 Background

As illustrated in Chapter 2, the cost of supplying CO_2 to support the growth of microalgae in an outdoor setup can be the highest operating cost. Instead of purchasing food-grade high purity CO_2 at a rate of \$40 tonne $^{-1}$, utilization of lower quality CO_2 from a waste source is well documented in the literature to be as effective in supporting the growth of microalgae. Studies show that low levels of NO_x and SO_x, such as in the natural gas combustion exhausts, do not inhibit the growth of microalgae, hence such flue gases can be injected directly into algal cultures [39], [107]. Otherwise, flue gases can be purified to deliver an almost 100% pure CO_2 gas to the algal ponds. If the CO_2 is not used locally, the latter option becomes more economically favorable because of the significant reduction in the compression and transportation cost of a much lower volume of gas for the same CO_2 supply [39]. However, crude injection might be justified when the CO_2 is used locally, e.g. algae cultivation in proximity of power production, as well as when compression for storing the CO_2 produced at night is avoided [108]. Note that in crude utilization, the flue gas must be injected at a microalgae safe temperature and typically, this means cooling

down the flue gas to below its dewpoint which is around 135 ^{o}F for natural gas combustion with standard air. Cooling has to be accomplished using corrosion-resistant condensing heat exchangers, because the CO_2, NO_x, and SO_x in the flue gas increase the water acidity.

Condensing heat exchangers can be categorized into direct and indirect contact, depending on the presence of separating walls for preventing mass transfer between the streams exchanging heat. Direct contact heat exchangers are more suitable for cooling the flue gas, because they can scrub pollutants from the flue gas without reducing its CO_2 content significantly [109]. Moreover, in a direct contact arrangement the overall heat transfer coefficient is in the range of 500-1000 Btu hr^{-1} ft^{-2} $^{o}F^{-1}$. In contrast, indirect contact condensing heat exchangers have much lower overall heat transfer coefficients at around 10 Btu hr^{-1} ft^{-2} $^{o}F^{-1}$ [109].

3.2 Process Description and Modeling

3.2.1 Microalgae Cultivation System

The microalgae cultivation system considered in this study is described in Chapter 2 with a summary provided herein for convenience. The study is centered on the cultivation of *Nannochloropsis Salina* in a 4 ha outdoor clay-lined open pond in southeastern California for an entire year starting from January. The high photosynthetic efficiency and lipid productivity of this robust algal strain make it promising for the production of biofuels [110]. The factors affecting the growth of microalgae considered are the water temperature, CO_2 availability, and irradiance level. The open pond is inoculated at 45 g of dry weight

microalgae (DW) m^{-2}. The actual daily weather conditions shown in the Appendix, including irradiance, wind speed, air temperature and humidity are used to predict the evolution of the water temperature varying on a daily basis [96]. A detailed model description for the open pond, growth kinetics of *Nannochloropsis Salina*, CO_2 transfer, and process economics is provided in Chapter 2.

3.2.2 Microalgae Cultivation and Flue Gas CO_2 Utilization

The option for purchasing pure CO_2 at \$40 $tonne^{-1}$ as in Chapter 2 is replaced with crude flue gas at 8% CO_2 injected throughout the growth culture in the two sump stations located at the pond middle. Before injection, the crude gas is cooled down to a maximum temperature of 50 ^oC using a packed tower serving as a direct contact condensing cooler. The proposed configuration of the open pond and packed tower is shown in Figure 3.1. Cooling water at 10 ^oC is assumed for cooling flue gas from a 2.93 MW natural gas-fired boiler. At 20% excess air, the boiler generates 4,220 kg hr^{-1} of flue gas at 177 ^oC containing 8% CO_2, 16% H_2O, 3% O_2, and 73% N_2 [111].

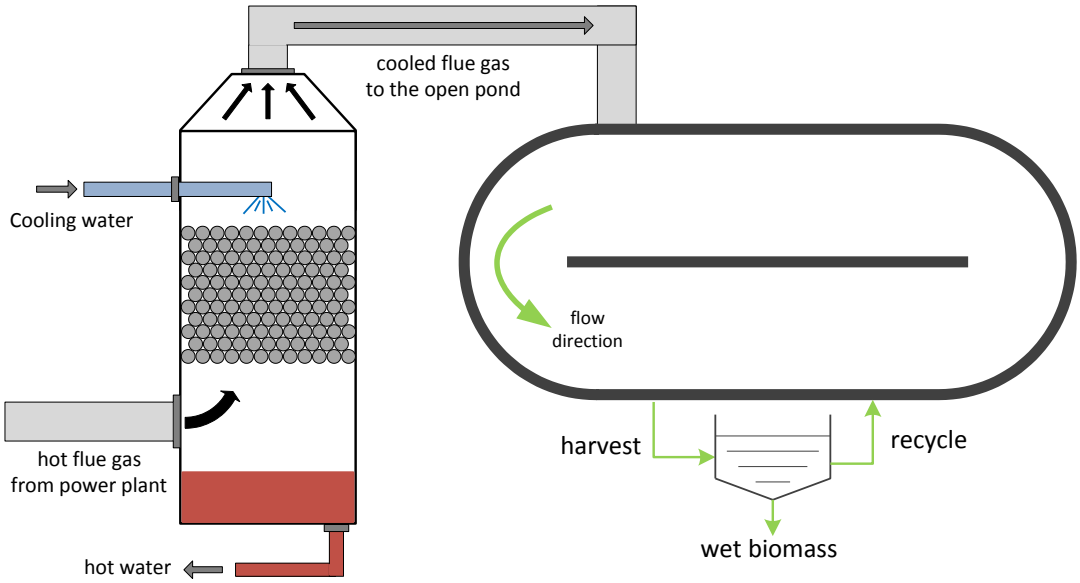

Figure 3.1: Schematic of the open pond and packed tower proposed configuration for the crude flue gas cooling and injection scenario.

3.2.3 Direct Contact Condensing Heat Exchanger Model

To simplify modeling of the direct contact heat exchanger, the water vapor contained in the gas is modeled separately and the gas calculations are done on a dry basis. Furthermore, steady state operation is assumed for the heat exchanger, as its dynamics are much faster than the algae growth and cultivation. Consequently, an energy balance around a direct contact condensing heat exchanger would give

$$H_{\mathrm{g,in}} + H_{\mathrm{v,in}} + H_{\mathrm{w,in}} = H_{\mathrm{g,\,out}} + H_{\mathrm{v,\,out}} + H_{\mathrm{w,\,out}} + H_{\mathrm{c,\,out}} \tag{3.1}$$

where H is the enthalpy of the stream and the subscripts refer to the gas (g), water vapor from the gas (v), liquid cooling water (w), and water condensate (c). The subscripts in and out denote that the stream is either entering or leaving the heat exchanger, respectively.

The amount of vapor condensing out of the hot gas (*Cond*) is calculated from the difference between the moisture content of the hot gas entering (X_{in}) and cooled gas leaving (X_{out}) the heat exchanger, respectively,

$$Cond = (X_{in} - X_{out}) F_{dry} \tag{3.2}$$

where F_{dry} is the flowrate of the flue gas on dry basis. Assuming that only steam condenses and other gases including CO_2 are non-condensable, Raoult's law for a single condensable component is used to calculate the mole fraction of water in the cooled flue gas (y_w)

$$y_{w,out} P_{T,out} = P_{vap,out} \tag{3.3}$$

where P_{vap} is the vapor pressure of water at the temperature of the cooled flue gas and P_T is the total pressure of this gas.

Direct contact heat exchangers include spray, packed, and tray columns [112]. High surface area packings can significantly improve the effectiveness of packed columns hence they are commonly used in direct contact heat recovery [109], [113]–[115]. The sensible heat gained by the cooling water in a packed tower can be estimated as

$$H_{w,out} - H_{w,in} = U_V Z_p A_{direct} \Delta T_{LMTD} \tag{3.4}$$

where Z_p is the packing height, A_{direct} is the column cross sectional area, and ΔT_{LMTD} is the log mean temperature difference. The volumetric overall heat transfer coefficient (U_V) can be estimated by

$$1/U_V = 1/h_g a_c + 1/h_l a_c \tag{3.5}$$

where a_c is the interfacial area, h_g is the gas side, and h_l is the liquid side volumetric heat

transfer coefficients. Determining the heat transfer area in a direct contact condensing heat exchanger is a difficult task, hence volumetric heat transfer coefficients are used. For packed columns those can be estimated using the correlation

$$h_{g/l}\, a = C\, G_s^{m1}\, L_s^{m2} \tag{3.6}$$

where G_s and L_s are the gas and liquid superficial mass velocities, respectively [112]. The values of the fluid and packing-specific fitting parameters C, m_1, and m_2 are shown in Table 3.1 for an air/water system with a random packing made of 38 mm Ceramic Intalox saddles.

Operating a column under flooding must be avoided, because it leads to operational problems such as higher pressure drops which could damage the packing and increase the energy consumption. The packed tower is designed considering the flood points which are determined using the calculations presented by Menzel (1979).

Table 3.1: Parameter values for the heat transfer coefficient correlation [112].

Coefficient	**Parameter**		
	C	m_1	m_2
$h_g\, a_c$	6,170	1.38	0.1
$h_l\, a_c$	42,570	0.2	0.69

3.3 Process Economics

The process economics detailed in Section 2.3 are adopted in this Chapter with some modifications. The unit production cost (*UPC*) is reformulated replacing the cost of purchasing CO_2 with the amortized capital cost (CC_{cooler}) and operating cost ($cost_{cooling}$) of the condensing cooler

$$UPC = \frac{CC_{\text{Pond}} + CC_{cooler} + \sum_{t=1}^{T_c} (cost_{\text{Nutrients},t} + cost_{\text{cooling},t} + cost_{\text{water},t} + cost_{\text{energy},t})}{\sum_{t=1}^{T_c} harvest_t} \tag{3.7}$$

where t is an integer denoting the number of the day starting from the beginning of the production cycle, and T_c is the length of the time horizon. The amortized capital cost of the open pond system (CC_{Pond}), and the costs of nutrients ($cost_{\text{Nutrients}}$), makeup water ($cost_{\text{water}}$), and energy ($cost_{\text{energy}}$) are calculated as shown in Section 2.3. A 1.35 m in diameter and 3 m long stainless steel tower packed with 2.4 m of ceramic packing would cost $57,100 including direct and indirect costs [117]. The expected stainless steel tower life is 20 years. Assuming the flue gas pressure drop is negligible, the cooling cost is

$$cost_{\text{cooling},t} = x_{\text{w}} Q_{\text{cooling water},t} + x_{\text{e}} Q_{\text{pumping power},t} \tag{3.8}$$

where x_{w} and x_{e} are the prices of water and power, respectively, and $Q_{\text{cooling water}}$ is the quantity of cooling water pumped to the packed tower. The amount of power ($Q_{\text{pumping power}}$) needed at the cooling water pump is given by

$$Q_{\text{pumping power},t} = \beta\, h \rho Q_{\text{water},t} / P_{\text{eff}} \tag{3.9}$$

where β is the number of hours the pump is operating daily, ρ is the water density, h is the head the pump overcomes to rise the cooling water to the tower top, P_{eff} is the pump efficiency, and Q_{water} is the cooling water flowrate [70]. The economic model parameter values are shown in Table 3.2.

Table 3.2: Parameter definitions and values for the process economics model.

Parameter	Description	Value
x_e	price of electricity (\$ kWh^{-1})	0.04 [102]
x_w	price of cooling water (\$ m^{-3})	0.016 [101]
β	number of hours the pump is operating daily (hr day^{-1})	12
ρ	density of water (g cm^{-3})	1.0
h	head the pump needs to overcome (m)	3
P_{eff}	Pump efficiency	85%

3.4 Dynamic Optimization

The several tradeoffs involved in outdoor cultivation of microalgae call for scheduling operations based on optimization. As discussed in Chapter 2, the two major parameters for operating an algae cultivation system are the dilution rate and the CO_2 gas flowrate. The dilution rate is the predominant factor in determining the amount of microalgae remaining in the open pond. The concentration of microalgae in the growth culture is an important factor, because it affects the productivity directly and it determines the effect of the shading and photoinhibition phenomena. Therefore, optimizing the dilution rate to achieve the optimal concentration of algae in the culture becomes vital. The CO_2 provides microalgae with the carbon necessary for growth. However, oversupply of CO_2 can inhibit the growth rate of microalgae. Additionally, dissolved CO_2 can degas to the atmosphere if not consumed by the microalgae, hence optimizing the CO_2 gas flowrate is necessary. The flowrate of the flue gas into the cooling packed tower dictates the availability of CO_2 for injection at the open pond as well as the cooling cost. Note that, a

higher flue gas flowrate would increase the cooling load, however, according to eq 3.6 this would improve the volumetric heat transfer coefficient and possibly reduce the cooling cost. A similar trade-off applies to the flowrate of the cooling water, which is therefore optimized in this case along with the dilution rate and the flue gas flowrate.

3.4.1 Base Case

In Chapter 2, the dilution rate and the CO_2 gas flowrate are optimized for a scenario where CO_2 is purchased from an external source at a price of \$40 tonne^{-1} which is the standard procedure for supplying CO_2 to an algae facility [27]. That case can serve as a base case in this Chapter.

3.4.2 Optimization Problem

The optimization problem seeks to determine the optimal monthly operating profiles of the dilution rate (D), flue gas flowrate (Q_{flue}), and the cooling water flowrate (Q_{water}) that

$$\underset{D,Q_{\text{flue}},Q_{\text{water}}}{\text{minimize}} \qquad UPC \text{ (eq 3.7)}$$

subject to the following constraints:

(1) mass and energy balances (eqs 2.1-2.14)

(2) growth kinetics (eqs 2.15-2.19, and 2.21-2.23)

(3) CO_2 transfer (eqs 2.24-2.29)

(4) heat transfer (eqs 3.1-3.6)

(5) process economics (eqs 2.31-2.32, 2.34-2.38, and 3.8-3.9)

(6) $0 \le Q_{\text{flue}} \le 4220$

(7) $0 \le D \le 0.5$

(8) $Q_{\text{water}} \ge 0$

Other constraints include a minimum harvest of 40 tonne DW year^{-1}, a maximum cooled flue gas temperature of 50 ^{o}C, a maximum column flooding of 90%, and a maximum cooling water exit temperature of 100 ^{o}C. The decision variables are manipulated on a monthly basis for a production horizon T_c = 1 year. The dilution rate is given an initial guess of 0.10 day^{-1} and the flue gas flowrate is assigned an initial guess of 1,100 kg hr^{-1}. The cooling water is assigned an initial guess flowrate of 1500 kg hr^{-1}.

3.4.3 Optimization Results

The flooding and cooling water exit temperature constraints, in particular, increase the computational time significantly. The optimizer spends 198,137 seconds to find the optimal operating profiles for the flue gas flowrate, dilution rate and cooling water flowrate shown in Figures 3.2-3.4. The corresponding column flooding factor shown in Figure 3.5 suggests that a column with smaller diameter can be used which can result in a reduced capital cost and an improved overall heat transfer coefficient according to eqs 3.5-3.6. Nevertheless, using the current heat exchanger in the utilization of the waste flue gas CO_2 can reduce the algal biomass production cost from \$672 tonne^{-1} down to \$602 tonne^{-1}. As shown in Figure 3.6 and Chart 3.1, the availability of a cheaper CO_2 source allows increasing the CO_2 supply rate liberally to prevent any CO_2 limitation on growth which

results in an increased annual algal biomass production from 45.7 tonne to 48.4 tonne. Moreover, Chart 3.1 illustrates how the utilization of flue gas CO_2 can generate good savings in the CO_2 cost while not incurring huge additional capital costs.

Since the crude flue gas contains 8% CO_2, it is expected to find that the optimal operating schedule for the flowrate of the crude CO_2 gas is at least an order of magnitude higher than in the pure CO_2 gas case as shown in Figure 3.2. Primarily, the flowrate of the CO_2 gas determines the amount of CO_2 supplied to the open pond culture, therefore the optimal profile in the base case suggests higher flowrates from May to September, where the productivity is higher as evidenced by the dilution rate profile shown in Figure 3.3. However, the optimal profile for the CO_2 gas flowrate in the flue gas injection scenario follows a different trend because the gas flowrate determines the cost of operating the heat exchanger as well. The optimal dilution rate profiles shown in Figure 3.3 are very similar. These findings suggest that under optimized operations, the CO_2 gas purity and price, within the studied limits, mainly change the CO_2 gas scheduling and the process economics without significantly affecting the other operating parameters.

Based on the analyzed scenario, it turns out that utilizing locally available crude CO_2 is economically better than supplying costly pure CO_2. However, purchasing CO_2 from an external source gives more flexibility in terms of locating the algae facility, i.e. it no longer has to be at the CO_2 source, which could greatly influence the economics. If locating an algae facility next to the CO_2 source would result in an additional cost, e.g. due

to a land cost higher than the reported production cost savings, then purchasing the CO_2 could be more economical.

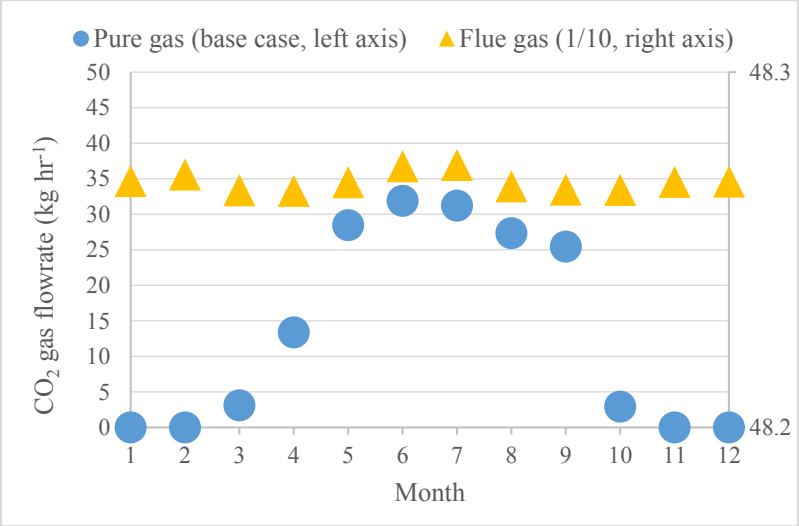

Figure 3.2: Optimal monthly schedules for the CO_2 gas flowrate in the flue gas and pure gas (base case) scenarios. These are the flowrates at each of the two sump stations.

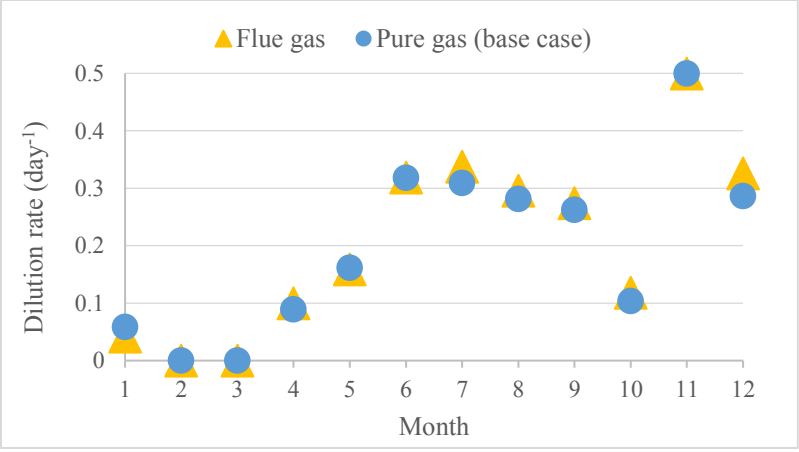

Figure 3.3: Optimal monthly schedules for the dilution rate in the flue gas and pure gas (base case) scenarios.

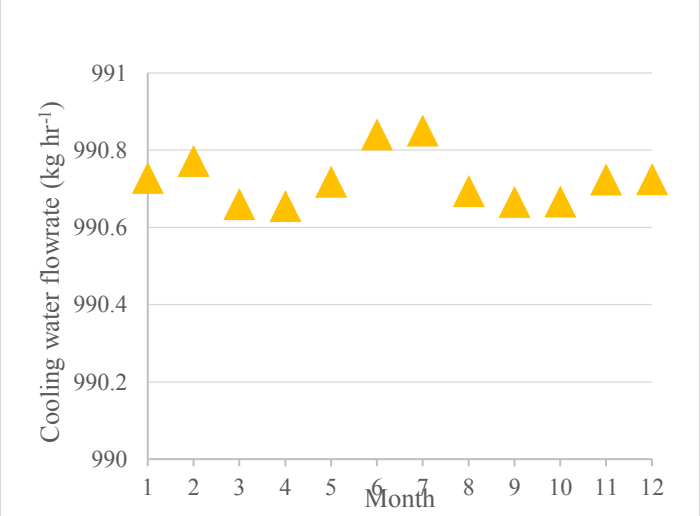

Figure 3.4: Optimal monthly schedule for the cooling water in the optimized flue gas injection scenario.

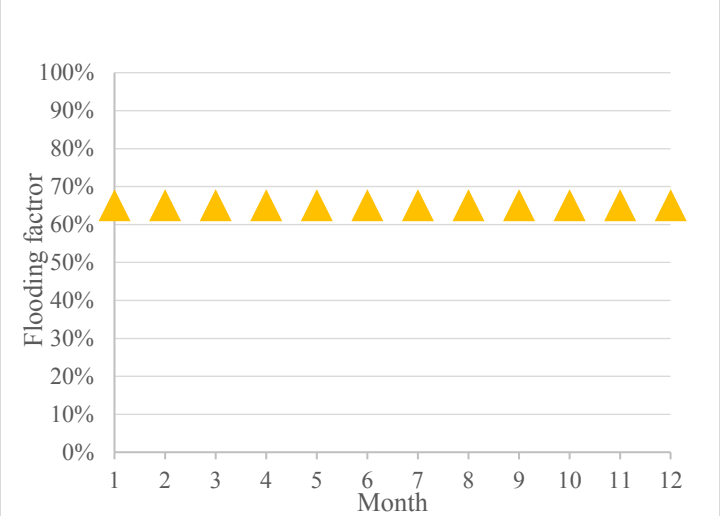

Figure 3.5: Profile of the resulting flooding factor in the packed column during operation under the optimized flue gas injection scenario.

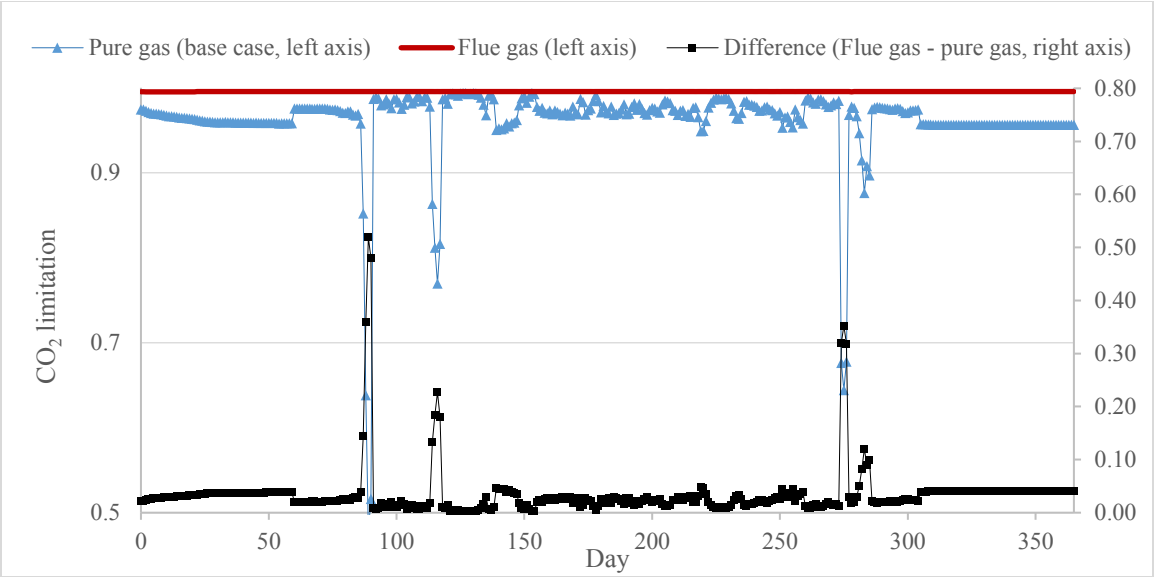

Figure 3.6: Difference between the CO_2 limitation on the growth rate in the flue gas and pure gas (base case) scenarios.

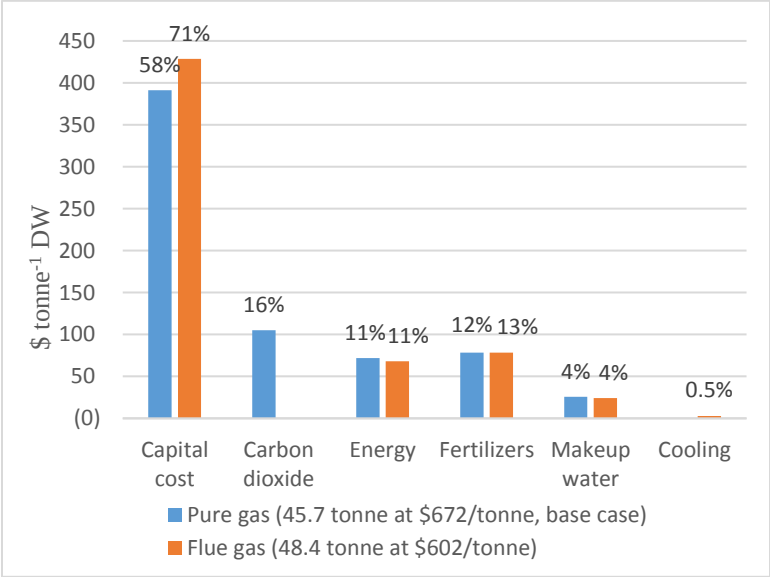

Chart 3.1: Breakdown of the unit production cost for the flue gas and pure gas (base case) scenarios.

3.5 Conclusions

This chapter analyzes the economic impact of using power plant flue gas CO_2 in cultivation of microalgae in an outdoor open pond. A model was developed for a packed tower used as a direct contact heat exchanger for cooling down the flue gas to estimate the performance and operating costs. Injection of the flue gas in crude form after cooling turned out to be more economical than purchasing pure CO_2. The trends in the optimal operations for both scenarios do not vary much except for the magnitude of the CO_2 gas flowrate, due to the difference in the CO_2 concentration in the flue gas and pure gas.

CHAPTER 4

Cultivation Coupled with Recovery of Waste Heat

4.1 Background

In Chapter 2 of this thesis, it was shown that cold ambient temperatures critically inhibit the growth of microalgae for a considerable period of time during the year. Current approaches for minimizing heat losses to the atmosphere include covering the photobioreactor surface with an insulating material during cold weather [118]. Others proposed a new open pond design where the culture is stored in a deep canal during the night to reduce the surface area of the culture exposed to the ambient air [119]. Consuming energy to warm up the huge quantities of culture water during cold climates is economically unfavorable [42].

Utilization of waste heat from power plants flue gases in heating algal growth cultures is suggested in the literature [27], [42]–[44]. Most gas-fired steam boiler power plants use economizers to recover waste heat and the exhaust gases exit the economizers at less than 450 ^{o}F; however, this low-temperature waste heat is suitable for domestic water heating [120]. In 2006, the waste heat inventory in the United States (US) industrial sector reached 1.5-3 quadrillion Btu per year which, if utilized, could provide substantial heating

to algal culture, hence, supporting algae growth [121]. Combustion flue gases are also high in moisture; as a result waste heat recovery (WHR) is commonly done in practice using condensing heat exchangers to capture the latent heat trapped in the flue gas [120].

As discussed in Chapter 3 (section 3.1), condensing heat exchangers are categorized into direct and indirect contact heat exchangers. Although direct contact heat exchangers are more advantageous for the purpose of cooling hot gases, for the purpose of waste heat recovery the indirect contact arrangement is more suitable. The maximum water heating attainable in a direct contact arrangement is limited by the flue gas dewpoint [122]. On the other hand, indirect contact condensing heat exchangers can heat the water up to 200 ^{o}F [123].

4.2 Process Description and Modeling

4.2.1 Microalgae Cultivation System

The algal biomass production configuration considered in this analysis is detailed in Chapter 2. To summarize, the study addresses a year-long cultivation of *Nannochloropsis Salina* in a 4 ha outdoor clay-lined open pond in southeastern California. The high photosynthetic efficiency and lipid productivity of this robust algal strain make it promising for the production of biofuels [110]. Growth limitations by water temperature, CO_2 availability, and irradiance level are considered in the model. The open pond inoculated at 45 g of dry weight microalgae (DW) m^{-2} is supplied with CO_2 by bubbling a CO_2 pure gas throughout the growth culture in the two sump stations located at the pond

middle. The actual daily weather conditions including irradiance, wind speed, air temperature, and humidity shown in the appendix are used to predict the evolution of the water temperature varying on a daily basis [96]. A detailed model description for the open pond, growth kinetics of *Nannochloropsis Salina*, CO_2 transfer, and process economics is provided in Chapter 2.

4.2.2 Microalgae Cultivation and Flue Gas Heat Recovery

Algal strains from the *N. Salina* species grow best at culture temperatures around 27 ^oC [75]. Heating of the growth medium can be accomplished using a shell and tube (indirect contact) heat exchanger configured to the open pond as shown in Figure 4.1. After harvesting the microalgae, the water is completely or partially pumped to the economizer for heating before recycling it to the open pond. Heating of water added to make up for evaporation losses is not included. The amount of cold pond water available for heating at the heat exchanger is limited by the harvest scheme at the open pond, hence the dilution rate affects the operations at the economizer as well. Waste heat is assumed to be available from a 2.93 MW natural gas-fired boiler flue gas at 177 ^oC. At 20% excess air, the boiler generates 4220 kg hr^{-1} of flue gas containing 8% CO_2, 16% H_2O, 3% O_2, and 73% N_2 [111]. The cooled gas could be directed to the open pond as needed for supplying the necessary CO_2 for the growth of microalgae. In order to make the case study applicable for CO_2-poor waste heat sources as well, pure CO_2 gas purchased at \$40 $tonne^{-1}$ is used herein.

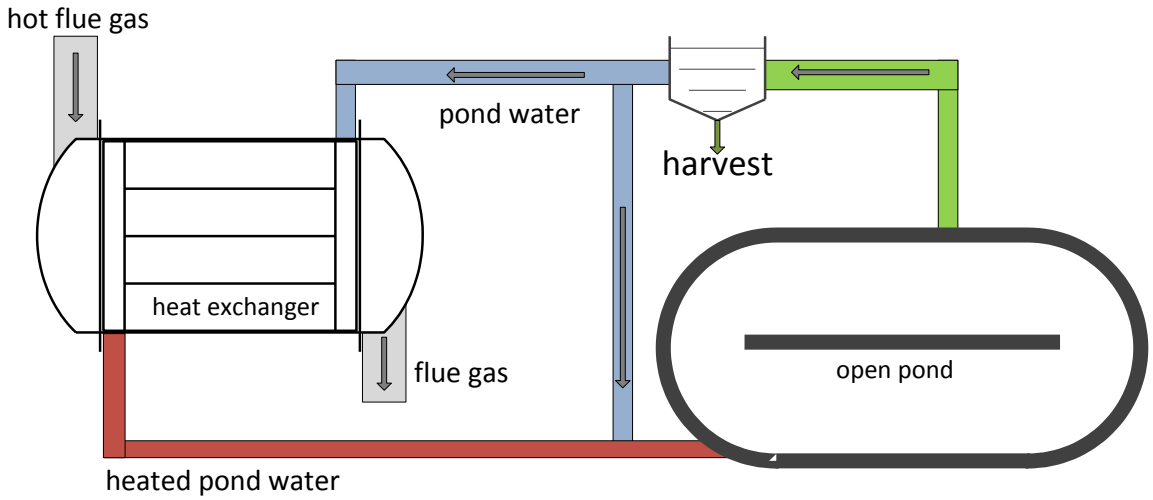

Figure 4.1: Schematic of the open pond and shell and tube heat exchanger proposed configuration for the waste heat recovery coupling.

4.2.3 Indirect Contact Condensing Heat Exchanger Model

The overall heat transfer coefficient in indirect contact can be assumed fairly constant around 10 Btu hr^{-1} ft^{-2} $^{o}F^{-1}$ [124], [125]. The heat exchanger model adopted from the gPROMS Model Libraries is used for the performance calculations of the indirect contact heat exchanger used in the WHR scenario [126]. For WHR applications, shell and tube is the most commonly used heat exchanger configuration when indirect contact arrangement is desired [124], [125], [127].

4.3 Process Economics

The process economics detailed in Section 2.3 are adopted in this Chapter with some modifications. The amortized capital cost of the heat exchanger (CC_{heater}) and its operating cost ($cost_{\text{heating}}$) are added to the unit production cost (UPC)

$$UPC = \frac{CC_{\text{Pond}} + CC_{\text{heater}} + \sum_{t=1}^{T_c} (cost_{\text{Nutrients},t} + cost_{\text{CO2},t} + cost_{\text{water},t} + cost_{\text{energy},t} + cost_{\text{heating},t})}{\sum_{t=1}^{T_c} harvest_t} \tag{4.1}$$

where t is an integer denoting the number of the day starting from the beginning of the production cycle, and T_c is the length of the time horizon. The costs of nutrients ($cost_{\text{Nutrients}}$), CO_2 ($cost_{CO_2}$), makeup water ($cost_{\text{water}}$), and energy ($cost_{\text{energy}}$) and the amortized capital cost of the open pond system (CC_{Pond}) are calculated as shown in Section 2.3. The purchased equipment cost of a 229 m^2 condenser made of corten steel with steel pipes and aluminum fins withstanding pH values above 8 is $14,430 (vendor-provided [128]). Assuming an installation factor of 1.9 and a yearly maintenance cost of 6 % of the installed cost, the capital cost of the heat exchanger amortized over its 15-year expected lifetime is $3,473 [124]. The cost of operating the economizer is estimated accordingly

$$cost_{\text{heating},t} = x_e \, Q_{\text{heater},t} \tag{4.2}$$

where x_e is the price of power, and Q_{heater} is the amount of power needed to overcome the drop in water pressure (ΔP) from flowing through the steel pipes of the heat exchanger

$$Q_{\text{heater},t} = \beta\, \Delta P\, S\, F_{\text{harvest}} / P_{\text{eff}} \tag{4.3}$$

where β is the number of hours the pump is operating daily, P_{eff} is the pump efficiency, F_{harvest} is the flowrate of the open pond harvest stream, and S is the splitting ratio which is a fraction between 0 and 1 dictating the amount of water available for heating [70]. The economic model parameter values are shown in Table 4.1.

Table 4.1: Parameter definitions and values for the process economics model.

Parameter	Description	Value
x_e	price of electricity (\$ kWh^{-1})	0.04 [102]
β	fractional length of a day having daylight	0.5
P_{eff}	efficiency of the water pump	85% assumed
ΔP	pressure drop of water flowing through the tubes (kPa)	7.5 [128]

4.4 Optimization

As demonstrated in Chapter 2, the dilution rate is an important operating parameter to be optimized for improving the economics of microalgae cultivation in outdoor open ponds. The dilution rate determines the concentration of microalgae in the open pond which plays an important role in the growth rate, and hence the productivity of microalgae. The tradeoffs involved in the dilution rate optimization for a traditional open pond system are discussed in Section 2.5.2.1. In the open pond culture heating scenario, an additional competing factor is introduced as increasing the dilution rate increases the amount of pond water available for heating which is encouraged for cases with abundant waste heat due to

the following reasons. First, indirect contact economizers can heat up water to a maximum of 93 ^{o}C using waste heat from boilers [123]. Second, heating up the water to such high temperatures can be lethal to the microalgae where the heated water is introduced at the open pond. Thus, having higher amounts of water available for heating during cold weather is preferable. This means using higher dilution rates, and consequently reducing the productivity when the low temperature is already inhibiting the growth rate. Thus, optimizing the dilution rate becomes critical in a culture heating scenario. In addition to optimizing the dilution rate, the actual amount of water pumped to the heat exchanger is optimized through varying the splitting ratio (*S*) for the junction after the harvest as shown in Figure 4.1.

4.4.1 Base Case

A base case resembling the no-heating scenario is created using the optimized dilution rate profile as determined in Section 2.5.5. The CO_2 gas flowrate is set based on the rate of CO_2 uptake from the growth medium and the makeup water flowrate is set to the level that compensates for evaporation losses. As shown in Figure 4.2, in the base case the growth rate is critically inhibited by the temperature limitation during January-March and November-December. One might expect cooler air temperatures during these months to cause higher heat losses from the pond water to the ambient air through conduction. Figure 4.3 shows that the opposite is true as the water gains heat from the air through conduction, because the air temperature is almost always higher than the water temperature

as shown in Figure 4.4. Furthermore, compared to the rest of the year, lower air temperatures during cooler weather does not significantly drop the amounts of heat radiated from the atmosphere/air to the pond water as clearly shown in Figure 4.3. One can conclude that lower irradiance levels in the winter compared to the summer are responsible for the reduced water temperatures. Moreover, as shown in Figure 4.4, water thermal radiation is the dominant heat loss term and it increases with higher water temperatures. Therefore, it is possible that heat gained through culture heating might get wasted through increased water thermal radiation to the surroundings before the growth rate improves by the higher water temperature.

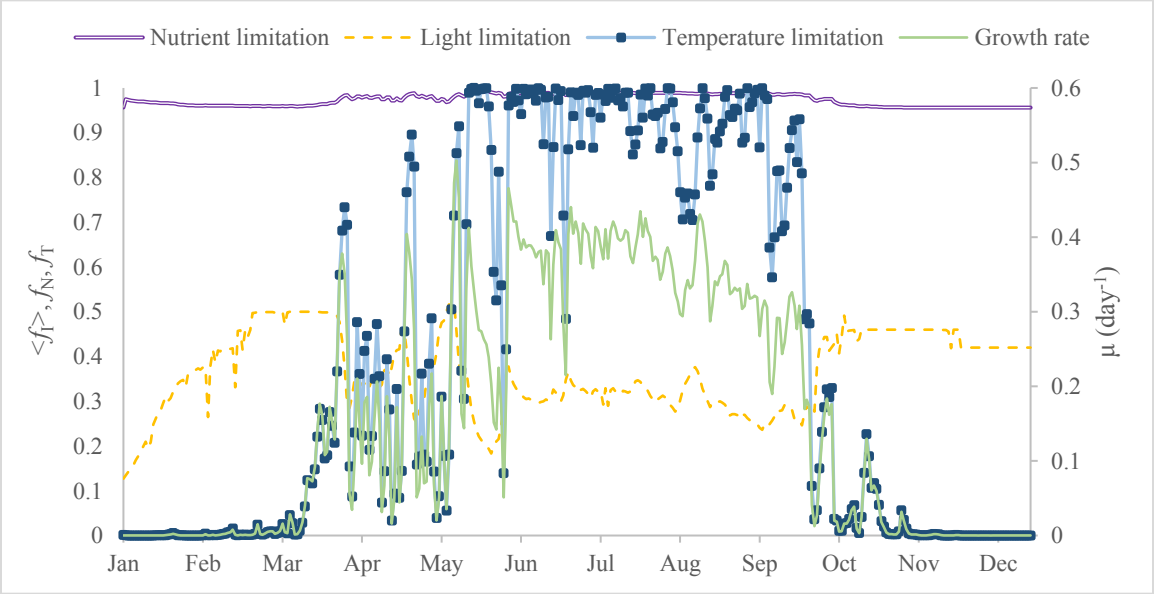

Figure 4.2: Effect of the temperature limitation on the growth rate for the base case (no-heating).

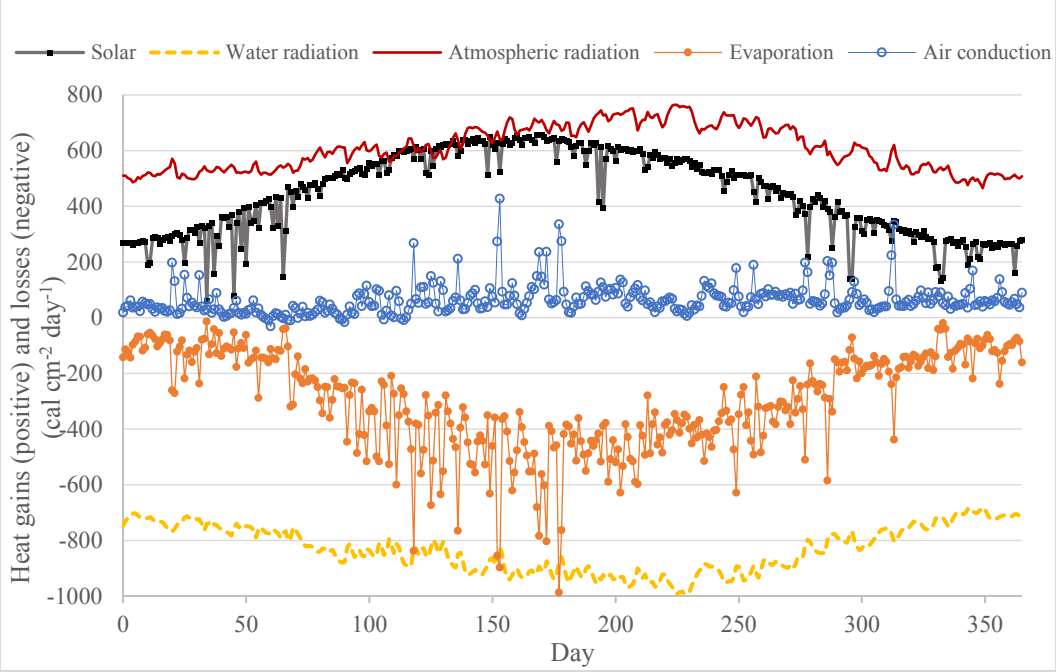

Figure 4.3: Heat gains and losses from the open pond surface for the base case (no-heating).

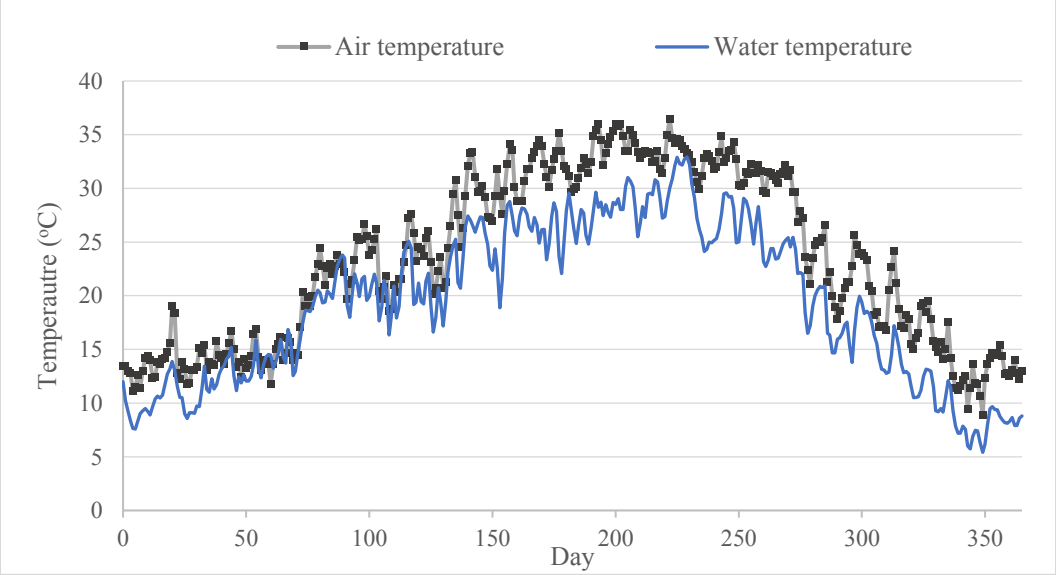

Figure 4.4: Comparing water and air temperatures in the base case (no-heating).

4.4.2 Optimization Problem

The optimization problem seeks to determine the optimal monthly operating profiles of the dilution rate (D), flue gas flowrate (Q_{flue}), and the splitting ratio (S) that

$$\underset{D, Q_{\text{flue}}, S}{\text{minimize}} \qquad UPC \text{ (eq 4.1)}$$

subject to the following constraints:

(1) mass and energy balances (eqs 2.1-2.14)

(2) growth kinetics (eqs 2.15-2.19 and 2.21-2.23)

(3) CO_2 transfer (eqs 2.24-2.29)

(4) heat transfer (see section 4.2.3)

(5) process economics (eqs 2.31-2.38 and 4.2-4.3)

(6) $0 \le Q_{\text{flue}} \le 4220$

(7) $0 \le D \le 0.5$

(8) $0 \le S \le 1$

Other constraints include a minimum harvest of 40 tonne DW year^{-1}, and a maximum heated water temperature of 100 ^{o}C. The decision variables are manipulated on a monthly basis for a production horizon T_c = 1 year. The dilution rate profile from the base case is used to provide the initial guess. The initial guess for S is 1. The flue gas flowrate is assigned an initial guess of zero for June to September and 4,220 kg hr^{-1} for the other months.

4.4.3 Optimization Results

The optimizer takes 6,587 seconds to find the optimal operating profiles for the heating scenario which slightly raise the temperature of the pond water as shown in Figure 4.5. Figures 4.6 and 4.7 show that heating reduces the temperature limitation which improves the growth rate. As a result the annual harvest increases from 47.4 to 48.6 tonne DW. As illustrated in Chart 4.1, the operating cost of the heat exchanger is negligible, but the capital cost of the heat recovery apparatus increases the biomass production cost from \$666 tonne^{-1} to \$727 tonne^{-1}.

Figure 4.8 shows that the heat gained through heating gets lost through radiative heat loss from the water. As discussed earlier, thermal radiation from water is the dominant cause of pond water heat losses, hence reducing the water thermal radiation could be more effective than heating the culture. Covering the huge open pond surface is expected to be uneconomical. Alternatively, one could seek options that reduce the water exposed surface to volume ratio to reduce heat exchange at night when heat gain by solar is unavailable. Although this would reduce the heat gain by atmospheric radiation, it is not as significant as the heat losses by water thermal radiation as concluded from Figure 4.3. The algal raceway integrated design (ARID) pond addresses this issue by storing the culture in an underground reservoir at night [119].

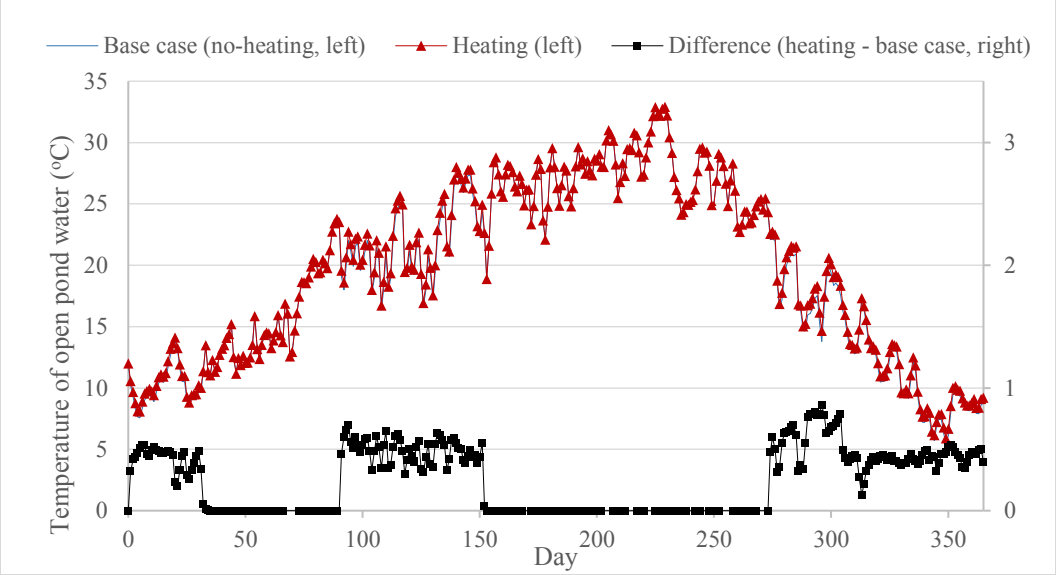

Figure 4.5: Difference between the temperature of the open pond water in the heating case and the base case (no-heating).

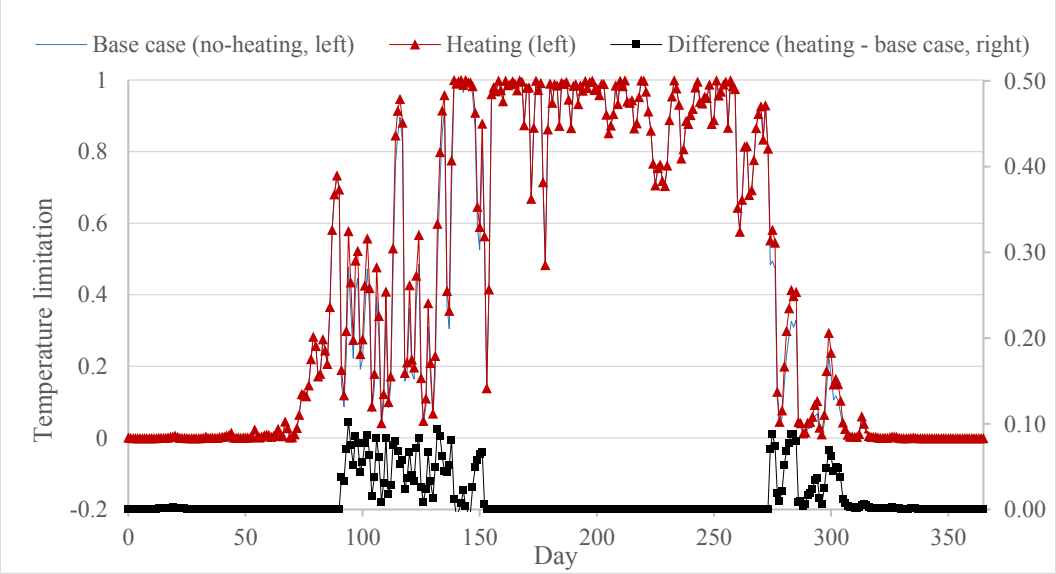

Figure 4.6: Difference between the temperature limitation on the growth rate between the heating case and the base case (no-heating).

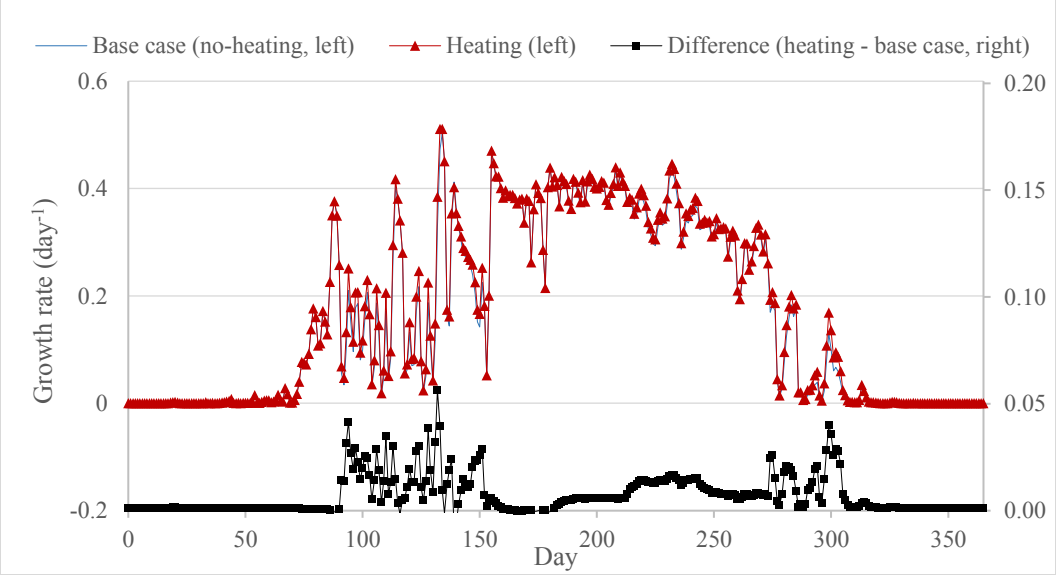

Figure 4.7: Comparison between the growth rate of microalgae in the open pond for the heating case and the base case (no-heating).

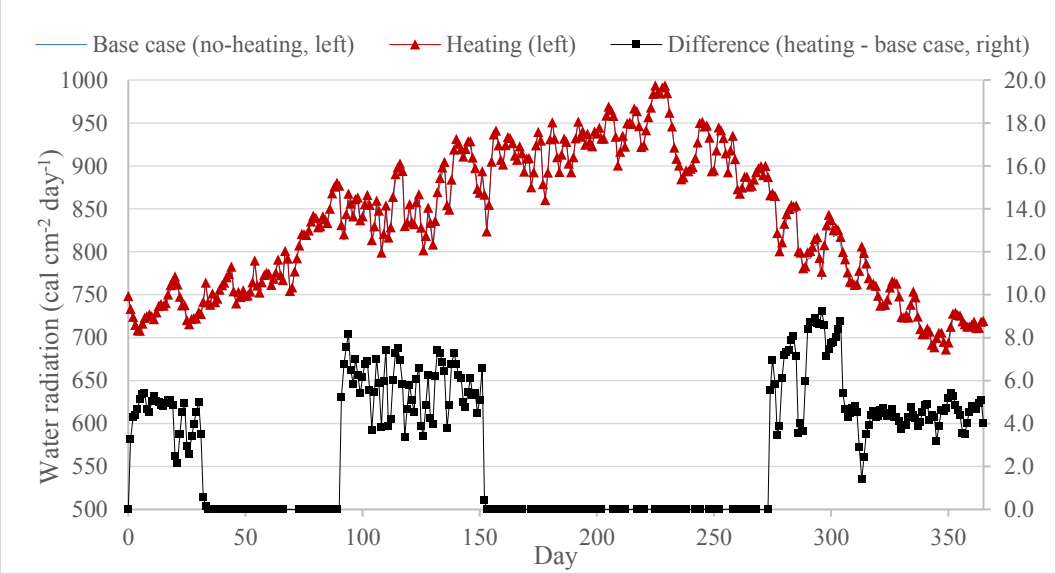

Figure 4.8: Comparison between the heat losses through water thermal radiation for the heating case and the base case (no-heating).

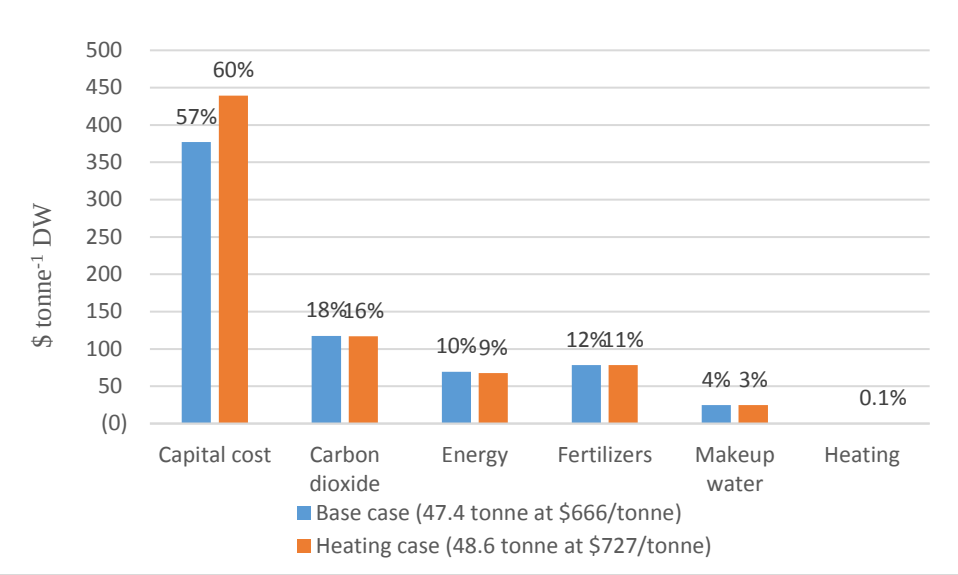

Chart 4.1: Unit production cost breakdown for the heating case and the base case (no-heating).

The monthly operating profiles for the dilution rate, flue gas flowrate and the splitting ratio are shown in Figures 4.9-4.11 suggesting heating only during the months of January, April, May, and October-December. Typically, one would expect the optimal solution to include heating during February and March. However, as shown in Figure 4.9, the optimal profile for the dilution rate agrees with the base case profile suggesting that no harvest be employed in February and March. Obviously, that's because the growth rate drops dramatically during these months as shown in Figure 4.7 and apparently heating can't prevent that. Although the growth rate is higher in March than January, the high inoculation at the begging of the year allows using a low dilution rate before the algae concentration drops significantly shortly after January and harvest has to stop as shown in Figure 4.12.

This means some water is available in January which is why the optimal solution suggests heating in that month.

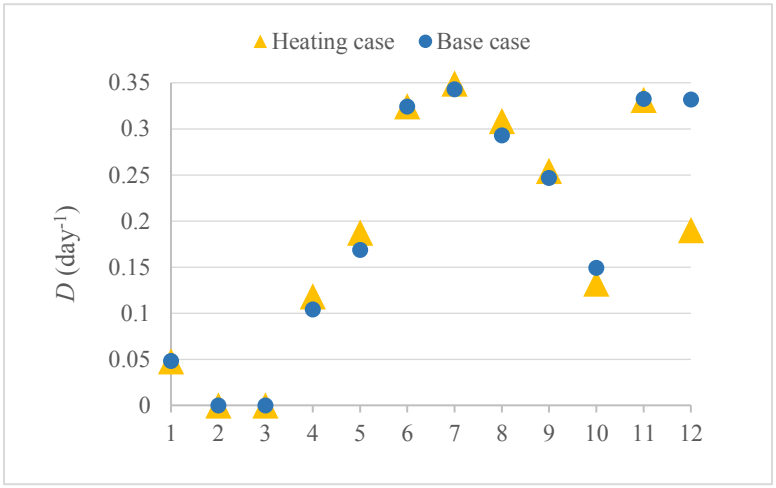

Figure 4.9: Dilution rate profile for the heating case and the base case (no-heating).

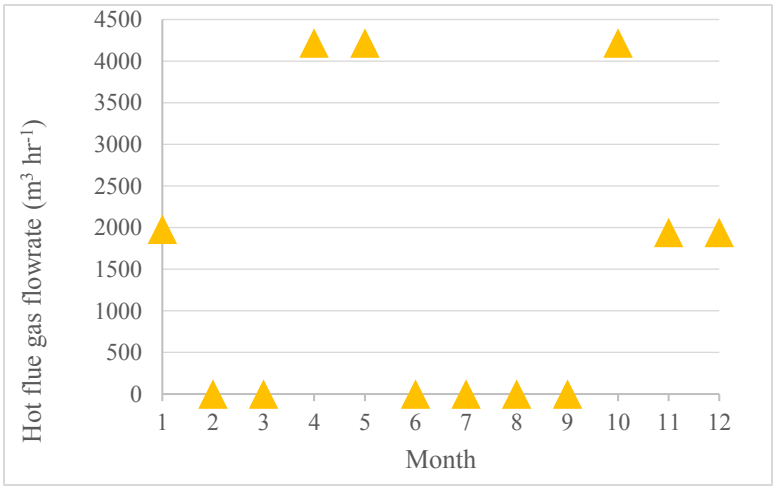

Figure 4.10: Optimal monthly schedule for the hot flue gas flowrate.

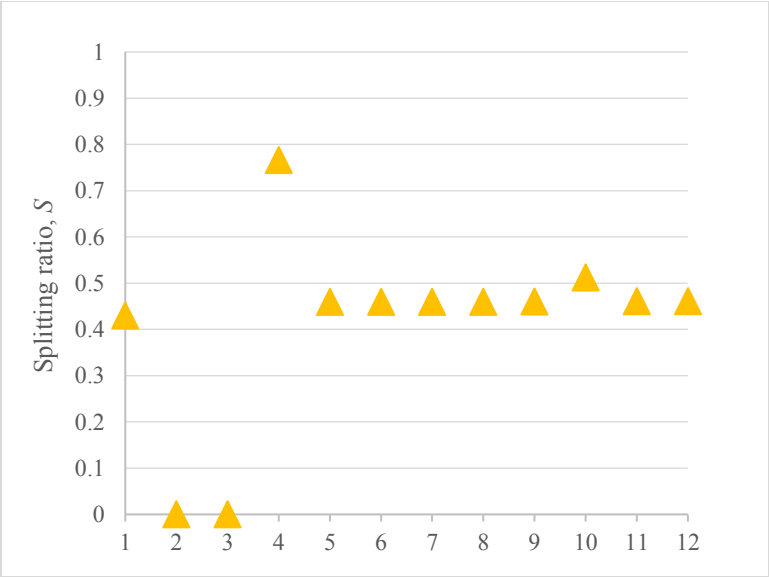

Figure 4.11: Optimal monthly schedule for the splitting ratio (*S*). This fraction determines the amount of harvest water redirected to the heat exchanger for heating.

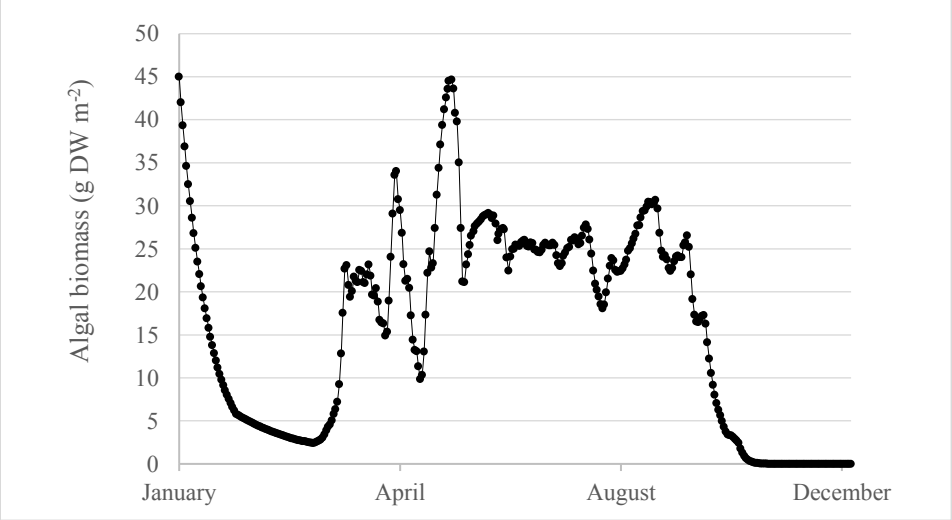

Figure 4.12: Algal biomass concentration in the open pond for the optimized case where culture heating is employed.

4.5 Conclusions

During cold weather, the temperature limitation significantly drops the growth rate of microalgae in outdoor cultivation. The difference in water temperature between winter and summer times is mainly due to the seasonal changes in solar irradiance. Heat losses from the open pond water are dominated by water thermal radiation to the atmosphere. Increasing the water temperature through waste heat recovery and its impact on the process economics is investigated in this chapter. A model was developed to estimate the operating cost and performance of an indirect contact heat exchanger used in recovering heat from a power plant natural gas boiler flue gas to the open pond water. In conclusion, heating improved the productivity of the system, but the high capital cost of the heat exchanger resulted in an increased algal biomass production cost from \$666 tonne^{-1} DW to \$727 tonne^{-1} DW.

CHAPTER 5

Cultivation Coupled with Recovery of Waste Nutrients

5.1 Background

In algal biomass cultivation, fertilizers such as ammonia, urea, sodium nitrate, diammonium phosphate, and potassium phosphate, are added to the growth culture to fulfill the requirement of elemental nitrogen and phosphorus necessary for the growth of microalgae, cell division and lipid accumulation [129]. Studies on nutrient optimization primarily focus on nitrogen and phosphorus because the other elements are needed in much smaller quantities including Co, Zn, Mn and Cu. For instance, *N. Salina* is commonly cultivated in the f/2 medium which contains 75 mg L^{-1} of $NaNO_3$, 5 mg L^{-1} of $NaH_2PO_4 \cdot H_2O$ and 0.0098 mg L^{-1} of $CuSO_4$ [106], [129], [130]. Nitrogen can make up 1-15% of the algal biomass of *N. Salina* [104]. The ideal ratio of nitrogen to phosphorus in algal biomass is around 16:1 [131].

In cultivation of microalgae in open ponds, fertilizers are introduced to the pond culture as needed to avoid growth limitation due to nutrient deficiency. As demonstrated in Chapter 2, the cost of nutrients (fertilizers) can be around 10-12% of the algal biomass unit production cost. For commercial application of algal biofuel in the near future, every

aspect of the cultivation process will have to be optimized. Utilization of waste nutrients through integration of microalgae cultivation with wastewater treatment is widely discussed in the literature [132]. A typical secondary wastewater treatment process would receive raw municipal wastewater at total nitrogen concentration (*TN*) of 30-100 mg L^{-1}, and total phosphorus concentration (*TP*) of 6-25 mg L^{-1} [133]. Strict regulations limiting nitrogen and phosphorus content of treated wastewater discharged to surface open waters are lacking [134]. Some of the consequences related to the discharge of waters containing those pollutants include eutrophication, drinking water contamination, and toxicity to marine life [25]. A tertiary treatment step dedicated for removal of nitrogen and other dissolved pollutants can be extremely costly [25]. On the other hand, pollutants in treated wastewater can be thought of as free nutrients for algal biomass cultivation. Moreover, growing microalgae in wastewater can reduce its biological oxygen demand through the oxygen generated during the photosynthesis reaction. Furthermore, microalgae can remove metal ions and coliform bacteria from wastewater [25]. An economic analysis on the cost of algal biofuels production in an integrated process for algae cultivation and secondary wastewater treatment can be found in reference [70]. Although microalgae cultivation can be used as a secondary treatment process, it is not as effective considering the retention time currently achieved in existing processes such as the activated sludge process [132].

Employing microalgae cultivation as a tertiary treatment step can be challenging if the nitrogen to phosphorus ratio is relatively low, hence leading to excessive phosphorus limitation [132]. Furthermore, algal biomass consists of 50% carbon, hence the

requirement for CO_2 in algae production is much higher than nitrogen and phosphorus and locating algae facilities at CO_2 sources becomes advantageous. Therefore, in cases were local wastewater is not available, using microalgae as a tertiary treatment step can be challenging, because transporting treated wastewater from a wastewater treatment plant to an algae facility can be costly. For an algae producer, the reduction in nutrient cost might not compensate the added transportation cost and this tradeoff can be addressed in a supply chain optimization formulation. Moreover, wastewater treatment plants can differ in effluent nutrient concentrations which could lead to nutrient deficiencies affecting the growth rate of microalgae. Therefore, in the case of wastewater utilization, the cultivation system operations should be optimized according to the received treated wastewater characteristics. The analysis presented in reference [70] addresses the algae facility location issue assuming monthly average productivities of the algal system.

The proposed supply chain formulation accounts for daily changes in weather conditions and embeds a process model for estimating growth rates on a daily basis. Moreover, the process model is used in preforming dynamic optimization to determine the optimal operating parameters for every individual supply chain considered in the analysis. The formulation compares this information to decide on the optimal facility location, daily supply of treated wastewater, and monthly operating profiles for the cultivation system.

5.2 Process Model

5.2.1 Microalgae Cultivation System

The microalgae cultivation system considered in this study is described in Chapter 2 with a summary provided herein for convenience. The study is centered on the cultivation of *Nannochloropsis Salina* in a 4 ha outdoor clay-lined open pond in southeastern California for an entire year. The factors affecting the growth rate of microalgae considered in the model are the water temperature, CO_2 availability, nitrogen availability, and irradiance level. The open pond is inoculated at 45 g of dry weight microalgae (DW) m^{-2}. Actual daily weather conditions available in the Appendix, including irradiance, wind speed, air temperature and humidity are used to predict the evolution of the water temperature varying on a daily basis [96].

5.2.2 Treated Wastewater Utilization

In this analysis, the algae cultivation system receives treated wastewater from secondary treatment wastewater processing plants. Typically, secondary treatment produces an effluent quality level of 30 mg L^{-1} of total suspended solids. Such low turbidity (0.003%) won't increase the water turbidity noticeably, also considering that only a fraction of the pond water is going to be replaced with treated wastewater [135].

Effluent flow and nutrients concentrations from wastewater treatment plants in Imperial County are shown in Table 5.1 as collected from the California Regional Water Quality Control Board webpage [136]. These are maximum daily values otherwise noted

as average and missing data was estimated. The wastewater treatment plants included in the study are ones with effluent discharge to surface waters or evaporation ponds. As discussed earlier, the ideal ratio of nitrogen to phosphorus in *N. Salina* cultivation is 16:1 [131]. Based on the data from Table 5.1, the average ratio of nitrogen to phosphorus is around 14:1 which suggests the growth rate will experience nitrogen limitation rather than phosphorus limitation. Therefore, only nitrogen limitation is considered in this analysis.

As demonstrated in Chapter 3, utilization of crude CO_2 from natural gas fired power plants can be economically advantageous. Table 5.2 shows annual amounts of CO_2 generated from power production at power plants in Imperial County according to the Emissions & Generation Resource Integrated Database (eGRID) [137]. According to the optimized operations found in Chapter 2 for the CO_2 gas flowrate, these power plants generate more than enough CO_2 for the scale of the cultivation system considered in this study. According to reference [70], types of land suitable for algae cultivation include agricultural, developed open-space, shrub, and bare land. The availability of such land at the candidate sites (power plants locations) is confirmed using data form the National Land Cover Database [138] as displayed in Figure 5.1. The wastewater treatment plants and power plants are geographically distributed as shown in Figure 5.2. A possible scenario is the cultivation of microalgae at the wastewater treatment plants where wastewater nutrients are freely available eliminating costly transportation. However, power plants flue gas CO_2 won't be available and pure CO_2 will have to be purchased. The other scenario is algal biomass production at the power plants, to benefit from the cheaper CO_2, with

transportation of treated wastewater from the wastewater treatment plants to the power plants for the nutrients supply. Door-to-door driving distances from the wastewater treatment plants to the power plants found using Google Maps are available in the Appendix [139].

Table 5.1: Effluent characteristics of wastewater treatment plants in Imperial County [136].

Wastewater Treatment Plant	**Flow** (million gal day^{-1})	**Total Nitrogen** ($g\ m^{-3}$)	**Total Phosphorus** ($g\ m^{-3}$)
El Centro	3.5	17	2 (average)
Calexico	2.68	98.84 (estimated)	3.32 (average)
Calipatria	1.73	92.8	12.47
Heber	0.27	26.8	10.11
Holtville	0.67	34.4	8.82
Imperial	2.4	125	11
Niland	0.28	15.1	3.1
Seeley	0.1	58.6	17 (estimated)
Westmorland	0.28	21.81	1.89
Brawley	3.9	59.96	16.65

Table 5.2: CO_2 emissions data for natural gas fired power plants in Imperial County [137].

Power Plant Name	**CO_2 Emissions** (tons $year^{-1}$)
El Centro	548,584
Niland Gas Turbine Plant	44,683
Rockwood	3,128
Spreckels Sugar Company	63,192

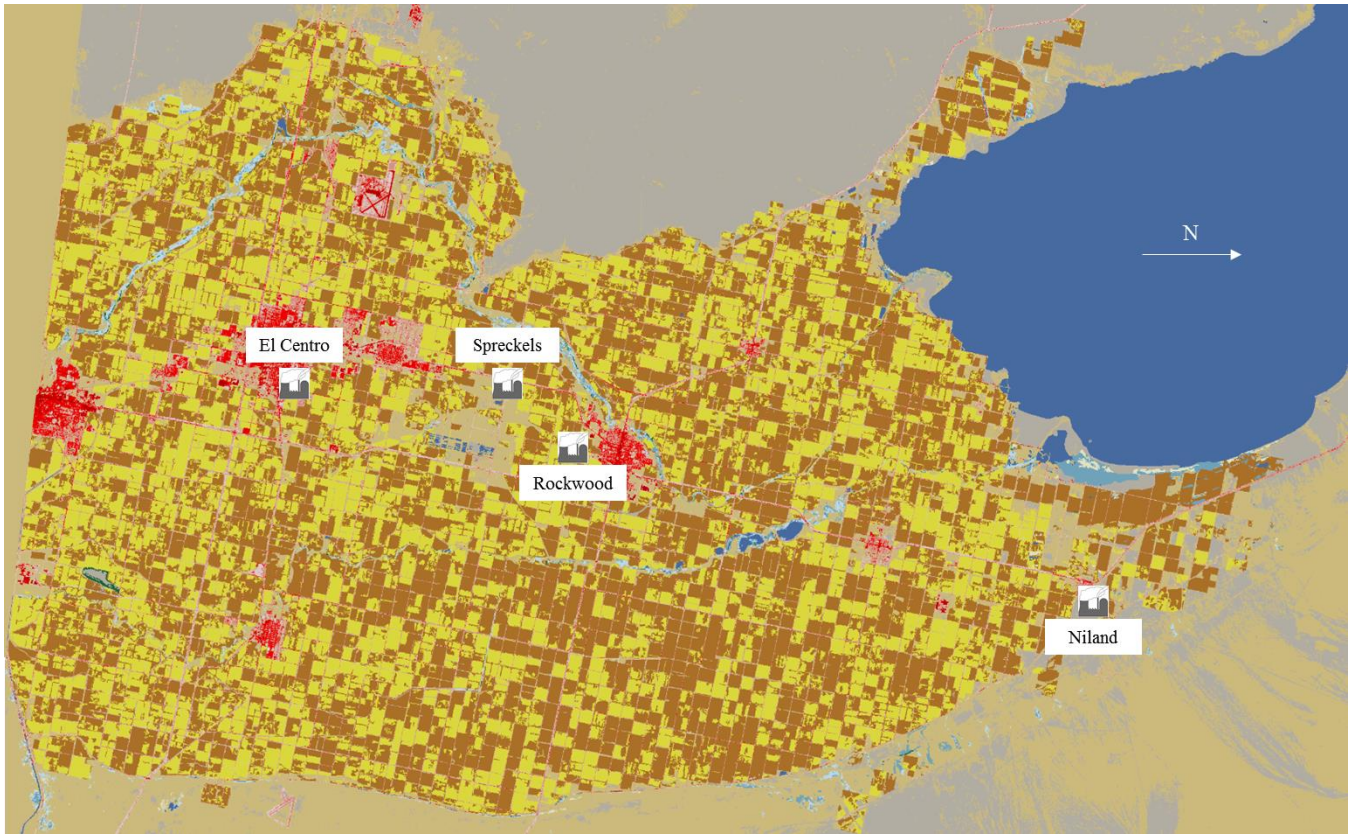

Figure 5.1: Map of Imperial County displaying the considered power plants locations (white font and black marker) and land availability: developed land (red), developed open-space (pink), agricultural (brown), and pasture land (yellow) [137], [138].

Figure 5.2: Map of Imperial County displaying the geographic distribution of the considered wastewater treatment plants and CO_2 power plants [136], [137], [140].

5.2.3 Kinetics of Nutrient Limitation on Growth

A detailed model description for the open pond, growth kinetics of *Nannochloropsis Salina*, and CO_2 transfer is provided in Chapter 2. In section 2.2.2, the nutrient limitation factor (f_{Nutrient}) is modeled assuming only carbon deficiency. In the presence of nitrogen deficiency, f_{Nutrient} becomes a combined effect of the carbon ($f_{\text{Nutrient\_C}}$) and nitrogen ($f_{\text{Nutrient\_N}}$) deficiencies

$$f_{\text{Nutrient},i} = f_{\text{Nutrient\_C},i}\ f_{\text{Nutrient\_N},i} \tag{5.1}$$

where $i \in [1,n]$, and n is the number of continuous stirred tank reactors an open pond is discretized to. The term $f_{\text{Nutrient\_C}}$ is modeled as shown in section 2.2.2. Nitrogen deficiency is modeled based on the analysis presented in reference [141] where nitrogen uptake and limitation on growth is related to the intercellular (q_{N}) and extracellular (C_{N}) concentration of nitrogen. According to the Droop model

$$f_{\text{Nutrient\_N},i} = \left[1 - \frac{q_{\text{N\_min}}}{q_{\text{N},i}}\right] \tag{5.2}$$

where $q_{\text{N\_min}}$ is the minimum nitrogen content of the algal cells where microalgae stop growing [142]. Assuming no remineralization of nitrogen from the algal biomass to the culture, the change in nitrogen content is determined from the specific uptake rate of nitrogen (U_{Nitrogen})

$$\frac{\mathrm{d}}{\mathrm{d}t}\left(q_{\mathrm{N},i}\right) = U_{\mathrm{Nitrogen},i} \tag{5.3}$$

which is calculated based on the intercellular and extracellular nitrogen concentration and assuming it is not affected by the temperature of the growth medium

$$U_{\mathrm{Nitrogen},i} = U_{\mathrm{Nitrogen\_max}}\ f_{\mathrm{Nutrient\_N},i}\ \frac{C_{\mathrm{N},i}}{K_{\mathrm{N}} + C_{\mathrm{N},i}} \tag{5.4}$$

where $U_{\mathrm{Nitrogen\_max}}$ is the maximum specific uptake rate of nitrogen and K_{N} is the half saturation constant for nitrogen uptake [143]. The following mass balance is used to track changes in the extracellular concentration of nitrogen in the culture

$$LW\frac{\mathrm{d}}{\mathrm{d}t}\left(H_i\, C_{\mathrm{N},i}\right) = F_{\mathrm{in},i}\, C_{\mathrm{N},i\text{-}1} - F_{\mathrm{out},i}\, C_{\mathrm{N},i} - LW\, H_i\, U_{\mathrm{Nitrogen},\,i}\, C_{\mathrm{algae},i} \tag{5.5}$$

where F_{in} is the flow of water from the preceding CSTR to the *i*-th CSTR of the segmented open pond. Similarly, F_{out} is the flow of water out to the succeeding CSTR in the direction of flow. For each CSTR, L is its length, W is its width, C_{algae} is the algae concentration, and H is the depth of water. Table 5.3 shows the parameter values for the nitrogen deficiency model.

Table 5.3: Parameter definitions and values for the nitrogen deficiency model including initial values [68], [141].

Parameter	Description	Value
q_{N_min}	minimum nitrogen content of the algal cells (gN g^{-1} DW)	0.01
K_N	half saturation constant for nitrogen uptake (gN m^{-3})	0.02
$U_{Nitrogen\_max}$	maximum specific uptake rate of nitrogen (gN g^{-1} DW day^{-1})	0.004
Variable	**Description**	**Value**
q_N	intracellular nitrogen content of the algal cells (gN g^{-1} DW)	0.06
C_N	extracellular nitrogen concentration in the open pond (gN m^{-3})	125

5.3 Process Economics

The process economics detailed in Section 2.3 are adopted in this Chapter with some modifications in the unit production cost (*UPC*). In the scenario with algae production at wastewater treatment plants, *UPC* is given by

$$UPC = \frac{CC_{\text{Pond}} + \sum_{t=1}^{T_c} (cost_{\text{energy},t} + cost_{\text{CO2},t})}{\sum_{t=1}^{T_c} harvest_t} \tag{5.6}$$

where t is an integer denoting the number of the day starting from the beginning of the production cycle, and T_c is the length of the time horizon. The amortized capital cost of the microalgae cultivation system (CC_{Pond}), cost of energy at the cultivation system ($cost_{\text{energy}}$), cost of pure CO_2 gas ($cost_{CO_2}$), and algal biomass harvest (*harvest*) are determined as shown in Section 2.3. In the case of algae production at power plants, *UPC* is determined assuming the operating cost of preparing the flue gas before injection to the open pond is negligible compared to the other costs as illustrated in Chart 3.1

$$UPC = \frac{CC_{\text{Pond}} + CC_{cooler} + \sum_{t=1}^{T_C} (cost_{\text{energy},t} + cost_{\text{trans},t})}{\sum_{t=1}^{T_C} harvest_t} \tag{5.7}$$

where CC_{cooler} is the amortized capital cost of the heat exchanger used in cooling down the flue gas. The heat exchanger design and costing is shown in Section 3.3. According to reference [144], the cost of transporting treated wastewater ($cost_{\text{trans}}$) using a rented truck is

$$cost_{\text{trans},t} = FC_{\text{trans}} + d_{\text{trans}} VC_{\text{trans}} \tag{5.8}$$

where d_{trans} is the travel distance. The fixed transportation cost (FC_{trans}) and the variable transportation cost (VC_{trans}) are given by

$$FC_{\text{trans}} = \frac{T_{\text{loading}} CO_{\text{trans}}}{60\ Cap} \tag{5.9}$$

$$VC_{\text{trans}} = \frac{CO_{\text{trans}}}{v_{\text{trans}} Cap} \tag{5.10}$$

where Cap is the truck capacity, CO_{trans} is the truck charge-out rate, T_{loading} is the total liquid loading and unloading time, and v_{trans} is the traveling speed. The loading time is determined assuming a water loading rate of 2 m^3 min^{-1} and the other parameters values are given in Table 5.4.

Table 5.4: Parameter definitions and values for the wastewater transportation cost [144].

Parameter	Description	Value
Cap	transporting capacity of rented truck (m^3)	40
CO_{trans}	truck charge-out rate ($ hr^{-1})	95.1
v_{trans}	Traveling speed (mile hr^{-1})	40

5.4 Supply Chain Optimization

When nutrient concentration in the wastewater is relatively high, sufficient addition of nutrients can be accomplished using treated wastewater in replacing makeup for evaporation losses. Otherwise, treated wastewater can be used in partial/full replacement of the harvest stream that is typically recycled to the open pond following harvest of the biomass. In such cases, any nutrients in the replaced portion of the harvest stream are wasted. Moreover, maintaining the salinity of the algal culture becomes a concern in marine microalgae cultivation and usually salts have to be added to the growth culture. Figure 5.3 shows daily evaporation losses from an open water surface as calculated based on eqs 2.4-2.6 and the weather conditions for Imperial County. Figure 5.4 shows the daily nitrogen requirement for supporting the growth of microalgae according to the optimized case in Chapter 2. Figure 5.5 shows the necessary concentration of nitrogen in makeup water to deliver the nitrogen requirement shown in Figure 5.4 using the makeup water flowrates based on the profile shown in Figure 5.3. From Figure 5.5 and Table 5.1, adequate nitrogen supply can be accomplished using treated wastewater in replacing only the evaporation losses which is the scenario considered in this analysis.

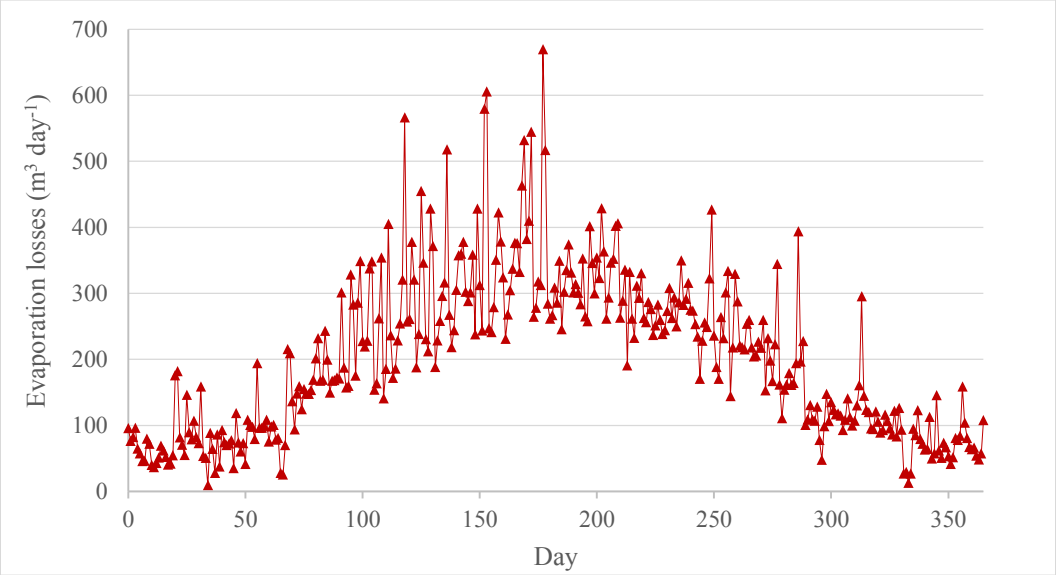

Figure 5.3: Daily evaporation losses from open surfaces in Imperial County.

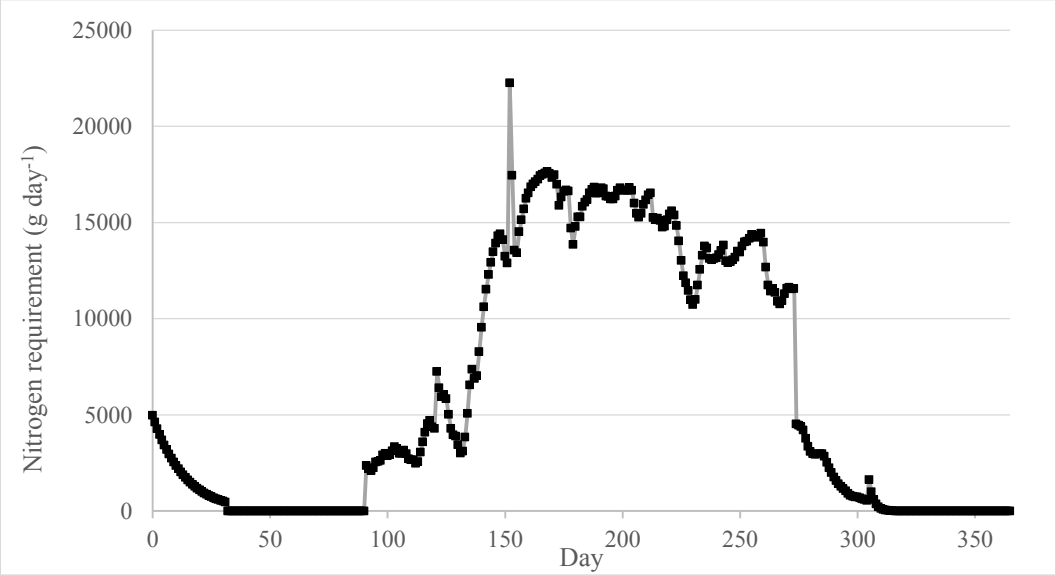

Figure 5.4: Nitrogen requirement for sustaining the growth rate of microalgae for the optimized case presented in Chapter 2.

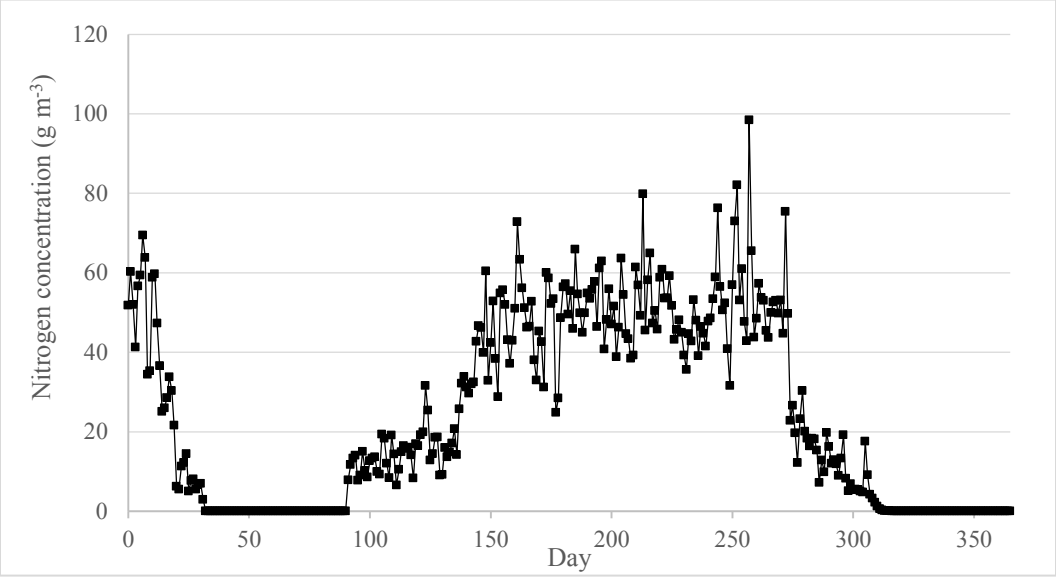

Figure 5.5: Necessary concentration of nitrogen in the makeup water calculated based on the profiles shown in Figures 5.3 and 5.4.

5.4.1 Microalgae Cultivation at Wastewater Treatment Plants

This case resembles microalgae cultivation at a wastewater treatment facility generating treated wastewater at a total nitrogen concentration of 55 g m^{-3} which is the average of the values in Table 5.1. The pure CO_2 gas flowrate is set based on the rate of CO_2 uptake rate from the growth culture with a price of \$40 $tonne^{-1}$ CO_2. In this case the optimization problem seeks to determine the optimal dilution rate (D) profile that

$$\underset{D}{\text{minimize}} \qquad UPC \text{ (eq 5.6)}$$

subject to the following constraints:

(1) mass and energy balances (eqs 2.1-2.14)

(2) growth kinetics (eqs 2.15-2.19 and 2.21-2.23)

(3) CO_2 transfer (eqs 2.24-2.29)

(4) Nitrogen limitation (eqs 5.1-5.5)

(5) process economics (eqs 2.31, 2.33, and 2.35-2.38)

(6) $0 \le D \le 0.5$

The initial total nitrogen concentration in the open pond is 55 g m^{-3}. The optimal dilution rate profile found in Chapter 2 is used as an initial guess. The resulting model is a nonlinear program (NLP).

5.4.2 Microalgae Cultivation at Power Plants

The rate of flue gas CO_2 injection into the open pond is set based on the CO_2 uptake rate from the pond medium. The optimization problem seeks to determine the optimal dilution rate (D) profile, the power plant site (PP) hosting the algae facility, and the wastewater treatment plant ($WWTP$) supplying the treated wastewater that

$$\underset{D,PP,WWTP}{\text{minimize}} \quad UPC \text{ (eq 5.7)}$$

subject to the following constraints:

(1) mass and energy balances (eqs 2.1-2.14)

(2) growth kinetics (eqs 2.15-2.19 and 2.21-2.23)

(3) CO_2 transfer (eqs 2.24-2.29)

(4) Nitrogen limitation (eqs 5.1-5.5)

(5) process economics (eqs 2.31, 2.35-2.38, and 5.8-5.10)

(6) $0 \le D \le 0.5$

Including a constraint that forces the evaporation losses to be replaced only with treated wastewater. The model adjusts the initial total nitrogen concentration in the open pond to match the chosen wastewater treatment plant during each optimization run. The optimal dilution rate profile found in Chapter 2 serves as an initial guess for the dilution rate. The initial guess for the power plant is El Centro and for the wastewater treatment plant is Brawley. *WWTP* and *PP* are binary variables creating a mixed integer nonlinear program (MINLP).

5.4.3 Optimization Results

The NLP is optimized in 1,396 seconds and the MINLP is optimized in 15,804 seconds. The cost of microalgae cultivation at the wastewater treatment plant using purchased CO_2 gas is found to be \$604 tonne^{-1} DW. On the other hand, the cost of growing microalgae at a power plant using treated wastewater from a nearby wastewater treatment plant is \$4,773 tonne^{-1} DW. As shown in Figure 5.6, the optimal solution for the supply chain scenario suggests growing microalgae at Niland Gas Turbine Plant and receiving treated wastewater from Niland wastewater treatment plant. The effluent from Niland wastewater treatment plant contains total nitrogen at 15.1 g m^{-3}. According to Figure 5.7, such concentration in the makeup water provides sufficient amounts of nitrogen to the growth culture achieving the minimum possible growth inhibition due to nitrogen deficiency of 0.93. The travel distance between these two sites is the shortest at 2.3 miles. As shown in Chart 5.1, the cost of transporting wastewater dominates the production cost in the supply chain scenario. This explains why the optimizer resorts to the closest available

sites considering that such supply chain scenario provides sufficient nitrogen to the algae growth medium. At a travel distance of 2.3 miles, the fixed cost of transporting water at \$2.38 m^{-3} constitutes 95% of the transportation cost. This suggests finding transportation alternatives with lower fixed cost is vital before hauling treated wastewater can be considered in the production of algal biomass.

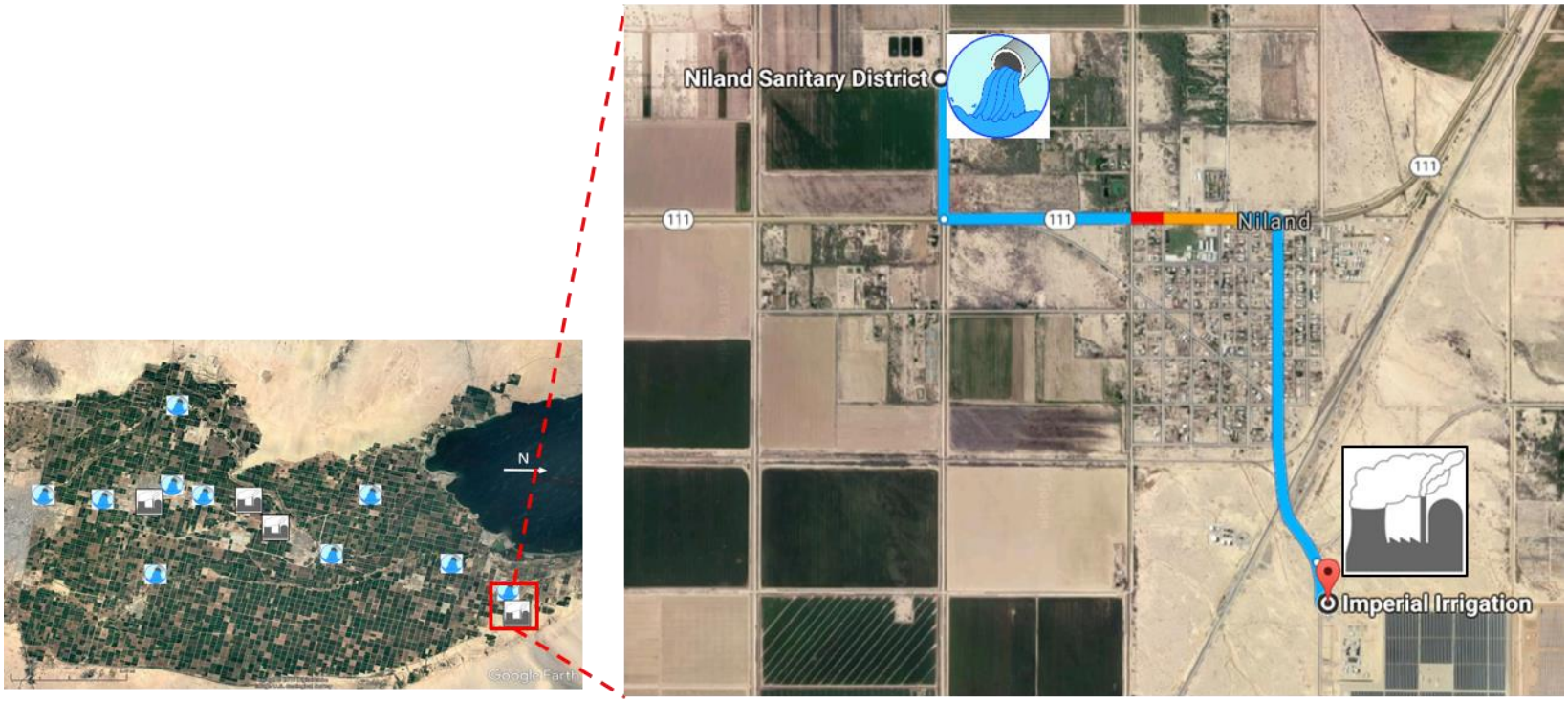

Figure 5.6: Map of Imperial County displaying the optimal solution for the supply chain optimization scenario. The optimal microalgae cultivation site is the Niland Gas Turbine Plant with treated wastewater received from Niland wastewater treatment plant.

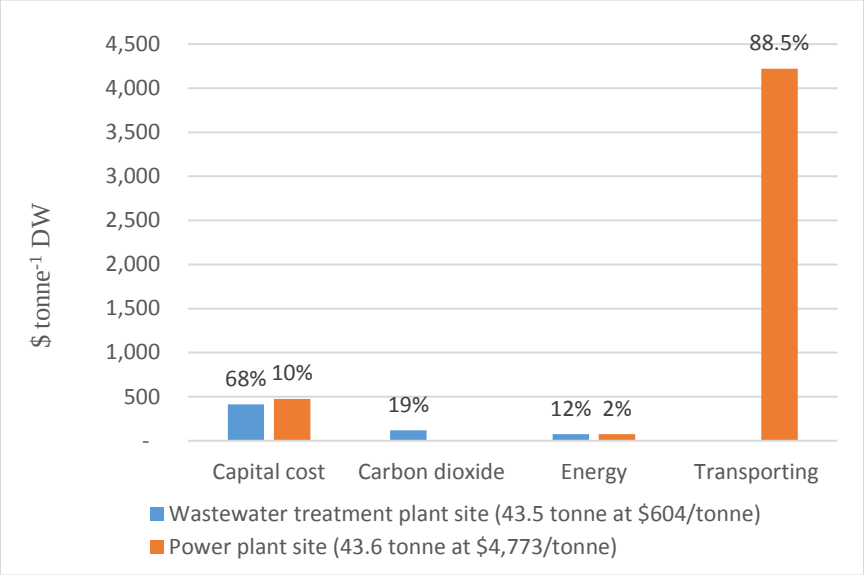

Chart 5.1: Comparing breakdown of the unit production costs for cultivating microalgae at a power plant and at a wastewater treatment plant.

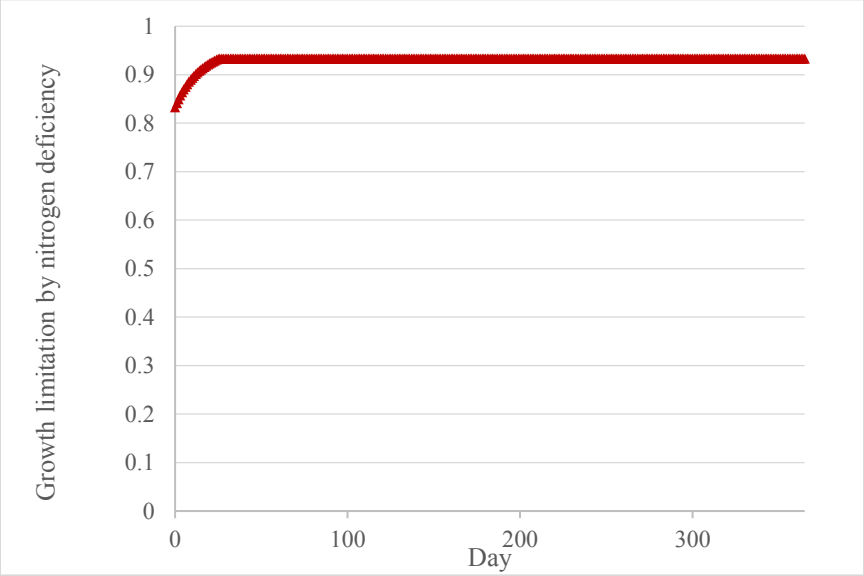

Figure 5.7: Limitation on the growth rate due to nitrogen deficiency in the optimal supply chain scenario.

5.5 Conclusions

This chapter addresses the issue of optimal siting of microalgae cultivation with respect to availability of waste nutrients, mainly nitrogen, and waste CO_2. A model is developed to estimate the effect of nitrogen deficiency on growth limitation. Also, a model is developed to determine the cost of transporting treated wastewater from a wastewater treatment plant to an algae cultivation facility using a rented truck. In the first analyzed scenario, microalgae is cultivated at a wastewater treatment plant benefiting from wastewater nutrients while purchasing pure CO_2 from an external source. In the other scenario, cultivation happens in a power plant where flue gas CO_2 is available but treated wastewater supplying nutrients is transported to the facility. A supply chain optimization framework is developed to determine the optimal location for an algae facility as well as the optimal operating profiles at the cultivation system. In conclusion, cultivation of microalgae utilizing wastewater nutrients can be economically advantageous when local treated wastewater is available. Transporting treated wastewater to an algal biomass production site can be extremely costly even for short travel distances due to the high fixed transportation cost. The cost of purchasing CO_2 is much lower than the cost of transporting wastewater.

CHAPTER 6

Conclusions and Future Work

6.1 Conclusions

Compared to other oil crops, microalgae can achieve much higher oil yields and CO_2 fixation rates making algal biomass a potential feedstock for the production of ecofriendly renewable biofuels [9]. However, the cost of cultivating algal biomass remains too high for creating low-value products such as transportation fuels [27]. Research has shown that the most economically promising configuration for production of algal biofuels is cultivation of microalgae in outdoor open ponds and in such systems algal cultures are susceptible to the effects of weather vagaries. In this research, a dynamic optimization formulation was developed to determine the optimal operations of an outdoor open pond for mitigating the impact of changing weather conditions on the growth of microalgae. The formulation incorporated daily weather conditions for a representative location for microalgae cultivation and the optimized operations included the dilution rate, CO_2 gas flowrate, and makeup water flowrate. Based on the case study presented in Chapter 2, optimizing the operations on a monthly basis can lower the cost of microalgae cultivation by 11% from a reference case price of \$758 $tonne^{-1}$.

The developed formulation provided the capacity to explore utilization of waste heat recovery in heating up the open pond culture to improve the growth conditions for cultivation during cold weather. Chapter 4 investigates the economic advantage of using hot flue gases from power production in heating the open pond water using a shell and tube heat exchanger. Based on the analyzed case, heating can indeed improve the growth rate of microalgae and consequently increase the annual harvest from 47.4 to 48.6 tonne DW. However, heating would increase the cost of cultivating microalgae from \$666 $tonne^{-1}$ to \$727 $tonne^{-1}$ due to the relatively high capital cost of the heat exchanger.

In addition, more economical alternatives were evaluated for the supply of CO_2, nitrogen, and phosphorus to the algal culture of the open pond. In Chapter 3, the utilization of waste CO_2 from industrial flue gases rich in CO_2 was analyzed for a case where exhausts from power production are cooled and injected to an open pond. The flue gas was found to be as effective in supporting the growth of microalgae and more economical than purchasing a pure CO_2 gas. For the supply of nutrients, the economic impact of recovering nitrogen and phosphorus from treated wastewater was investigated in Chapter 5 and found to be more economical than using fertilizers. Moreover, Chapter 5 includes a supply chain optimization for siting an algae facility where treated wastewater is supplied from nearby wastewater treatment plants to the candidate locations, i.e. power plants. The analysis shows that cultivating microalgae at a wastewater treatment plant using pure CO_2 is significantly more economical than transporting treated wastewater to a power plant.

Nevertheless, cultivation at power plants, using flue gases to supply CO_2 and fertilizers to supply nitrogen and phosphorus, was found to be the most economical configuration for algal biomass production as demonstrated in Chapter 3.

According to the scenarios considered in this research, the cost of cultivating algal biomass using an outdoor open pond in a suitable location favoring algae growth is at least \$602 tonne^{-1}. In laboratory studies, the algal species *N. Salina* achieved lipid content as high as 50%, however, a maximum lipid content of 20% was reported for cultivation in an outdoor open pond [119]. The lower lipid content is more realistic due to the suboptimal growth conditions and the desire to balance lipid content and biomass productivity in outdoor cultivation in open ponds. Assuming a lipid content of 20% and the density of algal oil to be equivalent to soybean oil at 918 kg m^{-3}, then the cost of crude algal oil would be at least \$10.5 gal^{-1} [71]. Although algal biofuels are technically feasible, further research is needed to improve their economic viability as compared with petroleum crude oil which costs around \$2 gal^{-1}. Possible directions for future research in modeling and optimization of outdoor microalgae cultivation are discussed in the following section.

There are several species of microalgae possessing unique set of characteristics that hold potential for algal biofuels production. Moreover, unlike conventional chemical plants, microalgae cultivation is highly sensitive to the geographic location due to the distinct combination of weather conditions at each candidate location. Therefore, modeling tools can provide a means to estimating productivities and economics of algal systems for

different species and potential sites. The developed formulation in this research accounts for the weather conditions at cultivation sites as well as the species-specific growth parameters making it valuable for guiding pilot studies and avoiding risky investments. As demonstrated throughout this research, there are several tradeoffs governing algal growth in outdoor systems in addition to the wide range of possible combinations of operating conditions in algae cultivation. Consequently, employing dynamic optimization can achieve substantial savings in time and other resources which otherwise would be spent on experimenting with models of algae growth. The novelty of the proposed optimization formulation resides in its capability of performing dynamic optimization for several operating conditions while incorporating data for daily weather conditions for an annual production cycle.

6.2 Future Work

6.2.1 Integration of Waste Heat and CO_2 Recovery

Supplying algal cultivation systems with CO_2 from waste sources such as industrial flue gases can be economically advantageous as investigated in Chapter 3 of this thesis. On the other hand, recovering waste heat from a flue gas to warm up the algal culture during cold weather is not encouraged due to the relatively high capital cost of the heat exchanger as shown in the case study presented in Chapter 4. Hot flue gases holding waste heat recovery potential are also CO_2-rich in a wide range of industries. The recovery of

waste heat and waste CO_2 in a single step is technically feasible using an absorber-type column at the same time serving as a direct contact heat exchanger. A future direction of this work is to evaluate the economic advantage of integrating waste heat recovery and waste CO_2 recovery by developing a model for a tray absorber capturing the heat as well as mass transfers occurring in the column. Moreover, the operations of the column can be optimized to maximize CO_2 recovery over heat recovery or both at the same time depending on the need at the algal cultivation system.

In Chapter 4, it was shown that heat losses from the open pond surface are dominated by the loss of heat through thermal radiation from the water surface. A future direction is to investigate the economics of different alternatives for reducing the exposed area of the pond water especially at night to minimize heat losses. For example, one option is to store the pond water in a container providing lower exposed surface area to volume ratio. Moreover, the analysis could be combined with waste heat recovery because the heat recovered can be better maintained in such scenarios of minimized heat losses to the surrounding environment.

6.2.2 Siting of Algae Facilities Worldwide

Based on the analysis presented in Chapter 2, algae facilities adopting outdoor open ponds and having access to local meteorological data can use the presented formulation to lower the cultivation cost by identifying optimal operating conditions. Furthermore, the

proposed formulation can be useful for determining facility locations for algal biomass production by comparing candidate sites based on optimized operations.

The developed model for analyzing algal biomass production in an outdoor open pond can be applied to any other location in the world given weather conditions for the particular site are available. A future direction is to expand the search for optimal algae cultivation sites beyond Imperial County especially where weather conditions favor algae growth and waste sources for heat, CO_2 and nutrients are also available. Moreover, in addition to the algal strain of *N. Salina*, the developed framework for estimating the growth of microalgae can accommodate other strains that hold potential in algal biofuels production.

6.2.3 Alternative Harvesting Schemes

In Chapter 2, it was shown that the dilution rate is the most important operating parameter in outdoor cultivation of microalgae production using open ponds. The case studies analyzed in this research were optimized for an open pond operating in continuous mode. Several studies in the literature adopt batch (semi-continuous) cultivation of algal biomass in open ponds [104]. The developed dynamic optimization formulation provides a valuable tool for exploring batch mode cultivation while optimizing the cultivation time.

a	total interfacial area of CO_2 gas bubbles (m^{-1})
a_c	interfacial area between the flue gas bubbles and cooling water droplets (m^{-1})
α_1	atmospheric attenuation coefficient
α_2	Bowen's coefficient (mmHg $^oC^{-1}$)
α_3	radiation absorption factor
α_4	fraction accounting for the visible portion of solar irradiance
α_5	reflection coefficient
α_6	correction factor for the compression of gas under water
α_7	kinetic loss coefficient
α_8	conversion factor (9.8 Watt s kg^{-1} m^{-1})
α_9	daily hours the paddle wheel is operating (24 h day^{-1})
A	cooling tower cross sectional area (m^2)
B	rate of basal metabolism processes (day^{-1})
B_m	metabolic rate at reference temperature (day^{-1})
β	fractional length of a day with daylight
$cost_{CO_2}$	cost of CO_2 supplied to the open pond (\$ day^{-1})
$cost_{cooling}$	cost of operating the heat exchanger used in cooling the flue gas (\$ day^{-1})
$cost_{energy}$	cost of energy supplied to the pond (\$ day^{-1})
$cost_{heating}$	cost of operating the heat exchanger used in heating the pond water (\$ day^{-1})
$cost_{Nutrients}$	cost of nutrients supplied to the pond (\$ day^{-1})
$cost_{trans}$	cost of transporting treated wastewater to an algae facility (\$ day^{-1})
$cost_{water}$	cost of freshwater supplied to the pond (\$ day^{-1})
c_p	specific heat capacity of water (cal K^{-1} g^{-1})
C	fitting parameter for the volumetric heat transfer coefficients
C_{algae}	mass concentration of microalgae in the pond (g DW m^{-3})
$C_{algae_{feed}}$	concentration of algae in the feed (g DW m^{-3})
C_{CO_2}	molar concentration of CO_2 in the pond (mol m^{-3})
$C_{CO_2,atm}$	equilibrium concentration of atmospheric CO_2 in water at 20 ^oC (mol m^{-3})
C_N	extracellular concentration of nitrogen (gN m^{-3})
Cap	truck capacity for transporting water (m^3)
$Cond$	amount of vapor condensing out of the flue gas (kg hr^{-1})
CC_{cooler}	amortized capital cost of the cooling tower/heat exchanger (\$ $year^{-1}$)
CC_{heater}	amortized capital cost of the shell and tube heat exchanger used for heating (\$ $year^{-1}$)
CC_{Pond}	amortized capital cost of the open pond cultivation system (\$ $year^{-1}$)
CO_{trans}	truck charge-out rate for transporting water (\$ hr^{-1})

d_b	diameter of CO_2 gas bubble (mm)
d_{trans}	travel distance for transporting wastewater (mile)
D	dilution rate (day^{-1})
E	heat exchanged through the water surface of the CSTR (cal cm^{-2} day^{-1})
E_a	heat added to the CSTR water from the atmospheric long-wave (cal cm^{-2} day^{-1})
E_c	heat lost from the CSTR water by conduction to atmosphere (cal cm^{-2} day^{-1})
E_{mixing}	energy requirement for mixing the open pond water (kWh day^{-1})
E_s	heat added to the CSTR water from the absorbed solar irradiance (cal cm^{-2} day^{-1})
E_v	latent heat flux (cal cm^{-2} day^{-1})
E_w	heat lost from the CSTR water through water long-wave (cal cm^{-2} day^{-1})
ε	water emissivity
ε_g	gas hold up
$f_I, f_T, f_{Nutrient}$	attenuation factors for light, temperature, and nutrient limitations
$f_{Nutrient\_C}$	attenuation factor due to carbon deficiency
$f_{Nutrient\_N}$	attenuation factor due to nitrogen deficiency
F_{dry}	flowrate of the flue gas on dry basis (kg hr^{-1})
F_{evap}	water evaporating from a CSTR in the open pond (m^3 day^{-1})
F_{feed}	flowrate of the open pond feed stream (m^3 day^{-1})
$F_{harvest}$	flowrate of the open pond harvest stream (m^3 day^{-1})
F_{in}	water entering a CSTR from a previous CSTR within an open pond (m^3 day^{-1})
F_{makeup}	makeup water flowrate (m^3 day^{-1})
F_{out}	water leaving a CSTR to the following CSTR within the open pond (m^3 day^{-1})
FC_{trans}	fixed transportation cost for shipping water (\$ m^{-3})
g	acceleration of gravity (m s^{-2})
G	rate of CO_2 bubbling into the pond water (mol day^{-1})
G_s	flue gas superficial mass velocity inside the cooling tower (kg m^{-2} s^{-1})
h	head the pump overcomes to rise the cooling water to the tower top (m)
$harvest$	algal biomass harvested daily (tonne day^{-1})
$h_{friction/bend}$	head loss from friction and from flow around the bends and sumps (m)
h_g	gas side volumetric heat transfer coefficient (J s^{-1} m^{-2} K^{-1})
h_l	liquid side volumetric heat transfer coefficient (J s^{-1} m^{-2} K^{-1})
H	depth of water in a CSTR in the open pond (m)
H_e	dimensionless Henry's constant
H_{eff}	efficiency of algal biomass harvest (%)
$H_{g,\ in}$	enthalpy of the flue gas entering the heat exchanger on dry basis (J hr^{-1})
$H_{g,\ out}$	enthalpy of the flue gas exiting the heat exchanger on dry basis (J hr^{-1})
$H_{v,\ in}$	enthalpy of the water vapor in the flue gas entering the heat exchanger (J hr^{-1})
$H_{v,\ out}$	enthalpy of the water vapor in the flue gas exiting the heat exchanger (J hr^{-1})
$H_{w,\ in}$	enthalpy of the cooling water entering the heat exchanger (J hr^{-1})
$H_{w,\ out}$	enthalpy of the cooling water exiting the heat exchanger (J hr^{-1})
$H_{c,\ out}$	enthalpy of the condensed vapor from the flue gas exiting the heat exchanger (J hr^{-1})
i	index for the location of the CSTR relative to the other CSTRs in the open pond

I	visible irradiance absorbed at the pond surface over daylight hours (μE m^{-2} s^{-1})
I_a	daily average solar irradiance at the pond surface (W m^{-2})
I_{max}	maximum irradiance above which algae growth does not increase (μE m^{-2} s^{-1})
k_B	exponential fitting constant for metabolic rate ($^oC^{-1}$)
k_e	extinction coefficient related to water turbidity and algae concentration (m^{-1})
k_w	water (background) turbidity (m^{-1})
$k_{T,1}$,$k_{T,2}$	fitting constants of the attenuation factor due to temperature limitation ($^oC^{-2}$)
K_{atm}	mass transfer coefficient for diffusion of CO_2 to/from the atmosphere (m day^{-1})
K_C	half saturation constant for CO_2 (mol CO_2 m^{-3})
K_L	mass transfer coefficient for CO_2 transfer from gas phase to liquid phase (m day^{-1})
K_N	half saturation constant for nitrogen uptake (gN m^{-3})
K_s	inhibition constant for CO_2 (mol CO_2 m^{-3})
L	length of the CSTR in the open pond (m)
L_e	latent heat of evaporation (cal g^{-1})
L_s	cooling water superficial mass velocity inside the cooling tower (kg m^{-2} s^{-1})
$m_{1,2}$	fitting parameters for the volumetric heat transfer coefficients
M_{eff}	efficiency of the paddle wheel mixing system
μ	growth rate of microalgae (day^{-1})
μ_{max}	maximum algae growth rate (day^{-1})
n	number of compartments the open pond is segmented to
n_o	Gauckler-Manning coefficient; a roughness factor (day $m^{-1/3}$)
N_o	number of bubbles of gas formed at the sump bottom (s^{-1})
P_{air}	vapor pressure in the overlaying air (mmHg)
P_{eff}	cooling water pump efficiency (%)
P_g	pressure of CO_2 gas (atm)
Pr	productivity of algal biomass in the open pond (g DW m^{-2} day^{-1})
P_{sat}	saturation vapor pressure for a given water temperature (mmHg)
P_T	total pressure of the flue gas exiting the heat exchanger (Pa)
P_{vap}	vapor pressure of water at the temperature of the cooled flue gas (Pa)
PP	candidate power plant site for hosting an algae cultivation facility
ΔP	pressure drop of the pond water due to heating (kPa)
q_N	intercellular concentration of nitrogen (gN g^{-1} DW)
q_{N_min}	minimum intercellular concentration of nitrogen where growth ceases (gN g^{-1} DW)
$Q_{cooling\ water}$	quantity of cooling water pumped to the cooling tower (m^3 day^{-1})
Q_{flue}	flue gas flowrate (m^3 day^{-1})
Q_g	CO_2 gas flowrate (m^3 day^{-1})
Q_{heater}	power needed to overcome the drop in water pressure while heating (kWh day^{-1})
$Q_{pumping\ power}$	power needed at the cooling water pump (kWh day^{-1})
Q_{water}	cooling water flowrate (m^3 day^{-1})
r	hydraulic radius of pond channel (m)
R_g	universal gas constant (atm m^3 mol^{-1} K^{-1})
R_{CO_2}	carbon dioxide requirement (mol CO_2 g^{-1} DW)

R_{Chl}	algal biomass chlorophyll content (g Chl kg^{-1} DW)
R_{DAP}	phosphorus content of diammonium phosphate (g DAP g^{-1} P)
R_N	nitrogen content of algal biomass (g N g^{-1} DW)
R_{NH_3}	nitrogen content of ammonia (g NH3 g^{-1} N)
R_P	phosphorus content of algal biomass (g P g^{-1} DW)
ρ	density of water (g cm^{-3})
ρ_{CO_2}	density of CO_2 gas (g cm^{-3})
σ	Stefan-Boltzmann constant (cal cm^{-2} d^{-1} K^{-4})
S	splitting ratio in the pond water heating scenario
t_p	length of a day in hours (24 h)
T_{air}	daily average local air temperature (°C)
T_B	reference temperature for metabolic rate (°C)
T_c	time horizon of a production cycle
T_g	temperature of CO_2 gas (°C)
$T_{loading}$	total liquid loading and unloading time (min)
T_{opt}	optimal temperature for algae growth (°C)
T_w	temperature of the water in the CSTR (°C)
ΔT_{LMTD}	log mean temperature difference in the cooling tower (K)
U	wind speed above the open pond water (m s^{-1})
$U_{Nitrogen}$	specific uptake rate of nitrogen from the algal culture (gN g^{-1} DW day^{-1})
$U_{Nitrogen\_max}$	maximum specific uptake rate of nitrogen from the algal culture (gN g^{-1} DW day^{-1})
UPC	yearly average algal biomass unit production cost ($ $tonne^{-1}$)
U_v	volumetric overall heat transfer coefficient (J s^{-1} m^{-3} K^{-1})
v	water velocity in the open pond (cm s^{-1})
v_b	gas terminal velocity (cm s^{-1})
v_{trans}	traveling speed for transporting water (mile hr^{-1})
VC_{trans}	variable transportation cost for shipping water ($ m^{-3} $mile^{-1}$)
W	width of the CSTR in the open pond (m)
W_s	width of the CO_2 gas sump station (m)
$WWTP$	candidate wastewater treatment plant for supplying treated wastewater
x_{CO_2}	price of CO_2 ($ $tonne^{-1}$)
x_{DAP}	price of diammonium phosphate ($ $tonne^{-1}$)
x_e	price of electricity ($ kWh^{-1})
x_{NH_3}	price of ammonia ($ $tonne^{-1}$)
x_w	price of agricultural water ($ m^{-3})
X_{in}	moisture content of the flue gas entering the heat exchanger (kg vapor kg^{-1} dry gas)
X_{out}	moisture content of the flue gas exiting the heat exchanger (kg vapor kg^{-1} dry gas)
$y_{in/out}$	CO_2 mole in the inlet/outgassing bubbles
y_w	mole fraction of water in the cooled flue gas
z	vertical distance from the water surface in the pond (m)
Z_p	height of the packing in the cooling tower/heat exchanger (m)

Bibliography

[1] IPCC, “Contribution of Working Groups I, II and III to the Fourth Assessment Report of the Intergovernmental Panel on Climate Change,” 2007.

[2] M. Steinacher, F. Joos, and T. F. Stocker, “Allowable carbon emissions lowered by multiple climate targets,” *Nature*, vol. 499, no. 7457. pp. 197–201, 2013.

[3] J. G. J. Oliviera, J. A. Van Aardenneb, and F. J., “Recent trends in global greenhouse gas emissions: regional trends 1970–2000 and spatial distribution of key sources in 2000,” *Environ. Sci.*, vol. 2, no. 2–3, pp. 81–99, 2005.

[4] A. Hooijer, M. Silvius, H. Wösten, and S. Page, “PEAT-CO2, Assessment of CO2 emissions from drained peatland in SE Asia,” 2006.

[5] J. G. J. Olivier, G. Janssens-Maenhout, M. Muntean, and J. A. H. W. Peters, “Trends in global CO2 emissions: 2014 Report,” 2014.

[6] C. Davenport, “A Climate Accord Based on Global Peer Pressure.” [Online]. Available: http://www.nytimes.com/2014/12/15/world/americas/lima-climate-deal.html. [Accessed: 01-Jun-2015].

[7] D. S. Powlson, A. B. Riche, and I. Shield, “Biofuels and other approaches for decreasing fossil fuel emissions from agriculture.,” *Ann. Appl. Biol.*, no. 146, pp. 193–201, 2005.

[8] International Energy Agency, “Key World Energy Statistics 2011.” [Online]. Available: http://www.iea.org/publications/freepublications/publication/name,20938,en.html. [Accessed: 06-Sep-2012].

[9] Y. Chisti, “Biodiesel from Microalgae,” *Biotechnol. Adv.*, vol. 25, no. 25, pp. 294–306, 2007.

[10] Á. T. Martínez, M. Speranza, F. J. Ruiz-Dueñas, P. Ferreira, S. Camarero, F. Guillén, M. J. Martínez, A. Gutiérrez, and J. C. del Río, “Biodegradation of lignocellulosics: microbial, chemical, and enzymatic aspects of the fungal attack of lignin,” *Int. Microbiol.*, vol. 8, pp. 195–204, 2005.

[11] Y. Zheng, Z. Pan, and R. Zhang, “Overview of biomass pretreatment for cellulosic ethanol production,” *Int J Agric Biol Eng*, vol. 2, no. 3, pp. 51–68, 2009.

[12] J. R. Benemann and W. J. Oswald, “Systems and Economic Analysis of Microalgae Ponds for Conversion of C02 to Biomass,” 1996.

[13] S. Mandal and N. Mallick, “Microalga Scenedesmus obliquus as a Potential Source for biodiesel Production,” *Appl. Microbiol. Biotechnol.*, vol. 2, no. 84, pp. 281–291, 2009.

[14] X. Miao and Q. Wu, “Biodiesel production from heterotrophic microalgal oil.,” *Bioresour. Technol.*, vol. 97, no. 6, pp. 841–6, Apr. 2006.

[15] S. Aaronson and Z. Dubinsky, “Mass Production of Microalgae,” *Cell. Mol. life Sci.*, vol. 1, no. 38, pp. 36–40, 1982.

[16] J. C. Weissman, R. P. Goebel, and J. R. Benemann, “Photobioreactor Design: Mixing, Carbon Utilization, and Oxygen Accumulation,” *Biotechnol. Bioeng.*, vol. 31, pp. 336–344, 1988.

[17] K. Sander and G. S. Murthy, “Life cycle analysis of algae biodiesel,” *Int. J. Life Cycle Assess.*, vol. 15, no. 7, pp. 704–714, Jun. 2010.

[18] K. Lum and X. G. Lei, “Potential of Defatted Algal Meal Derived From Biofuel Production as a New Generation of Feed Protein Supplement,” in *2011 Cornell Nutrition Conference for Feed Manufacturers*, pp. 111–113.

[19] J. A. Stamey, D. M. Shepherd, M. J. de Veth, and B. A. Corl, “Use of algae or algal oil rich in n-3 fatty acids as a feed supplement for dairy cattle,” *J. Dairy Sci.*, vol. 95, no. 9, pp. 5269–5275, 2012.

[20] S. Hemaiswarya, R. Raja, R. R. Kumar, V. Ganesan, and C. Anbazhagan, “Microalgae: a sustainable feed source for aquaculture,” *World J Microbiol Biotechnol*, no. 27, pp. 1737–1746, 2011.

[21] E. W. Becker, “Micro-algae as a source of protein,” *Biotechnol. Adv.*, no. 25, pp. 207–210, 2007.

[22] W. Oswald, “Advanced Integrated Wastewater Pond Systems.,” in *ASCE Convention: Supplying Water and Saving the environment for Six Billion People*, 1990, pp. 74–81.

[23] P. Pienkos and A. Darzins, “The Promise and Challenges of Microalgal-derived Biofuels,” *Biofuels Bioprod. Biorefin.*, vol. 4, no. 3, pp. 431–440, 2009.

[24] L. Christenson and R. Sims, “Production and harvesting of microalgae for wastewater treatment, biofuels, and bioproducts,” *Biotechnol. Adv.*, vol. 29, no. 6, pp. 686–702, 2011.

[25] N. Abdel-Raouf, A. A. Al-Homaidan, and I. B. M. Ibraheem, “Microalgae and wastewater treatment,” *Saudi Journal of Biological Sciences*, vol. 19, no. 3. pp. 257–275, 2012.

[26] P. M. Foley, E. S. Beach, and J. B. Zimmerman, “Algae as a source of renewable chemicals: opportunities and challenges,” *Green Chem.*, vol. 13, p. 1399, 2011.

[27] R. Davis, A. Aden, and P. T. Pienkos, “Techno-economic analysis of autotrophic microalgae for fuel production,” *Appl. Energy*, vol. 88, no. 10, pp. 3524–3531, 2011.

[28] R. Radakovits, R. E. Jinkerson, A. Darzins, and M. C. Posewitz, “Genetic Engineering of Algae for Enhanced Biofuel Production,” *Eukaryot. Cell*, vol. 9, no. 4, pp. 486–501, 2010.

[29] C. U. Ugwu, H. Aoyagi, and H. Uchiyama, “Photobioreactors for mass cultivation of algae.,” *Bioresour. Technol.*, vol. 99, no. 10, pp. 4021–4028, Jul. 2008.

[30] J. Gong and F. You, “Optimal Design and Synthesis of Algal Biore fi nery Processes for Biological Carbon Sequestration and Utilization with Zero Direct Greenhouse Gas Emissions: MINLP Model and Global Optimization Algorithm,” *Ind. Eng. Chem. Res.*, vol. 53, no. 4, pp. 1563–1579, 2014.

[31] M. Martín and I. E. Grossmann, “Simultaneous Optimization and Heat Integration for Biodiesel Production from Cooking Oil and Algae,” *Ind. Eng. Chem. Res.*, vol. 51, pp. 7998–8014, 2012.

[32] J. D. Smith, A. A. Neto, S. Cremaschi, and D. W. Crunkleton, “CFD-Based Optimization of a Flooded Bed Algae Bioreactor,” *Ind. Eng. Chem. Res.*, vol. 52, p. 7181−7188, 2013.

[33] M. Gross, “Development and optimization of algal cultivation systems.,” Iowa State University, 2013.

[34] K.-H. Park and C.-G. Lee, “Optimization of Algal Photobioreactors Using

Flashing Lights," *Biotechnol. Bioprocess Eng.*, vol. 5, pp. 186–190, 2000.

[35] K. McKnight, "Optimizing Growth of Microalgae for Use as a Potential Biofuel Feedstock," Lawrence Berkeley National Laboratory, USA, 2013.

[36] A. Richmond and Z. Cheng-Wu, "Optimization of a flat plate glass reactor for mass production of Nannochloropsis sp. outdoors," *J. Biotechnol.*, vol. 85, pp. 259–269, 2001.

[37] A. Thornton, T. Weinhart, O. Bokhove, B. Zhang, D. M. van der Sar, K. Kumar, M. Pisarenco, M. Rudnaya, V. Savcenco, J. Rademacher, J. Zijlstra, A. Szabelska, J. Zyprych, M. van der Schans, V. Timperio, and F. Veerman, "Modeling and optimization of algae growth," 2010.

[38] L. He, V. R. Subramanian, and Y. J. Tang, "Experimental analysis and model-based optimization of microalgae growth in photo-bioreactors using flue gas," *Biomass and Bioenergy*, vol. 41, pp. 131–138, 2012.

[39] K. G. Zeiler, D. A. Heacox, S. T. Toon, K. L. Kadam, and L. M. Brown, "The use of microalgae for assimilation and utilization of carbon dioxide from fossil fuel-fired power plant flue gas," *Energy Convers. Manag.*, vol. 36, no. 6–9, pp. 707–712, 1995.

[40] G. Pokoo-Aikins, A. Nadim, M. M. El-Halwagi, and V. Mahalec, "Design and analysis of biodiesel production from algae grown through carbon sequestration," *Clean Technol. Environ. Policy*, vol. 12, no. 3, pp. 239–254, Mar. 2009.

[41] J. Doucha, F. Straka, and K. Lívanský, "Utilization of flue gas for cultivation of microalgae (Chlorella sp.) in an outdoor open thin-layer photobioreactor," *J. Appl. Phycol.*, vol. 17, no. 5, pp. 403–412, 2005.

[42] R. Baliga and S. E. Powers, "Sustainable algae biodiesel production in cold climates," *Int. J. Chem. Eng.*, 2010.

[43] L. F. Lira-Barragán, C. G. Gutiérrez-Arriaga, H. S. Bamufleh, F. Abdelhady, J. M. Ponce-Ortega, M. Serna-González, and M. M. El-Halwagi, "Reduction of greenhouse gas emissions from steam power plants through optimal integration with algae and cogeneration systems," *Clean Technol. Environ. Policy*, vol. 17, no. 8, pp. 2401–2415, 2015.

[44] E. W. Wilde, J. R. Benemann, J. C. Weissman, and D. M. Tillett, "Cultivation of algae and nutrient removal in a waste heat utilization process," *J. Appl. Phycol.*,

vol. 3, no. 2, pp. 159–167, 1991.

[45] B. Dong, N. Ho, K. L. Ogden, and R. G. Arnold, “Cultivation of Nannochloropsis salina in municipal wastewater or digester centrate,” *Ecotoxicol. Environ. Saf.*, vol. 103, no. 1, pp. 45–53, 2014.

[46] J. P. Sheets, X. Ge, S. Y. Park, and Y. Li, “Effect of outdoor conditions on Nannochloropsis salina cultivation in artificial seawater using nutrients from anaerobic digestion effluent,” *Bioresour. Technol.*, vol. 152, pp. 154–161, 2014.

[47] “gPROMS.” Process Systems Enterprise, London, U.K., 2015.

[48] D. Piñol, J. C. Rodriguez, M. Halloran, M. Pons, and M. Woodman, “Thermodynamic and Physical Properties v1.0.” CAPE-OPEN, 2011.

[49] O. Perez-Garcia, F. M. E. Escalante, L. E. De-Bashan, and Y. Bashan, “Heterotrophic cultures of microalgae: Metabolism and potential products,” *Water Res.*, vol. 45, pp. 11–36, 2011.

[50] L. Rodolfi, G. C. Zittelli, N. Bassi, G. Padovani, N. Biondi, G. Bonini, and M. R. Tredici, “Microalgae for Oil: Strain Selection, Induction of Lipid Synthesis and Outdoor Mass Cultivation in a Low-Cost Photobioreactor,” *Biotechnol. Bioeng.*, vol. 102, no. 1, pp. 100–112, 2009.

[51] S. HA and M. HW, “The chemical composition of Chlorella: Effect of environmental conditions,” *Plant Physiol*, vol. 24, pp. 120–149, 1949.

[52] Y. Chisti, “Biodiesel from microalgae beats bioethanol.,” *Trends Biotechnol.*, vol. 26, no. 3, pp. 126–31, Mar. 2008.

[53] M. R. Tredici, P. Carlozzi, G. C. Zittelli, and R. Materassi, “Avertical alveolar panel (VAP) for outdoor mass cultivation of microalgae and cyanobacteria,” *Bioresour. Technol.*, vol. 38, no. 2–3, pp. 153–159, 1991.

[54] W. F. R. Bare, N. B. Jones, and E. J. Middlebrooks, “Algae Removal Using Dissolved Air Flotation,” *Water Pollut. Control Fed.*, vol. 47, no. 1, pp. 153–169, 1975.

[55] M. R. Teixeira and M. J. Rosa, “Comparing dissolved air flotation and conventional sedimentation to remove cyanobacterial cells of Microcystis aeruginosa: Part I: The key operating conditions,” *Sep. Purif. Technol.*, vol. 52, no. 1, pp. 84–94, 2006.

[56] W. V. Jr., M. J. Hammer, E. M. Perez, and P. A. Chadik, *Water Supply and Pollution Control*. Upper Saddle River, New Jersey: Prentice Hall, 2004.

[57] J. Kim, G. Yoo, H. Lee, J. Lim, K. Kim, C. W. Kim, M. S. Park, and J. W. Yang, "Methods of downstream processing for the production of biodiesel from microalgae," *Biotechnology Advances*, vol. 31, no. 6. pp. 862–876, 2013.

[58] J. L. Faeth and P. E. Savage, "The Effects of Heating Rate and Reaction Time On Hydrothermal Liquefaction of Microalgae," in *AICHE annual meeting*, 2012.

[59] "Algae Basics." [Online]. Available: http://allaboutalgae.com/algae-basics-photos/. [Accessed: 28-Dec-2016].

[60] "Algal Bioreactors." [Online]. Available: http://www.cambia.org/daisy/eos/4148.html. [Accessed: 28-Dec-2016].

[61] J. W. Richardson, M. D. Johnson, and J. L. Outlaw, "Economic comparison of open pond raceways to photo bio-reactors for profitable production of algae for transportation fuels in the Southwest," *Algal Res.*, vol. 1, no. 1, pp. 93–100, 2012.

[62] S. B. Miller and H. O. Buhr, "Mixing characteristics of a high-rate algae pond," *Water*, vol. 7, pp. 8–15, 1981.

[63] H. O. Buhr and S. B. Miller, "A dynamic model of the high-rate algal-bacterial wastewater treatment pond," *Water Res.*, vol. 17, no. 1, pp. 29–37, 1983.

[64] H. Jupsin, E. Praet, and J. L. Vasel, "Dynamic mathematical model of high rate algal ponds (HRAP)," *Water Sci. Technol.*, vol. 48, no. 2, pp. 197–204, 2003.

[65] A. Yang, "Modeling and Evaluation of CO2 Supply and Utilization in Algal Ponds," *Ind. Eng. Chem. Res.*, vol. 50, pp. 11181–11192, 2011.

[66] S. C. James and V. Boriah, "Modeling Algae Growth in an Open-Channel Raceway," *J. Comput. Biol.*, vol. 17, no. 7, pp. 895–906, 2010.

[67] C. F. Cerco and T. Cole, "User's Guide to the CE-QUAL-ICM Three-Dimensional Eutrophication Model," 1995.

[68] B. Ketheesan and N. Nirmalakhandan, "Modeling microalgal growth in an airlift-driven raceway reactor," *Bioresour. Technol.*, vol. 136, pp. 689–696, 2013.

[69] S. C. Chapra, *Surface Water-Quality Modeling*. Boulder: The McGRAW-Hill

Companies, INC., 1997.

[70] T. J. Lundquist, I. C. Woertz, N. W. T. Quinn, and J. R. Benemann, “A Realistic Technology and Engineering Assessment of Algae Biofuel Production,” Berkeley, California, 2010.

[71] K. M. Weyer, D. R. Bush, A. Darzins, and B. D. Willson, “Theoretical Maximum Algal Oil Production,” *Bioenerg. Res.*, vol. 3, pp. 204–213, 2010.

[72] A. Vonshak and L. Tomaselli, *Arthrospira (Spirulina): systematics and ecophysiology. In: Whitton, B.A.; Potts, M. (Eds.), Ecology of Cyanobacteria.*. The Netherlands: Kluwer Academic Publishing, 2000.

[73] M. J. Griffiths and S. L. Harrison, “Lipid productivity as a key characteristic for choosing algal species for biodiesel production,” *J Appl Phycol*, vol. 21, no. 5, pp. 493–507, 2009.

[74] A. Belay, Y. Ota, K. Miyakawa, and H. Shimamatsu, “Current knowledge on potential health benefits of Spirulina,” *J. Appl. Phycol.*, vol. 5, pp. 235–241, 1993.

[75] S. Boussiba, A. Vonshak, Z. Cohen, Y. Avissar, and A. Richmond, “Lipid and biomass production by the halotolerant microalga Nannochloropsis salina,” *Biomass*, vol. 12, no. 1, pp. 37–47, 1987.

[76] E. M. Grima, F. G. A. Ferna´ndez, F. G. Camacho, and Y. Chisti, “Photobioreactors: light regime, mass transfer, and scaleup,” *J. Biotechnol.*, vol. 70, pp. 231–247, 1999.

[77] J. L. P. Van Oorschot, “Conversion of Light Energy in Algal Cultures,” *Med. van. Lund. Wang.*, vol. 55, p. 225‑277, 1955.

[78] M. H. Huesemann, J. Van Wagenen, T. Miller, A. Chavis, S. Hobbs, and B. Crowe, “A Screening Model to Predict Microalgae Biomass Growth in Photobioreactors and Raceway Ponds,” *Biotechnol. Bioeng.*, vol. 110, no. 6, pp. 1583–1594, 2013.

[79] J. H. Steele, “Microbial Kinetics and Dynamics,” in *Chemical reactor theory*, Englewood Cliffs, N.J.: Prentice-Hall, 1977, pp. 405–483.

[80] G. A. Riley, “Oceanography of Long Island Sound, 1952-1954. II. Physical Oceanography,” *Bull. Bingham. Ocean. Collect.*, vol. 15, pp. 15–46, 1956.

[81] J. U. Grobbelaar, “Algal Nutrition,” in *Handbook of Microalgal Culture Biotechnology and Applied Phycology*, Oxford: Blackwell, 2006, pp. 97–115.

[82] D. Kaplan, A. E. Richmond, Z. Dubinsky, and S. Aaronson, “Algal nutrition,” in *Handbook of microalgal mass culture.*, Boca Raton: CRC Press, 1986, pp. 147–198.

[83] D. F. McGinnis and J. C. Little, “Predicting diffused-bubble oxygen transfer rate using the discrete-bubble model,” *Water Res.*, vol. 36, no. 18, pp. 4627–4635, 2002.

[84] J. C. Weissman and R. P. Goebel, “Design and analysis of microalgal open pond systems for the purpose of producing fuels: A subcontract report,” Fairfield, California, 1987.

[85] N. W. Hudson, *Field measurement of soil erosion and runoff*. Ampthill, UK: Food and Agriculture Organization of the United Nations, 1993.

[86] C. Jime´nez, B. R. Cossı´o, D. Labella, and F. X. Niell, “The Feasibility of industrial production of Spirulina (Arthrospira) in Southern Spain,” *Aquaculture*, vol. 217, pp. 179–190, 2003.

[87] C. Jime´neza, B. R. Cossı´o, and F. X. Niell, “Relationship between physicochemical variables and productivity in open ponds for the production of Spirulina: a predictive model of algal yield,” *Aquaculture*, vol. 221, pp. 331–345, 2003.

[88] Z. Cheng-Wu, O. Zmora, and R. Kopel, “An industrial-size flat plate glass reactor for mass production of Nannochloropsis sp. (Eustigmatophyceae),” *Aquaculture*, vol. 195, pp. 35–49, 2001.

[89] “Satel-Light, The European Database of Daylight and Solar Radiation.” [Online]. Available: http://www.satel-light.com/indexs.htm. [Accessed: 16-Jun-2015].

[90] “Tutiempo Network, S.L., Climate Malaga / Aeropuerto - Climate data (84820).” [Online]. Available: http://en.tutiempo.net/climate/07-1997/ws-84820.html. [Accessed: 16-Jun-2015].

[91] H. G. Stefan and J. J. Cardoni, “Model of Light Penetration in a Turbid Lake,” *Water Resour. Res.*, vol. 19, no. 1, pp. 109–120, 1983.

[92] S. Bhattacharya and M. K. Shivaprakash, “Evaluation of three Spirulina species

grownunder similar conditions for their growthand biochemicals," *J Sci Food Agric*, vol. 85, pp. 333–336, 2005.

[93] "National Alliance For Advanced Biofuels And Bioproducts Synopsis (NAABB): Full Final Report Section II.," 2014.

[94] A. Vonshak, "Spirulina: growth, physiology and Biochemistry," in *Spirulina platensis (Arthrospira): physiology, cell-biology, and biotechnology*, London: Taylor & Francis, 1997, pp. 43–65.

[95] J. K. Volkman, M. R. Brown, G. A. Dunstan, and S. W. Jeffrey, "The Biochemical Composition of Marine Microalgae from the Class Eustigmatophyceae," *J. Phycol*, vol. 29, pp. 69–78, 1993.

[96] "National Solar Radiation Data Base," *1991- 2005 Update: Typical Meteorological Year 3*, 2015. [Online]. Available: http://rredc.nrel.gov/solar/old_data/nsrdb/1991-2005/tmy3/. [Accessed: 16-Jun-2015].

[97] B. E. W, *Microalgae. Biotechnology and Microbiology*. Cambridge, UK: Cambridge University Press, 1994.

[98] G. A. Hughmark, "Holdup and Mass Transfer in Bubble Columns," *Ind. Eng. Chem. Proc. Des. Dev.*, vol. 6, pp. 218–220, 1967.

[99] P. Talbot, M. P. Gortares, R. W. Lencki, and J. de la Noiie, "Absorption of CO2 in Algal Mass Culture Systems: A Different Characterization Approach," *Biotechnol. Bioeng.*, vol. 37, pp. 834–842, 1991.

[100] A. P. C. Malcata and F. Xavier, "Transfer of Carbon Dioxide within Cultures of Microalgae: Plain Bubbling versus Hollow-Fiber Modules," *Biotechnol. Prog.*, vol. 17, pp. 265–272, 2001.

[101] "About IID Water," *Imperial Irrigation District*. [Online]. Available: http://www.iid.com/water/about-iid-water. [Accessed: 29-Jun-2015].

[102] "Wholesale Electricity and Natural Gas Market Data," *U.S. Energy Information Administration (EIA)*, 2015. [Online]. Available: http://www.eia.gov/electricity/wholesale/index.cfm. [Accessed: 27-Aug-2015].

[103] "Fertilizer Use and Price." [Online]. Available: https://www.ers.usda.gov/data-products/fertilizer-use-and-price.aspx. [Accessed: 01-Jan-2016].

[104] J. Quinn, L. de Winter, and T. Bradley, “Microalgae bulk growth model with application to industrial scale systems.,” *Bioresour. Technol.*, vol. 102, no. 8, pp. 5083–92, Apr. 2011.

[105] R. number PH3/14, “Leading options for the capture of CO2 emissions at power stations,” 2000.

[106] M. L. Bartley, W. J. Boeing, B. N. Dungan, F. O. Holguin, and T. Schaub, “pH effects on growth and lipid accumulation of the biofuel microalgae Nannochloropsis salina and invading organisms,” *J. Appl. Phycol.*, pp. 1–7, 2013.

[107] M. Negoro, A. Hamasaki, Y. Ikuta, T. Makita, K. Hirayama, and S. Suzuki, “Carbon dioxide fixation by microalgae photosynthesis using actual flue gas discharged from a boiler,” *Appl. Biochem. Biotechnol.*, vol. 39–40, no. 1, pp. 643–653, 1993.

[108] K. L. Kadam, “Microalgae Production from Power Plant Flue Gas: Environmental Implications on a Life Cycle Basis,” 2001.

[109] V. Bontozoglou and A. J. Karabelas, “Direct-contact steam condensation with simultaneous noncondensable gas absorption,” *AIChE J.*, vol. 41, no. 2, pp. 241–250, 1995.

[110] X. N. Ma, T. P. Chen, B. Yang, J. Liu, and F. Chen, “Lipid production from Nannochloropsis,” *Mar. Drugs*, vol. 14, no. 4, 2016.

[111] T. Robert, “Condensing Heat Recovery for Industrial Process Applications,” *Process Heat.*, no. February, 2015.

[112] J. R. Fair, “Direct Contact Gas-Liquid Heat Exchange for Energy Recovery Energy,” *Sol. Energy Eng.*, vol. 112, pp. 216–222, 1990.

[113] I. Veidenbergs, D. Blumberga, E. Vigants, and G. Kozuhars, “Heat and Mass Transfer Processes in Scrubber of Flue Gas Heat Recovery Device,” *Sci. J. Riga Tech. Univ. Environ. Clim. Technol.*, vol. 4, no. 1, pp. 109–115, 2011.

[114] A. A. Al-Farayedhi, P. Gandhidasan, and M. A. Al-Mutairi, “Evaluation of heat and mass transfer coefficients in a gauze-type structured packing air dehumidifier operating with liquid desiccant,” *Int. J. Refrig.*, vol. 25, no. 3, pp. 330–339, 2002.

[115] Y. Li, J. F. Klausner, R. Mei, and J. Knight, “Direct contact condensation in packed beds,” *Int. J. Heat Mass Transf.*, vol. 49, no. 25–26, pp. 4751–4761, 2006.

[116] D. B. Menzel, *EPA Air Pollution Control Cost Manual*, vol. 203, no. 4380. 1979.

[117] R. Turton, R. C. Bailie, W. B. Whiting, and J. A. Shaeiwitz, *Analysis, Synthesis, and Design of Chemical Processes*, 3rd ed. Boston: Pearson Education, Inc, 2009.

[118] E. W. Becker, *Microalgae. Biotechnology and Microbiology*. Cambridge: Cambridge University Press, 1994.

[119] B. Crowe, S. Attalah, S. Agrawal, P. Waller, R. Ryan, J. Van Wagenen, A. Chavis, J. Kyndt, M. Kacira, K. L. Ogden, and M. Huesemann, "A comparison of nannochloropsis salina growth performance in two outdoor pond designs: Conventional raceways versus the arid pond with superior temperature management," *Int. J. Chem. Eng.*, 2012.

[120] C. Arzbaecher, G. Hamilton, and K. Parmenter, "Condensing Boiler Economizers," Walnut Creek, CA, 2009.

[121] BCS Incorporated, "Waste Heat Recovery: Technology Opportunities in the US Industry," 2008.

[122] D. Bharathan, B. K. Parsons, and J. Althof, "Direct-Contact Condensers for Open-Cycle OTEC Applications," Golden, Colorado, 1988.

[123] U.S. Department of Energy, "Considerations When Selecting a Condensing Economizer," *Energy Efficiency & Renewable Energy*, 2012. [Online]. Available: https://www1.eere.energy.gov/manufacturing/tech_assistance/pdfs/steam26b_condensing.pdf. [Accessed: 08-Jan-2016].

[124] Q. Chen, K. Finney, H. Li, X. Zhang, J. Zhou, V. Sharifi, and J. Swithenbank, "Condensing boiler applications in the process industry," *Appl. Energy*, vol. 89, no. 1, pp. 30–36, 2012.

[125] M. Terhan and K. Comakli, "Design and economic analysis of a flue gas condenser to recover latent heat from exhaust flue gas," *Appl. Therm. Eng.*, vol. 100, pp. 1007–1015, 2016.

[126] Process Systems Enterprise Ltd., "PML: Heat Exchange. gPROMS Process Model Library Documentation." Process Systems Enterprise, 2015.

[127] K. Y. Leong, R. Saidur, T. M. I. Mahlia, and Y. H. Yau, "Modeling of shell and tube heat recovery exchanger operated with nanofluid based coolants," *Int. J. Heat Mass Transf.*, vol. 55, no. 4, pp. 808–816, 2012.

[128] “Flue gas condenser,” *Thermeta*. [Online]. Available: http://www.thermeta.nl/documents/FLDR_EKA0705.03-EN.pdf.

[129] H. Campos, W. J. Boeing, B. N. Dungan, and T. Schaub, “Cultivating the marine microalga Nannochloropsis salina under various nitrogen sources: Effect on biovolume yields, lipid content and composition, and invasive organisms,” *Biomass and Bioenergy*, vol. 66, pp. 301–307, 2014.

[130] R. R. L. Guillard and J. H. Ryther, “Studies of marine planktonic diatoms: I. Cyclotella nana Hustedt, and Detonula confervacea (Cleve) Gran,” *Can. J. Microbiol.*, vol. 8, no. 1140, pp. 229–239, 1962.

[131] R. E. Hecky and P. Kilham, “Nutrient limitation of phytoplankton in freshwater and marine environments: A review of recent evidence on the effects of enrichment,” *Limnol. Oceanogr.*, vol. 33, no. 4_part_2, pp. 796–822, 1988.

[132] L. Wang, M. Min, Y. Li, P. Chen, Y. Chen, Y. Liu, Y. Wang, and R. Ruan, “Cultivation of green algae Chlorella sp. in different wastewaters from municipal wastewater treatment plant,” *Appl. Biochem. Biotechnol.*, vol. 162, no. 4, pp. 1174–1186, 2010.

[133] M. Henze and Y. Comeau, “Wastewater Characterization,” *Biological Wastewater Treatment: Principles Modelling and Design.* pp. 33–52, 2008.

[134] “Action towards Limiting Total Nitrogen, Total Phosphorus, and Total Inorganic Nitrogen Loads from NPDES-Permitted Facilities.” [Online]. Available: http://www.waterboards.ca.gov/coloradoriver/board_decisions/adopted_orders/boardorders2014.shtml. [Accessed: 12-Nov-2016].

[135] T. Cai, S. Y. Park, R. Racharaks, and Y. Li, “Cultivation of Nannochloropsis salina using anaerobic digestion effluent as a nutrient source for biofuel production,” *Appl. Energy*, vol. 108, pp. 486–492, 2013.

[136] “California Regional Water Quality Control Board - Colorado River Basin Board Orders – Year 2014.” [Online]. Available: http://www.waterboards.ca.gov/coloradoriver/board_decisions/adopted_orders/boardorders2014.shtml. [Accessed: 01-Nov-2016].

[137] “The Emissions & Generation Resource Integrated Database (eGrid) - Energy and the Environment.” [Online]. Available: https://www.epa.gov/energy/egrid. [Accessed: 01-Nov-2016].

[138] K. Homer, C.G., Dewitz, J.A., Yang, L., Jin, S., Danielson, P., Xian, G., Coulston, J., Herold, N.D., Wickham, J.D., and Megown, "Completion of the 2011 National Land Cover Database for the conterminous United States-Representing a decade of land cover change information," *Photogramm. Eng. Remote Sensing*, vol. 81, no. 5, pp. 345–354, 2015.

[139] "Google Maps." Google Inc., 2016.

[140] "Imperial County in California." Google Earth, 2016.

[141] J. Quinn, L. de Winter, and T. Bradley, "Microalgae bulk growth model with application to industrial scale systems," *Bioresour. Technol.*, vol. 102, pp. 5083–5092, 2011.

[142] V. Lemesle and L. Mailleret, "A mechanistic investigation of the algae growth 'droop' model," *Acta Biotheor.*, vol. 56, no. 1–2, pp. 87–102, 2008.

[143] R. J. Geiderl, H. L. Maclntyre, and T. M. Kana, "A dynamic regulatory model of phytoplanktonic acclimation to light, nutrients, and temperature," *Limnol. Ocean.*, vol. 43, no. 4, pp. 679–694, 1998.

[144] M. Marufuzzaman, S. D. Ekşioğlu, and R. Hernandez, "Truck versus pipeline transportation cost analysis of wastewater sludge," *Transportation Research Part A: Policy and Practice*, vol. 74. pp. 14–30, 2015.

[145] A. Malek, L. C. Zullo, and P. Daoutidis, "Modeling and Dynamic Optimization of Microalgae Cultivation in Outdoor Open Ponds," *Ind. Eng. Chem. Res.*, vol. 55, no. 12, pp. 3327–3337, 2016.

Table A.1: Daily weather conditions from typical metrological year data in imperial county California USA [96].

Day	Wind speed ($m\ s^{-1}$)	Humidity	Air temperature (^oC)	Irradiance ($W\ m^{-2}$)	Photoperiod
1	2.47	0.41	13.5	144	0.42
2	2.24	0.32	13	144	0.42
3	3.3	0.3	12.8	145	0.42
4	1.68	0.34	11.1	140	0.42
5	1.38	0.36	11.5	145	0.42
6	0.99	0.44	12.6	145	0.42
7	1.28	0.52	11.4	147	0.42
8	3.83	0.46	13	149	0.42
9	2.08	0.35	14.2	146	0.42
10	0.64	0.46	14.4	102	0.42
11	1.26	0.49	14	107	0.42
12	2.49	0.6	12.3	154	0.42
13	1.51	0.54	12.4	156	0.42
14	2.47	0.46	13.8	155	0.42
15	1.72	0.45	13.6	143	0.42
16	1.61	0.5	14.1	150	0.42
17	1.13	0.6	14.2	154	0.42
18	1.23	0.63	14.8	157	0.38
19	2.06	0.59	15.6	149	0.38
20	8.17	0.53	19	159	0.38
21	5.88	0.38	18.4	162	0.38
22	1.61	0.41	12.8	164	0.38
23	1.36	0.42	12.2	160	0.38
24	1.35	0.47	13.8	151	0.38
25	7.87	0.51	13.2	105	0.38
26	5.41	0.53	11.8	155	0.38
27	3.49	0.46	11.9	169	0.38
28	3.15	0.27	13.1	169	0.38
29	1.78	0.27	13.1	163	0.38
30	1.4	0.33	13.4	175	0.38
31	6.53	0.39	15.1	144	0.38
32	2.58	0.55	14.7	178	0.38
33	2.93	0.67	15.4	174	0.38
34	3.98	0.85	13.1	33	0.38
35	5.74	0.61	13.8	178	0.38

36	2.84	0.61	13.6	183	0.42
37	3.15	0.74	13.5	85	0.42
38	5.34	0.56	15.8	158	0.42
39	4.06	0.76	14.5	139	0.42
40	4.36	0.63	14.2	195	0.42
41	2.08	0.58	13.6	192	0.42
42	2.15	0.61	14.6	194	0.42
43	2.01	0.57	15.6	176	0.42
44	1.93	0.55	16.7	199	0.42
45	3.28	0.71	15	42	0.42
46	6.41	0.6	13.4	183	0.46
47	2.74	0.56	13.8	205	0.46
48	4.78	0.76	12.4	133	0.42
49	2.4	0.54	14.1	213	0.46
50	1.91	0.68	13.3	104	0.46
51	4.81	0.57	13.5	215	0.46
52	4.05	0.53	14.4	184	0.50
53	5.25	0.6	16.4	188	0.50
54	4.45	0.72	16.9	218	0.50
55	6.76	0.55	14.3	174	0.50
56	3.19	0.51	13.1	222	0.50
57	2.93	0.54	13.7	222	0.50
58	2.2	0.5	14	226	0.50
59	2.02	0.46	13.6	230	0.50
60	2.55	0.76	11.8	214	0.50
61	3.75	0.59	13.6	173	0.50
62	3.18	0.52	15	233	0.50
63	2.99	0.62	15.5	177	0.50
64	1.8	0.59	16.2	232	0.50
65	1.71	0.86	14	78	0.50
66	1.72	0.8	14.7	168	0.50
67	2.04	0.72	16.1	253	0.50
68	6.62	0.63	15.7	243	0.50
69	6.71	0.49	14	215	0.50
70	4.84	0.5	14.7	246	0.50
71	2.37	0.55	14.5	233	0.50
72	3.62	0.46	17.1	259	0.50
73	3.23	0.38	20.3	252	0.50
74	2.02	0.49	19	247	0.50
75	3.05	0.45	19.9	232	0.50
76	2.02	0.39	19	257	0.50
77	1.72	0.37	20	256	0.50
78	1.94	0.38	21.7	260	0.50
79	2.45	0.38	23	250	0.50
80	3.47	0.35	24.5	236	0.50
81	3.93	0.32	22.8	259	0.50
82	2.15	0.34	21	268	0.50
83	2.28	0.37	22.6	270	0.50
84	4.07	0.35	23	271	0.50

85	3.35	0.37	22	270	0.50
86	1.83	0.43	22.8	274	0.50
87	1.88	0.44	23.8	278	0.50
88	2.45	0.55	23	277	0.50
89	1.8	0.5	23.1	286	0.50
90	2.91	0.62	22.2	271	0.46
91	4.33	0.26	19.7	268	0.46
92	2.93	0.28	21.1	279	0.46
93	2.53	0.43	21.5	282	0.50
94	1.25	0.39	23.3	283	0.50
95	4.57	0.26	25.5	287	0.50
96	4.11	0.23	25.2	290	0.50
97	2.12	0.34	25.3	278	0.50
98	4.32	0.31	26.7	276	0.50
99	4.78	0.18	25.6	287	0.50
100	3.47	0.29	23.8	300	0.50
101	3.01	0.31	24.2	293	0.50
102	2.95	0.31	25.3	298	0.50
103	4.99	0.28	26.2	297	0.50
104	7.67	0.46	20.4	276	0.50
105	3.26	0.5	19.7	303	0.50
106	2.56	0.52	20.8	303	0.50
107	4.79	0.44	21.8	280	0.50
108	7.77	0.44	18.6	286	0.50
109	2.46	0.44	18.8	309	0.50
110	2.54	0.41	21	315	0.50
111	8.37	0.47	20.3	313	0.50
112	5.48	0.47	21.6	322	0.54
113	2.87	0.53	21.6	322	0.54
114	1.66	0.46	23.1	321	0.54
115	1.85	0.35	24.7	322	0.54
116	2.81	0.36	27.3	325	0.54
117	3.97	0.33	27.6	327	0.54
118	8.32	0.27	25.9	308	0.54
119	4.35	0.31	23.2	330	0.54
120	3.91	0.32	24.5	325	0.54
121	5.42	0.22	24.4	306	0.54
122	5.93	0.35	23.7	327	0.54
123	2.65	0.34	25.4	280	0.54
124	3.33	0.32	26	277	0.54
125	7.78	0.36	23.1	322	0.54
126	7.63	0.41	20.2	294	0.54
127	4.61	0.37	20.7	326	0.54
128	3.28	0.38	22.3	332	0.54
129	7.09	0.34	23.6	331	0.54
130	6.55	0.3	20.7	333	0.54
131	2.45	0.3	21.3	335	0.54
132	2.35	0.27	24.5	334	0.54
133	2.43	0.25	26.5	335	0.58

134	2.77	0.22	29.5	341	0.58
135	3.01	0.22	30.8	334	0.58
136	7.45	0.3	27.5	312	0.58
137	4.05	0.3	24.5	322	0.58
138	2.02	0.3	26.3	343	0.58
139	1.88	0.32	29.3	344	0.58
140	2.34	0.25	32.1	335	0.58
141	2.88	0.19	33.3	342	0.58
142	2.92	0.17	33.4	345	0.58
143	4.8	0.34	31.1	339	0.58
144	4.28	0.45	29.7	347	0.58
145	3	0.38	29.8	341	0.58
146	2.55	0.3	30.2	341	0.58
147	4.33	0.35	29.2	336	0.58
148	3.59	0.45	27.3	276	0.58
149	5.78	0.31	27.2	350	0.58
150	4.04	0.26	27	334	0.58
151	2.06	0.24	29.3	327	0.58
152	6.82	0.2	31.8	337	0.58
153	8.48	0.2	29.3	282	0.58
154	3.83	0.3	27.6	336	0.58
155	2.58	0.35	29.8	346	0.58
156	2.63	0.36	32.3	341	0.58
157	3.59	0.33	34.1	334	0.58
158	4.99	0.33	33.6	337	0.58
159	4.85	0.37	30.1	347	0.58
160	3.63	0.32	28.8	352	0.58
161	2.32	0.45	28.8	343	0.58
162	2.85	0.47	28.8	334	0.58
163	2.5	0.32	30.7	348	0.58
164	2.84	0.26	31.8	347	0.58
165	3.48	0.22	31.8	349	0.58
166	4.06	0.25	32.8	344	0.58
167	4.17	0.35	33.4	337	0.58
168	5.03	0.26	34	353	0.58
169	5.91	0.21	34.5	353	0.58
170	4.73	0.29	33.9	353	0.58
171	4.83	0.3	32.3	349	0.58
172	6.95	0.27	31.1	342	0.58
173	2.73	0.27	30.1	343	0.58
174	2.45	0.31	31.7	345	0.58
175	3.23	0.36	32.7	347	0.58
176	2.25	0.23	33.5	301	0.58
177	6.71	0.14	35.2	341	0.58
178	5.82	0.13	33.5	345	0.58
179	2.87	0.22	32.1	343	0.58
180	2.77	0.39	31.8	341	0.58
181	2.38	0.44	31.2	340	0.58
182	1.65	0.24	29.7	330	0.58

183	2	0.23	29.9	313	0.58
184	3.3	0.19	30.1	332	0.58
185	1.95	0.3	31	338	0.58
186	2.92	0.34	31.9	337	0.58
187	3.52	0.32	32.8	323	0.58
188	4.23	0.26	32.3	296	0.58
189	3.49	0.22	31.4	322	0.58
190	3.19	0.28	32.4	337	0.58
191	2.64	0.25	34.9	334	0.58
192	2.06	0.28	35.4	338	0.58
193	2.62	0.28	36	224	0.58
194	5.38	0.45	34.5	331	0.58
195	5.58	0.54	32.2	211	0.58
196	3.8	0.46	33.3	306	0.58
197	3.83	0.25	34.1	332	0.58
198	3.31	0.24	34.8	326	0.58
199	2.79	0.3	35.3	323	0.58
200	3.43	0.27	36	302	0.58
201	2.94	0.29	35.8	330	0.58
202	4.28	0.25	36	324	0.58
203	4.57	0.35	34.9	326	0.58
204	3.69	0.52	33.5	326	0.58
205	3.78	0.53	33.5	323	0.58
206	3.82	0.41	35.4	325	0.58
207	4.61	0.45	35	320	0.58
208	4.38	0.32	34.2	322	0.58
209	3.6	0.14	33.4	322	0.58
210	2.58	0.3	32.8	327	0.58
211	2.83	0.34	33.2	317	0.58
212	3.88	0.32	33.5	285	0.58
213	2.67	0.52	33.4	291	0.58
214	3.56	0.4	33.3	314	0.58
215	2.75	0.44	32.5	309	0.58
216	2.15	0.51	32.6	321	0.58
217	3.32	0.45	33.5	315	0.58
218	3.1	0.43	31.8	308	0.58
219	3.32	0.31	31.4	310	0.58
220	1.98	0.28	32.8	309	0.58
221	1.78	0.3	35	299	0.58
222	2.23	0.31	36.5	306	0.54
223	4.44	0.55	34.7	293	0.54
224	3.8	0.63	34.2	300	0.54
225	2.9	0.58	34.6	307	0.54
226	3.14	0.53	34.5	301	0.54
227	3.75	0.61	34	304	0.54
228	3.2	0.64	33.7	306	0.54
229	3.26	0.66	33.3	306	0.54
230	4.89	0.7	33.1	302	0.54
231	5.58	0.64	32.4	292	0.54

232	2.73	0.45	31.5	300	0.54
233	2.93	0.34	30.6	287	0.54
234	1.82	0.28	29.9	295	0.54
235	3.23	0.29	31.2	281	0.54
236	3.76	0.18	32.8	280	0.50
237	2.96	0.2	33.2	280	0.50
238	3.15	0.23	33	282	0.50
239	3.96	0.27	32.6	278	0.50
240	3.07	0.27	31.8	286	0.50
241	2.53	0.23	32	285	0.50
242	2.03	0.24	33.4	286	0.50
243	1.76	0.29	34.9	273	0.50
244	3.4	0.62	32.4	246	0.50
245	2.58	0.48	32.8	263	0.50
246	2.83	0.42	33.5	275	0.50
247	2.54	0.41	33.6	283	0.50
248	3.96	0.36	34.3	270	0.50
249	5.59	0.29	32.7	275	0.54
250	3.43	0.38	30.3	276	0.54
251	2.63	0.49	30.2	275	0.54
252	3.07	0.65	30.5	277	0.54
253	3.72	0.51	31.5	274	0.54
254	2.58	0.44	31.3	273	0.54
255	3	0.28	32.3	275	0.54
256	6.68	0.45	31.4	242	0.54
257	3.7	0.58	31.4	224	0.54
258	2.72	0.46	32.2	271	0.54
259	3.77	0.3	31.6	262	0.54
260	3.12	0.2	29.8	254	0.54
261	2.16	0.22	29.6	255	0.50
262	2.81	0.27	31.5	229	0.50
263	2.41	0.29	31.4	252	0.50
264	2.7	0.25	31.2	254	0.50
265	2.86	0.22	30.8	245	0.50
266	2.22	0.25	30.5	251	0.50
267	2.27	0.29	31.3	231	0.50
268	2.23	0.31	31.5	241	0.50
269	2.56	0.3	32.2	240	0.50
270	3.23	0.39	31.2	238	0.46
271	2.83	0.25	31.7	240	0.46
272	2.46	0.49	29.7	234	0.46
273	3.98	0.41	29.7	199	0.46
274	2.99	0.35	26.9	206	0.54
275	2.35	0.35	27.9	226	0.54
276	4.7	0.43	27.2	216	0.54
277	8.08	0.44	23.6	201	0.54
278	6.44	0.49	22.4	118	0.54
279	2.88	0.46	21.1	215	0.54
280	3.12	0.39	23.5	229	0.54

281	2.73	0.36	24.7	224	0.54
282	2.68	0.33	25.1	237	0.54
283	1.71	0.32	25	231	0.54
284	2.02	0.32	25.4	215	0.50
285	3.6	0.36	26.6	226	0.50
286	8.65	0.4	21.3	211	0.50
287	6.14	0.43	22.2	204	0.50
288	7.94	0.47	20	135	0.46
289	2.65	0.41	18.9	194	0.46
290	1.48	0.39	17.8	224	0.50
291	2.52	0.37	18.6	204	0.46
292	2.08	0.41	19.8	206	0.46
293	1.69	0.41	20.7	196	0.46
294	2.36	0.38	21.3	198	0.46
295	1.98	0.42	21.3	75	0.46
296	1.66	0.41	22.8	75	0.46
297	3.46	0.38	25.7	175	0.46
298	3.56	0.4	24.7	192	0.46
299	2.25	0.49	23.9	193	0.46
300	2.39	0.39	24	168	0.46
301	2.7	0.4	23.7	161	0.46
302	2.27	0.41	23.3	189	0.46
303	1.73	0.42	20.9	191	0.46
304	1.66	0.4	20.4	187	0.46
305	1.51	0.47	18.2	163	0.46
306	1.9	0.38	18.5	190	0.46
307	2.54	0.26	17.1	187	0.46
308	1.27	0.22	17.2	186	0.46
309	1.36	0.28	17.2	180	0.46
310	1.4	0.24	16.8	178	0.46
311	2.79	0.21	20.5	169	0.46
312	6.42	0.4	22.7	149	0.46
313	9.33	0.46	24.2	187	0.46
314	3.23	0.35	21.2	185	0.46
315	2.55	0.35	18.8	171	0.46
316	2.53	0.31	17.2	168	0.46
317	1.44	0.3	17	169	0.46
318	1.98	0.32	18.2	164	0.46
319	2.86	0.28	17.8	167	0.46
320	1.94	0.25	15.5	162	0.46
321	1.89	0.28	15	147	0.46
322	2.11	0.26	16.1	166	0.46
323	2.84	0.22	16.5	160	0.46
324	2.8	0.24	19	156	0.46
325	1.88	0.27	19.3	168	0.46
326	1.29	0.32	18.5	156	0.46
327	3.42	0.31	19.5	152	0.46
328	1.69	0.36	17.8	152	0.46
329	3.58	0.31	15.8	146	0.46

330	3.82	0.35	15.2	97	0.46
331	3.2	0.58	14.8	99	0.46
332	3.59	0.56	15.7	70	0.46
333	1.93	0.65	14.1	77	0.42
334	1.61	0.6	15	148	0.46
335	3.38	0.39	17.5	150	0.46
336	2.18	0.39	14.2	153	0.46
337	4.33	0.35	12.5	144	0.42
338	2.42	0.31	11.4	147	0.42
339	2.36	0.32	11.2	139	0.42
340	1.72	0.32	11.6	146	0.42
341	2.41	0.38	12.1	151	0.42
342	4.48	0.31	12.5	137	0.42
343	1.48	0.39	9.5	101	0.42
344	4.54	0.46	11.4	114	0.42
345	6.03	0.29	13.6	143	0.42
346	1.63	0.33	11.9	146	0.42
347	2.12	0.43	11.8	118	0.42
348	3.13	0.34	10.7	114	0.42
349	2.17	0.29	8.9	143	0.42
350	1.08	0.29	12.4	141	0.42
351	1.34	0.43	13.6	142	0.42
352	1.43	0.43	14.2	144	0.42
353	2.74	0.35	14.7	134	0.42
354	2.39	0.33	14.5	141	0.42
355	3.15	0.35	14.7	138	0.42
356	5.17	0.24	15.4	144	0.42
357	3.82	0.29	14.4	142	0.42
358	2.75	0.32	12.7	141	0.42
359	1.95	0.33	12.8	143	0.42
360	2.15	0.38	12.5	142	0.42
361	2.76	0.41	13.1	142	0.42
362	2.2	0.38	14	86	0.42
363	1.46	0.41	12.8	139	0.42
364	1.58	0.41	12.2	148	0.42
365	5.27	0.44	13	150	0.42

Table A.2: Travel distances in miles between the considered wastewater treatment plants and power plants in Imperial County, California, United States of America [139].

Wastewater treatment plant \ Power plant	El Centro	Niland Gas Turbine Plant	Rockwood	Spreckels Sugar Company
El Centro	5.24	32.76	12.18	7.35
Calexico	12.81	43.42	22.26	21.21
Calipatria	30.5	9.2	15.57	19.01
Heber	5.27	39.33	18.17	17.12
Holtville	8.98	37.17	17.76	16.71
Imperial	5.63	33.82	9.53	4.51
Niland	33.99	2.3	19.71	27.21
Seeley	12.89	41.18	20.82	15.99
Westmorland	25.68	20.8	9.97	12.83
Brawley	18.84	18.16	7.33	12.06